MARINE NATURAL PRODUCTS AS ANTIMICROBIAL CHEMICAL DEFENSES AND SOURCES OF POTENTIAL DRUGS

A Dissertation
Presented to
The Academic Faculty

by

Amy L. Lane

In Partial Fulfillment
of the Requirements for the Degree
Doctor of Philosophy in Chemistry in the
School of Chemistry & Biochemistry

Georgia Institute of Technology
December 2008

MARINE NATURAL PRODUCTS AS ANTIMICROBIAL CHEMICAL DEFENSES AND SOURCES OF POTENTIAL DRUGS

Approved by:

Dr. Julia Kubanek
School of Biology and School of Chemistry and Biochemistry
Georgia Institute of Technology

Dr. Mark E. Hay
School of Biology
Georgia Institute of Technology

Dr. Facundo M. Fernandez
School of Chemistry and Biochemistry
Georgia Institute of Technology

Dr. Nicholas V. Hud
School of Chemistry and Biochemistry
Georgia Institute of Technology

Dr. Stephen C. Harvey
School of Biology
Georgia Institute of Technology

Date Approved: August 26, 2008

ACKNOWLEDGEMENTS

I am grateful to many people who have made my thesis journey both successful and largely enjoyable. First, I would like to especially thank my advisor, Dr. Julia Kubanek. Dr. Kubanek's mentoring over the past five years has been instrumental in all aspects of my scientific development, and I am grateful for her advice, constructive criticism, friendship, and ceaseless confidence in my ability to achieve my goals. I also wish to thank committee members Facundo Fernandez, Mark Hay, Steve Harvey, and Nick Hud for their guidance during my time at Georgia Tech. I am grateful for funding from an NSF-IGERT Fellowship, as well as a GAANN Drug Discovery Fellowship, a Georgia Tech Presidential Fellowship, and a Sam Nunn Security Fellowship.

I've been fortunate to have excellent support from both past and present members of the Kubanek lab. E. Paige Stout has been a great resource for countless organic chemistry discussions and collaboration. Staci Padove was instrumental in manuscript editing and all things related to molecular biology. Kelsey Poulson and Drew Sieg were sources of microscopy advice. Clare Redshaw provided valuable LC-MS advice, while Emily Prince and Tracey Myers were great sources of experimental assistance. Renwang Jiang provided advice on natural product structure elucidation and was a valuable collaborator. Melissa Hicks, Lauren Mylacraine, Anne Prusak, and Ruth Armour also provided beneficial discussions as well as experimental assistance. Finally, undergraduate assistants Elizabeth Drenkard, Ankur Fadia, Laurlynn Mular, and Angela Wang were invaluable in completion of countless antimicrobial assays.

I would also like to thank the many who assisted with algal collections during field expeditions to Fiji, including Alex Chequer, Sebastian Engel, Mark Hay, Paul Jensen, Chris Kauffman, Cynthia Kicklighter, Anne Prusak, Tonya Shearer, E. Paige Stout, and Gunilla Toth. Sara Edge was an excellent resource in locating field sites in Fiji and provided extensive collection assistance as well as travel companionship. Bill Aalbersberg, Klaus Feussner, and Mukesh Sharma greatly aided my work in Fiji, providing experimental assistance and laboratory facilities. Further, I thank the government and people of Fiji for facilitating this work.

Paul Jensen and Sebastian Engel donated fungal cultures used in ecological experiments as well as microbiological advice. Tracy Hazen was also a valuable source of microbiology assistance and advice. Facundo Fernandez, Leonard Nyadong, and Asiri Galhena were essential in mass spectrometry imaging experiments, providing experimental assistance, immense knowledge of the subject, and instrumentation. I also acknowledge assistance from Les Gelbaum in collection of NMR data and interpretation of results, as well as services provided by David Bostwick and Cameron Sullards of the Georgia Tech Mass Spectrometry Lab.

I wish to thank friends and colleagues who have been a source of scientific advice and camaraderie: Kimberly Catton, Theresa Davenport, Kelly Fletcher, Tracy Hazen, Rachel Horak, Jennifer Jackson, Liliana Lettieri, Wendy Morrison, Staci Padove-Cohen, Anton Petrov, and Stacy Shinneman. I am also grateful to Tom Caulfield for sharing the dissertation journey with me. Finally, my parents, brother, and extended family have been an endless source of enthusiasm for my scientific career, and I am grateful for their continuing support.

TABLE OF CONTENTS

LIST OF TABLES

LIST OF FIGURES AND SCHEMES

LIST OF SYMBOLS AND ABBREVIATIONS

COSY	Correlation spectroscopy
DAPI	4',6-diamidino-2-phenylindole
DEPT	Distortionless enhancement by polarization transfer
DESI-MS	Desorption electrospray ionization mass spectrometry
DMSO	Dimethyl sulfoxide
EC_{50}	Half maximal effective concentration
HMBC	Heteronuclear multiple bond correlation
HSQC	Heteronuclear single quantum coherence
IC_{50}	Half maximal inhibitory concentration
NMR	Nuclear magnetic resonance
NOE	Nuclear overhauser effect
NOESY	Nuclear overhauser effect spectroscopy
ROESY	Rotating frame overhauser effect spectroscopy
SAR	Structure-activity relationship
SD	Standard deviation
SE	Standard error
δ	Chemical shift (in ppm) of a specific NMR peak

SUMMARY

Marine organisms including macroalgae, sponges, and microbes are widely recognized sources of an impressive array of structurally unusual compounds. Marine natural products have exhibited interesting biomedical activities, provided targets for synthetic organic chemists, and afforded opportunities for elucidation of enzymatic mechanisms involved in biosyntheses of these molecules. Secondary metabolite pathways probably evolved to mediate interactions between organisms in their natural habitats; however, the ecological functions of natural products remain poorly understood for the vast majority of cases. In the present series of investigations, I evaluate the hypothesis that macroalgal natural products play a role in defending these organisms against potentially pathogenic microbes in the marine environment. Further, I combine these ecology-driven investigations with evaluation of algal natural products as sources of novel human drugs.

This combined approach resulted in discovery of 15 novel natural products from two tropical red algae, *Callophycus serratus* and an unidentified crustose red alga. These new molecules included seven novel carbon-carbon connectivity patterns, not previously reported in the synthetic or natural product literature, illustrating the abundance of secondary metabolite diversity among marine macroalgae. Further, many compounds exhibited both biomedical and ecological activities, suggesting the synergistic potential of combined biomedical/ecological investigations in providing drug leads as well as insights into the natural functions of secondary metabolites.

Bromophycolides and callophycoic acids, natural products from *C. serratus*, inhibited growth of the marine fungal pathogen *Lindra thalassiae*. Spatially-resolved

desorption ionization mass spectrometry (DESI-MS) revealed that antifungal natural products were found at specific sites on algal surfaces. Inspection of these distinct regions suggested the presence of relatively large, heterotrophic microbes not found elsewhere on *C. serratus*, perhaps indicative of chemical defense localization to areas of the alga under threat. The heterogeneous presentation of antimicrobial chemical defenses on host surfaces suggests the potential importance of spatial scale in understanding host-pathogen interactions, and illustrates the capacity of mass spectrometry imaging in understanding chemically-mediated biological processes.

Finally, assessment of antimicrobial chemical defenses among extracts from 72 collections of tropical red algae revealed that nearly all algae were defended against at least one marine pathogen or saprophyte and further suggested the untapped potential of ecological investigations in the discovery of novel chemistry. Future investigations of chemically-mediated interactions between hosts and microbes will continue to increase understanding of these highly complex biological interactions and may provide valuable insights for drug discovery.

CHAPTER 1

INTRODUCTION: MARINE NATURAL PRODUCTS AS SOURCES OF NOVEL CHEMISTRY, ECOLOGY, AND DRUGS

Seaweeds, corals, and other benthic organisms face constant challenge on coral reefs. Fish may take more than 150,000 bites per square meter on the ocean floor every day, removing nearly 100% of daily productivity (Carpenter, 1986). Sessile marine organisms battle for space on limited reef substrates (McClintock and Baker, 2001), and microbial foulers and pathogens can devastate susceptible species (Harvell et al., 1999). The multitude of adversaries faced by marine organisms creates substantial selection pressure for the evolution of mechanisms to improve fitness in the face of these challengers.

Chemical defenses represent one way organisms may resist their enemies, and many studies have demonstrated roles for secondary metabolites in defense against consumers (Hay, 1996; Hay and Fenical, 1988). However, far less is known about the role of natural products in mediating other biological interactions, including those between hosts and microbes. Microbial-borne diseases have significantly impacted some marine organisms. Coralline lethal orange disease ravaged South Pacific coralline algal populations in the 1990s (Littler and Littler, 1995), a wasting epidemic caused near extinction of *Zosteria marina* eelgrass in the North Atlantic during the 1930s (Muehlstein et al., 1991), Caribbean populations of the sea urchin *Diadema antillarum* were devastated by an uncharacterized pathogen in the 1980s (Lessios et al., 1984), and white band disease has contributed to declines in reef-building corals (Gladfelter, 1982). Disease outbreaks affect not only susceptible species, but can also disturb the structure

and function of entire marine communities (Hughes, 1994). Harvell and co-workers report that marine diseases are increasing in both prevalence and severity, suggesting the urgent need for improved understanding of marine host-pathogen interactions (Harvell et al., 1999). Evaluation of natural mechanisms by which some marine organisms evade pathogen attack while others are devastated represents an essential facet of such studies.

Analogous to the recognized importance of secondary metabolites as defenses against consumers (Hay, 1996; Hay and Fenical, 1988), natural products may offer some marine species resistance to deleterious microbes. However, only a handful of studies have evaluated this hypothesis and even fewer have identified specific defensive compounds (Engel et al., 2006; Jensen et al., 1998; Jiang et al., In press.; Kjelleberg et al., 1997; Kubanek et al., 2003; Puglisi et al., 2006; Puglisi et al., 2004). Among marine plants, only four classes of antimicrobial chemical defenses have previously been described: a flavone glycoside isolated from the seagrass *Thalassia testudinum* inhibits a zoosporic fungus (Jensen et al., 1998), sulfated triterpenes from green algae *Penicillus capitatus* and *Tydemania expeditionis* exhibit growth inhibitory activity against a marine pathogenic fungus (Jiang et al., In press.; Puglisi et al., 2004), a macrocyclic polyketide from *Lobophora variegata* defends this brown alga against fungi (Kubanek et al., 2003), and furanones from the red alga *Delisea pulchra* interfere with acylated homoserine lactone (AHL) bacterial communication systems, thus inhibiting colonization of this alga (Kjelleberg et al., 1997). Yet, surveys of tropical reef plants suggest antimicrobial defenses are common (Engel et al., 2006; Puglisi et al., 2006). The paucity of knowledge regarding existing antimicrobial chemical defenses in marine algae suggests that this may represent a particularly fertile area for increased understanding of chemically-mediated

host-microbe interactions (Engel et al., 2002). Further, such ecologically-motivated studies may also be valuable in discovery of natural products with potential pharmaceutical applications.

Natural products play a dominant role as sources of new drugs. Between 1981 and 2002, over 60% of all novel drugs were derived from natural products, and over 75% of antimicrobial drugs can be traced to a natural origin (Newman et al., 2003). Nature has afforded scientists secondary metabolites with surprising structural diversity and unprecedented biological activity, although interest in natural products as sources of novel drugs fell in recent decades, giving way to high-throughput combinatorial chemistry approaches (Newman et al., 2003). However, there is now a resurgence of interest in natural product drug discovery research, driven by the low productivity of alternative strategies as well as the immediate need for novel pharmaceuticals (Newman et al., 2003). In particular, it is widely perceived that the pipeline for novel antibiotics is running dangerously low (Walsh, 2003). Tropical coral reefs, sites of high biodiversity and intense competition, predation, and parasitism, represent particularly promising sources of novel drugs to fill this pipeline. Although marine natural product studies are young relative to terrestrial investigations, biomedically-motivated marine natural product studies have already yielded structurally novel compounds with potencies and selectivities justifying clinical trials (Blunt et al., 2007; Blunt et al., 2008; Faulkner, 2000), and two natural product drugs are now on market (Newman and Cragg, 2007).

Combined studies of the ecological roles and pharmaceutical potential of marine natural products may afford particular benefits. By understanding natural functions of secondary metabolites, the relative promise of various organisms may be more readily

predicted. Understanding the ecological roles of natural products may also offer opportunities to manipulate production of these molecules in nature. For example, macroalgae have been shown to respond to small grazers by increasing chemical defenses (Cronin and Hay, 1996; Pavia and Toth, 2000; Taylor et al., 2002; Toth and Pavia, 2000), and such approaches may prove valuable in drug discovery efforts. Likewise, natural products discovered on the basis of biomedical activity may offer starting points for evaluation of ecological function, suggesting promising chemically-rich model systems. Such synergistic ecological and biomedical approaches may result in substantial advances in both fields, offering promise in filling the drug discovery pipeline and in understanding the evolutionary narrative behind natural product biosynthesis.

The following chapters represent combined explorations of marine natural product ecological roles and biomedical potentials. In the next chapter, 10 novel, biomedically-interesting diterpene-shikimate acids and alcohols are reported from the red alga *Callophycus serratus*. Chapter three then centers on discovery of three new, but related macrolides, including two new carbon connectivity motifs, from the same species. Natural products from *C. serratus* are later proposed as antifungal defenses marshaled to specific sites of challenge on algal surfaces (chapter 5). Evaluation of 72 collections of macroalgae for growth inhibitory activity against known algal pathogens and saprophytes then reveals nearly all collections harbored antimicrobial natural products, suggesting the vast untapped potential of ecological leads in natural product discovery (chapter 6). As one example of this approach, two novel sesquiterpene hydroquinones are reported from a crustose red alga on the basis of antimicrobial activity against a marine pathogenic

bacterium. Finally, specific molecular structural features are evaluated for their roles in antiherbivore chemical defense of a freshwater plant (chapter 7).

Works Cited

Blunt, J. W., Copp, B. R., Hu, W. P., Munro, M. H. G., Northcote, P. T., and Prinsep, M. R. (2007). Marine natural products. Natural Product Reports *24*, 31-86.

Blunt, J. W., Copp, B. R., Hu, W. P., Munro, M. H. G., Northcote, P. T., and Prinsep, M. R. (2008). Marine natural products. Natural Product Reports *25*, 35-94.

Carpenter, R. C. (1986). Partitioning herbivory and its effects on coral reef algal communities. Ecological Monographs *56*, 345-363.

Cronin, G., and Hay, M. E. (1996). Induction of seaweed chemical defenses by amphipod grazing. Ecology *77*, 2287-2301.

Engel, S., Jensen, P. R., and Fenical, W. (2002). Chemical ecology of marine microbial defense. Journal of Chemical Ecology *28*, 1971-1985.

Engel, S., Puglisi, M. P., Jensen, P. R., and Fenical, W. (2006). Antimicrobial activities of extracts from tropical Atlantic marine plants against marine pathogens and saprophytes. Marine Biology *149*, 991-1002.

Faulkner, D. J. (2000). Marine pharmacology. Antonie Van Leeuwenhoek International Journal of General and Molecular Microbiology *77*, 135-145.

Gladfelter, W. B. (1982). White-band disease in *Acropora palmata* - Implications for the structure and growth of shallow reefs. Bulletin of Marine Science *32*, 639-643.

Harvell, C. D., Kim, K., Burkholder, J. M., Colwell, R. R., Epstein, P. R., Grimes, D. J., Hofmann, E. E., Lipp, E. K., Osterhaus, A., Overstreet, R. M.*, et al.* (1999). Emerging marine diseases - Climate links and anthropogenic factors. Science *285*, 1505-1510.

Hay, M. E. (1996). Marine chemical ecology: What's known and what's next? Journal of Experimental Marine Biology and Ecology *200*, 103-134.

Hay, M. E., and Fenical, W. (1988). Marine plant-herbivore interactions: The ecology of chemical defense. Annual Review of Ecology and Systematics *19*, 111-145.

Hughes, T. P. (1994). Catastophes, phase shifts, and large-scale degradation of a Caribbean coral reef. Science *265*, 1547-1551.

Jensen, P. R., Jenkins, K. M., Porter, D., and Fenical, W. (1998). Evidence that a new antibiotic flavone glycoside chemically defends the sea grass *Thalassia testudinum* against zoosporic fungi. Applied and Environmental Microbiology *64*, 1490-1496.

Jiang, R. W., Lane, A. L., Hay, M. E., Hardcastle, K., and Kubanek, J. (In press.). Molecular structure and absolute configuration of sulfate conjugated triterpenoids: Chemical defenses of the marine green alga *Tydemania expeditionis*. Journal of Natural Products.

Kjelleberg, S., Steinberg, P., Givskov, M., Gram, L., Manefield, M., and deNys, R. (1997). Do marine natural products interfere with prokaryotic AHL regulatory systems? Aquatic Microbial Ecology *13*, 85-93.

Kubanek, J., Jensen, P. R., Keifer, P. A., Sullards, M. C., Collins, D. O., and Fenical, W. (2003). Seaweed resistance to microbial attack: A targeted chemical defense against marine fungi. Proceedings of the National Academy of Sciences of the United States of America *100*, 6916-6921.

Lessios, H. A., Robsertson, D. R., and Cubit, J. D. (1984). Spread of *Diadema* mass mortality through the Caribbean. Science *226*, 335-337.

Littler, M. M., and Littler, D. S. (1995). Impact of Clod Pathogen on Pacific Coral Reefs. Science *267*, 1356-1360.

McClintock, J. B., and Baker, B. J., eds. (2001). Marine Chemical Ecology (CRC Press).

Muehlstein, L. K., Porter, D., and Short, F. T. (1991). *Labyrinthula zosterae* Sp-Nov, the causative agent of wasting disease of eelgrass, *Zostera marina*. Mycologia *83*, 180-191.

Newman, D. J., and Cragg, G. M. (2007). Natural products as sources of new drugs over the last 25 years. Journal of Natural Products *70*, 461-477.

Newman, D. J., Cragg, G. M., and Snader, K. M. (2003). Natural products as sources of new drugs over the period 1981-2002. Journal of Natural Products *66*, 1022-1037.

Pavia, H., and Toth, G. B. (2000). Inducible chemical resistance to herbivory in the brown seaweed Ascophyllum nodosum. Ecology *81*, 3212-3225.

Puglisi, M., Engel, S., Jensen, P., and Fenical, W. (2006). Antimicrobial activities of extracts from Indo-Pacific marine plants against marine pathogens and saprophytes. Marine Biology.

Puglisi, M. P., Tan, L. T., Jensen, P. R., and Fenical, W. (2004). Capisterones A and B from the tropical green alga Penicillus capitatus: unexpected anti-fungal defenses targeting the marine pathogen Lindra thallasiae. Tetrahedron *60*, 7035-7039.

Taylor, R. B., Sotka, E., and Hay, M. E. (2002). Tissue-specific induction of herbivore resistance: seaweed response to amphipod grazing. Oecologia *132*, 68-76.

Toth, G. B., and Pavia, H. (2000). Water-borne cues induce chemical defense in a marine alga (*Ascophyllum nodosum*). Proceedings of the National Academy of Sciences of the United States of America *97*, 14418-14420.

Walsh, C. (2003). Where will new antibiotics come from? Nature Reviews Microbiology *1*, 65-70.

CHAPTER 2

CALLOPHYCOIC ACIDS AND CALLOPHYCOLS FROM THE FIJIAN RED ALGA *CALLOPHYCUS SERRATUS*

Abstract

Callophycoic acids A-H (**1-8**) and callophycols A-B (**9-10**) were isolated from extracts of the Fijian red alga *Callophycus serratus*, and identified by NMR, X-ray, and mass spectral analyses. These natural products represent four novel carbon skeletons, providing the first examples of diterpene-benzoic acids and diterpene-phenols in macroalgae. Compounds **1-10** exhibited antibacterial, antimalarial, and anticancer activity, although they are less bioactive than diterpene-benzoate macrolides previously isolated from this red alga. The identification of distinct chemotypes from different populations of *C. serratus* justifies evaluation of multiple collections of a single species.

Introduction

Red macroalgae are well-known producers of bioactive secondary metabolites, including isoprenoid and phenolic metabolites (Blunt et al., 2005). However, the discovery of metabolites with novel carbon skeletons and mixed biosynthetic origin is uncommon. Recently, 10 novel bioactive diterpene-benzoate macrolides, representing two new carbon skeletons, were isolated from a Fijian collection of *Callophycus serratus* (Kubanek et al., 2006; Kubanek et al., 2005), a member of the largely unstudied Solieriaceae family of red algae. To further characterize the secondary metabolism of *C. serratus*, a second Fijian population was analyzed. This exploration led to the isolation

of eight novel bioactive diterpene-benzoic acids (**1**-**8**) and two novel halogenated diterpene-phenols (**9**-**10**), whose structure elucidation and biological activities are presented herein.

Results and discussion

A toxicity assay based upon ingestion rates of the invertebrate rotifer *Brachionus calyciflorus* was used to guide the initial fractionation of *Callophycus serratus* extract by liquid-liquid partitioning. Liquid chromatography-mass spectrometry (LC-MS) was applied to identify fractions with isotopic signatures or molecular masses corresponding to putative brominated C_{27} natural products analogous to diterpene benzoate macrolides isolated from a previous *C. serratus* collection (Kubanek et al., 2006; Kubanek et al., 2005). Reversed and normal-phase high-performance liquid chromatography (HPLC) separation of these fractions led to isolation of callophycoic acids A-H (**1-8**) and callophycols A-B (**9-10**).

High-resolution mass spectral data established the molecular formula of callophycoic acid A (**1**) as $C_{27}H_{35}O_3Br$ (*m/z* 485.1697 $[M - H]^-$). X-ray diffraction analysis of **1** revealed two identical tricyclic diterpene-benzoic acids in the asymmetric unit, with one having the end of its pendant carbon chain rotated with respect to the other (Figure 2.1). The structure derived from X-ray diffraction data established 6*R*, 7*S*, and 24*S* absolute stereochemistries for **1**, indicated an *E* configuration at $\Delta^{10,11}$ and $\Delta^{21,22}$ (Appendix A), and was supported by NMR spectral data. Analysis of ^{13}C chemical shifts and HMBC correlations established the aryl moiety of this 3,4-substituted benzoic acid-based molecule, a structural theme common to **1-7**, and a combination of HMBC and

COSY correlations established connectivity throughout the tricyclic ring system (Table 2.1; Appendix A). Finally, the linear diterpene head was assembled primarily with strong two- and three-bond HMBC correlations from singlet methyl protons.

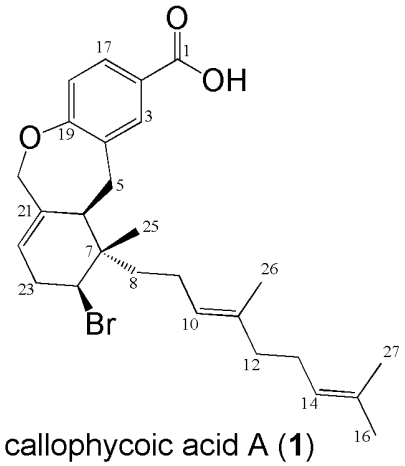

callophycoic acid A (**1**)

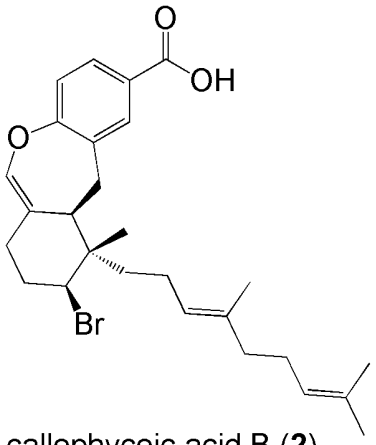

callophycoic acid B (**2**)

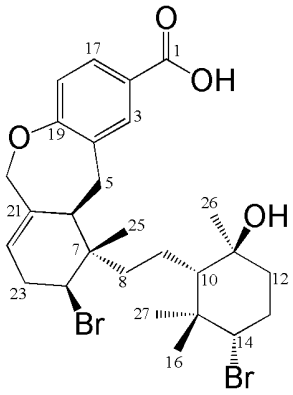

callophycoic acid C (**3**)

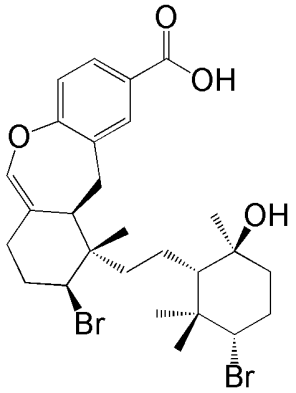

callophycoic acid D (**4**)

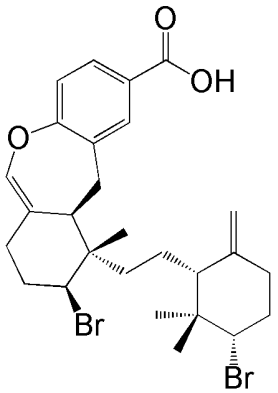

callophycoic acid E (**5**)

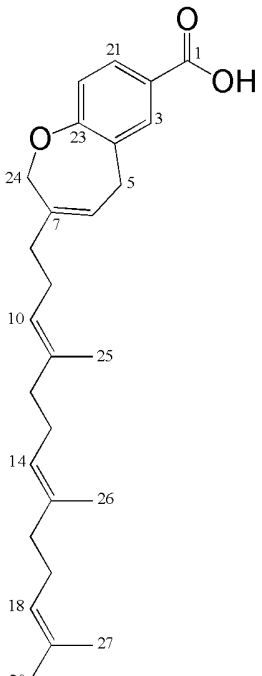

callophycoic acid F (**6**)

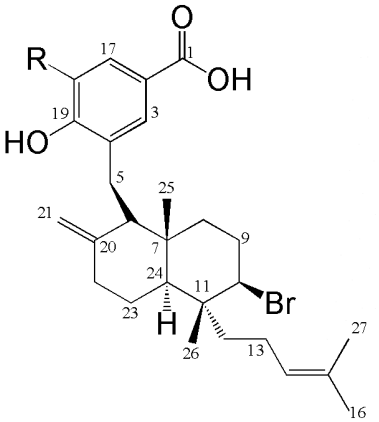

callophycoic acid G, R=H (**7**)
callophycoic acid H, R=Br (**8**)

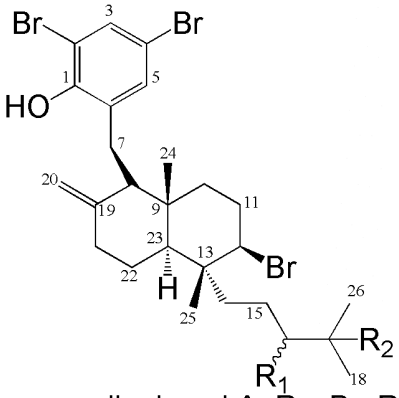

callophycol A, R_1=Br, R_2=Cl (**9**)
callophycol B, R_1=Cl, R_2=Br (**10**)

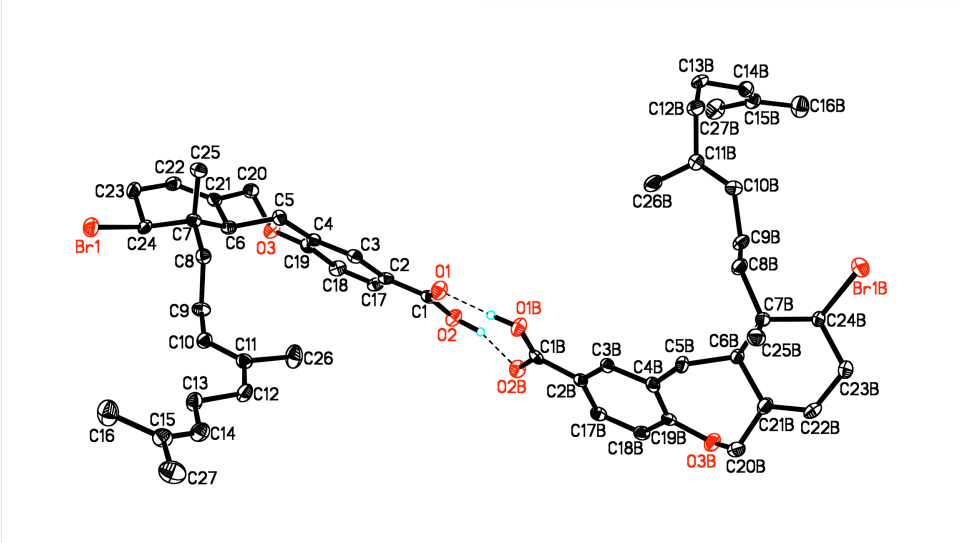

Figure 2.1 Perspective drawings of X-ray crystal structures of callophycoic acid A (1). These structures differ only in diterpenoid chain rotation.

Table 2.1 ^{13}C and ^{1}H NMR spectral data for callophycoic acids A-H (**1-8**) (500 MHz; in $CDCl_3$ for **1-2** and **5-8**; in $(CD_3)_2CO$ for **3**-**4**).

#	**1**		**2**		**3**		**4**		**5**		**6**		**7**		**8**	
	δ ^{13}C	δ ^{1}H ($J_{H,H}$)	δ ^{13}C	δ ^{1}H ($J_{H,H}$)	δ ^{13}C	δ ^{1}H ($J_{H,H}$)	δ ^{13}C	δ ^{1}H ($J_{H,H}$)	δ ^{13}C	δ ^{1}H ($J_{H,H}$)	δ ^{13}C	δ ^{1}H ($J_{H,H}$	δ ^{13}C	δ ^{1}H ($J_{H,H}$)	δ ^{13}C	δ ^{1}H ($J_{H,H}$)
1	171.5	-	171.2	-	167.2	-	167.1	-	169.9	-	171.4	-	170.0	-	169.0	-
2	122.6	-	125.8	-	124.2	-	127.4	-	125.0	-	124.1	-	121.2	-	122.0	-
3	134.5	7.85br s	132.1	7.88br s	135.6	7.91br s	133.0	8.08br s	132.1	7.91br s	131.4	7.80 br s	132.3	7.83brs	131.5	7.77br s
4	128.0	-	132.7	-	129.1	-	134.5	-	132.8	-	134.0	-	127.8	-	130.0	-
5	33.0	2.83d (15.3) 3.08dd (15.3, 12.1)	30.8	2.85dd (13.3, 4.2) 3.19dd (13.3, 10.8)	33.3	3.02d (15.7), 3.14dd (15.1, 12.0)	30.5	3.20m, 3.28dd (13.3, 4.3)	31.0	2.86dd (13.4, 3.8) 3.18dd (13.0, 11.1)	31.0	3.48d (5.2)	23.5	2.70 (13.2, 2.0) 2.78 (15.5, 10.0)	24.4	2.80m
6	41.6	2.89brd (11.6)	43.4	2.42dd (10.5, 4.0)	42.8	2.98m	44.1	2.64dd (10.1, 3.7)	43.3	2.44dd (10.8, 3.3)	121.7	5.70t (5.3)	55.6	2.25m	55.3	2.25m
7	40.3	-	43.4	-	41.7	-	44.7	-	43.5	-	137.9	-	41.9	-	42.0	-
8	37.6	1.57m 1.78m	37.6	1.54m 1.79m	41.4	1.78dd (13.4, 5.2), 2.16dd (13.8, 4.4)	41.8	1.76m, 1.96m	37.4	1.48m 1.73m	34.8	1.92m 2.06m	40.2	1.38m 1.91m	40.1	1.40m 1.90m
9	21.0	1.79m 1.94m	20.6	1.95m 2.05m	20.8	1.41m, 1.46m	20.5	1.43m, 1.74m	19.0	1.53m 1.70m	26.7	2.04m	31.2	2.19m 2.27m	31.2	2.19m 2.27m
10	123.3	5.08t (6.4)	123.4	5.20m	57.6	1.29dd (3.9, 3.9)	58.0	1.35m	53.9	1.79m	123.3	5.05m	64.0	4.32dd (12.5, 4.2)	64.0	4.33dd (12.5, 4.0)
11	135.7	-	135.7	-	73.0	-	73.4	-	146.8	-	135.9	-	41.5	-	41.9	-
12	39.6	1.87m 1.98m	39.7	2.02m	44.4	1.60m, 1.69m	44.5	1.70m, 1.84m	35.7	2.14m 2.49m	39.7	1.94m	39.7	1.40m 1.55m	39.7	1.40m 1.56m
13	26.6	1.89m 1.99m	26.7	2.08m	32.7	2.00dd (12.9, 3.3), 2.08m	33.5	2.13m	35.7	2.10m 2.29m	26.7	2.04m	21.0	1.83m 1.92m	21.1	1.83m 1.93m

14	124.3	5.03tm (7.0)	124.3	5.10m	68.9	4.10dd (12.2, 4.4)	68.9	4.15dd (11.0, 5.4)	66.5	4.17dd (10.1, 4.1)	124.4	5.07m	123.9	5.08dd (7.0, 7.0)	123.9	5.09dd (6.3, 6.3)
15	131.3	-	131.4	-	41.6	-	41.9	-	41.9	-	135.0	-	131.8	-	131.8	-
16	25.7	1.65s	25.7	1.68s	30.8	1.16s	30.8	1.19s	28.7	1.22s	39.7	1.94m	17.6	1.63s	17.6	1.63s
17	130.2	7.83d (8.4)	130.0	7.87m	129.9	7.73d (8.4)	130.0	7.83d (8.0)	130.0	7.89br d (2.0)	26.6	1.93m	129.6	7.79dd (7.7, 1.9)	131.6	8.03br s
18	119.5	6.89d (8.4)	119.8	6.98d (9.0)	119.5	6.84d (8.4)	120.2	7.00d (8.1)	119.8	7.02d (8.2)	124.1	5.07m	115.0	6.75d (8.4)	110.4	-
19	163.4	-	163.8	-	163.2	-	164.2	-	163.8	-	131.3	-	158.0	-	154.5	-
20	74.7	4.42d (13.6) 4.85brd (13.6)	140.2	6.53br s	74.6	4.44d (13.5), 4.97d (13.5)	140.9	6.61br s	140.3	6.53br s	25.7	1.65s	147.3	-	146.6	-
21	137.6	-	121.1	-	138.9	-	122.6	-	120.7	-	130.4	7.89dd (8.3, 1.8)	108.3	4.68brs, 4.82brs	108.3	4.61br s 4.79br s
22	122.9	5.56brs	33.1	1.90m 2.04m	123.6	5.63br s	33.2	2.08m	33.2	1.94m 2.07m	121.2	7.01d (8.3)	37.7	2.03m 2.38m	37.7	1.99m 2.36m
23	35.0	2.63m 2.75dm (17.8)	34.2	2.07m 2.17m	36.1	2.66m, 2.77m	35.2	2.07m, 2.18m	34.0	2.09m 2.18m	163.2	-	25.1	1.48m 1.72m	25.1	1.48m 1.72m
24	58.8	4.39dd (11.0, 5.8)	62.2	4.30dd (12.3, 4.2)	60.6	4.68dd (10.9, 6.0)	63.9	4.61dd (11.5, 4.0)	62.4	4.29dd (12.1, 4.1)	72.5	4.56s	49.8	1.54m	49.9	1.54m
25	15.7	0.92s	17.5	0.95s	16.1	0.91s	17.9	0.92s	17.7	0.95s	16.0	1.53s	15.0	0.87s	15.0	0.87s
26	15.9	1.49s	16.1	1.69s	23.1	0.99s	23.5	1.32s	108.9	4.84br s 5.13br s	16.0	1.56s	19.6	0.94s	19.6	0.94s
27	17.7	1.56s	17.7	1.60s	17.7	0.87s	18.0	0.98s	18.5	0.92s	17.7	1.57s	25.7	1.67s	25.7	1.68s
OH	-	-	-	-	-	-	-	3.65br s	-	-	-	-	-	5.45brs	-	6.08br s

br=broad; s=singlet; d=doublet; dd=doublet of doublets; t=triplet; m=multiplet

For callophycoic acid B (**2**), mass spectral analysis indicated an isotopic splitting pattern identical to that of **1** and an *m/z* $[M - H]^-$ of 485.1665, supporting a molecular formula of $C_{27}H_{35}O_3Br$, isomeric to **1.** Analysis of ^{13}C NMR spectral data indicated significant differences at C-20 (δ 74.7 for **1**; δ 140.2 for **2**), C-21 (δ 137.6 for **1**; δ 121.1 for **2**), and C-22 (δ 122.9 for **1**; δ 33.1 for **2**) (Table 1). Further, DEPT-135 data for **1** showed that two protons (δ 4.42, δ 4.85) were attached at C-20, while this position in **2** possessed a single, more deshielded proton (δ 6.53). Conversely, at C-22, **1** had one directly attached, deshielded proton (δ 5.56), while **2** had two attached protons (δ 1.90, δ 2.04). This suggested the $\Delta^{21,22}$ olefin in **1** was isomerised to a $\Delta^{20,21}$ olefin in **2**, and the close correspondence of 2D correlations between **1** and **2** confirmed this conclusion (Appendix A).

Observed NOEs were similar for **1** and **2**, leading us to predict that these molecules share the same absolute stereochemistry (Appendix A). Specifically, a strong NOE was noted between H-6 (δ 2.42) and H-24 (δ 4.30), supporting 6*R* and 24*S* configurations for **2**. The lack of an observable NOE from either H-6 or H-24 to Me-25 (δ 0.95) further supported these configurations and prompted assignment of a 7*S* configuration. An *E* configuration was supported at the $\Delta^{10,11}$ olefin of **2** by NOEs observed between Me-26 (δ 1.69) and H-9b (δ 2.05) and between H-10 (δ 5.20) and H-12 (δ 2.02) and confirmed by the lack of an NOE between Me-26 and H-10. An *E* configuration was assigned at the $\Delta^{20,21}$ olefin based on similar arguments.

Callophycoic acid C (**3**) gave a parent ion at *m/z* 581.0895, supporting a molecular formula of $C_{27}H_{36}O_4Br_2$. Callophycoic acids A and C (**1** and **3**) exhibited nearly identical ^1H and ^{13}C chemical shifts and 2D NMR correlations for C-1 through C-8

and C-17 through C-25 (Table 1; Appendix A), indicating these molecules shared a common tricyclic structure. However, substantial differences in chemical shifts and 2D NMR correlations were found in the diterpenoid head. Assessment of sites of unsaturation indicated that this group included one more ring system than **1**-**2**.

For callophycoic acid C (**3**), COSY correlations were observed between H-8 (δ 1.78, δ 2.16) and H-9 (δ 1.41, δ 1.46), establishing connectivity between these methylenes. Likewise, COSY correlations between H-9 and H-10 (δ 1.29) established connectivity between these carbons, an assignment further supported by an HMBC correlation from H-10 to C-9 (δ 20.8). This proton also exhibited HMBC correlations to quaternary C-11 (δ 73.0) and C-15 (δ 41.6), and methyl C-16 (δ 30.8), establishing C-11—C-10—C-15—C-16 connectivity.

In callophycoic acid C (**3),** the singlets Me-16 (δ 1.16) and Me-27 (δ 0.87) shared identical HMBC correlations to C-10 (*δ* 57.6), C-14 (*δ* 68.9), and C-15, as well as to each other. These correlations were thus a starting point for establishing connectivity within spin systems of the cyclohexanol ring through COSY and additional HMBC correlations. Hydroxy and bromine groups were assigned at C-11 and C-14, respectively, on the basis of carbon and proton chemical shift arguments.(Silverstein and Webster, 1998)

NOEs for the tricyclic moiety of **3** matched closely those of **1** (Appendix A), leading us to predict 6*R*, 7*S*, and 24*S* absolute configurations, as in **1**-**2**. Relative stereochemistry within the cyclohexanol ring was then established based on observed NOEs. First, H-10 and H-14 were assigned to diaxial positions on the same face of the ring, with NOEs observed between these protons. Further, the diaxial orientation of these protons supported a chair conformation for the cyclohexanol ring, with the bulky alkyl

substituent on C-10 and bromine on C-14 assigned equatorial positions. Me-16 was then assigned to an equatorial position on the same face as H-10 and H-14, based on NOEs between both of these protons and Me-16, an assignment further supported by the lack of NOEs between H-10 or H-14 and axial Me-27. Finally, Me-26 was assigned in an axial position on the opposite side of the ring to H-10 and H-14, based on an NOE between Me-26 and Me-27, and supported by the absence of an NOE between Me-26 and H-10 or H-14.

With the relative stereochemistry of the cyclohexanol moiety of **3** elucidated, the absolute stereochemistry of this ring was determined with a series of NOEs that established the orientation of this ring relative to the 6*R*, 7*S,* 24*S* tricycle. First, the conformation of the bond between C-9 and C-10 was determined by NOEs between H-9a and both Me-16 and Me-27, which supported H-9a pointing towards these two methyls. This assignment was further supported by the lack of an NOE between H-9a and Me-26. An NOE between H-9b and Me-26, but not between H-9b and Me-16 or Me-27, analogously prompted placement of H-9b pointing towards Me-26, thus establishing the dominant conformation of the C-9—C-10 bond. Next, NOEs were observed between H-9a and H-24 and between H-9b and H-6, supporting a conformational preference of H-9a, Me-16, H-24, and Me-27 on one side of the molecule and H-9b, H-6, and Me-26 on the other side. Based on these correlations, a 10*S*, 11*S*, 14*S* stereochemistry was assigned for the cyclohexanol ring. The enantiomer (10*R*, 11*R*, 14*R*) should instead afford NOEs between H-9b and H-24 and between H-9a and H-6, but these correlations were not observed, thus confirming the cyclohexanol stereochemistry (Figure 2.2). With this

additional ring relative to callophycoic acids A-B (**1-2**), callophycoic acid C (**3**) provided a second novel carbon skeleton.

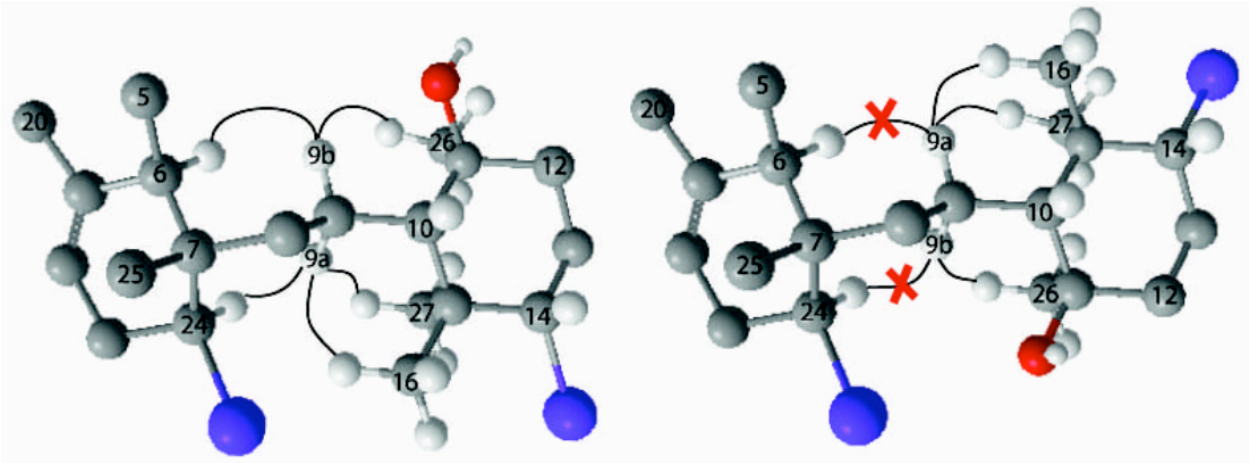

Figure 2.2 Proposed partial 3D structure of callophycoic acid C (3) (left) and incorrect configuration (right). Lines indicate selected observed NOEs that support 10*S*, 11*S*, 14*S* absolute stereochemistry. X's denote NOEs not observed.

Callophycoic acid D (**4**) appeared structurally similar to **3**, with an identical molecular formula ($C_{27}H_{36}O_4Br_2$ from $[M-H]^-$ *m/z* 581.0889). The major difference between **3** and **4** occurred in the tricyclic moiety. ^{1}H and ^{13}C chemical shifts, DEPT-135 data, and HMBC and COSY correlations for this group closely matched those observed for callophycoic acid B (**2**), prompting assignment of a tricycle identical to that of **2**. Hence, like **1** and **2**, callophycoic acids C and D (**3-4**) are isomers, differing only in the position of the olefin ($\Delta^{21,22}$ in **1** and **3** and $\Delta^{20,21}$ in **2** and **4**). The stereochemistry of **4** was established as 6*R*, 7*S,* 10*S*, 11*S*, 14*S*, 24*S* and the $\Delta^{20,21}$ olefin was assigned a *cis* conformation on the basis of NOE arguments analogous to those for **3**.

Comparison of NMR spectral data suggested that callophycoic acid E (**5**), with a parent ion of *m/z* 563.0807 (suitable for a molecular formula of $C_{27}H_{34}O_3Br_2$), was most similar to **4**, with similar ^{13}C and ^{1}H chemical shifts and 2D correlations throughout the tricyclic group. Further, spectral data were largely similar within the cyclohexane moiety, with the primary difference being the presence of an exo-methylene in **5** instead of the methyl and hydroxy groups observed in **4**. Assignment of the $\Delta^{11,26}$ olefin was confirmed by HMBC correlations from H-26 (δ 4.84, δ 5.13) to C-10 (δ 53.9) and C-12 (δ 35.7). Chemical shift assignments within the methylenecyclohexane system of **5** were further supported by close correspondence with previous reports of this group (Kuniyoshi et al., 2001). The stereochemistry of the tricyclic system was established as 6*R*, 7*S*, 24*S* on the basis of NOE arguments analogous to those for **1**-**4**. NOE correlations for **5** did not permit determination of the stereochemistry of the methylenecyclohexane ring relative to the tricyclic moiety, but, given the similarity between **3**, **4**, and **5**, stereochemistry within this group was proposed as 10*S*, 14*S*, and supported by NOEs between H-10 (δ 1.79) and H-14 (δ 4.17) and between H-10 and H-16.

High resolution mass spectral analysis established a molecular formula of $C_{27}H_{36}O_3$ (*m/z* 407.2574 $[M - H]^-$) for callophycoic acid F (**6**). Comparison of ^{1}H and ^{13}C chemical shifts and HMBC and COSY correlations between **1-5** and **6** indicated that this molecule contained a benzoic acid functionality fused to an unsaturated seven-membered ether ring. However, HMBC and COSY correlations indicated regioisomerisation of the olefin relative to **1-5**. For **6**, HMBC correlations from H-5 (δ 3.48) to olefinic carbons C-6 (δ 121.7) and C-7 (δ 137.9) supported a $\Delta^{6,7}$ olefin. This assignment was verified and the seven-membered ether ring sealed by HMBC

correlations from H-24 (δ 4.56) to C-7. HMBC correlations from H-6 and H-24 to C-8 (δ 34.8) connected the ring system to the side chain. This C-7–C-8 linkage completed one isoprene unit and left three sites of unsaturation, accounted for by six additional olefin signals evident from the ^{13}C NMR spectrum.

For callophycoic acid F (**6**), the COSY correlation between H-9 (δ 2.04) and H-10 (δ 5.05) and HMBC correlations from H-10 to C-8 and C-9 (δ 26.7) prompted placement of C-9 between C-8 and C-10 (δ 123.3). Strong two- and three-bond HMBC correlations from the Me-25 singlet (δ 1.53) to C-10 and C-11 (δ 135.9) supported linkage of these two olefinic carbons, with C-11 bearing the methyl substituent; an additional HMBC correlation between Me-25 and C-12 (δ 39.7) established the connectivity of C-11 with C-12 and completed the second isoprene unit. The third and fourth isoprene units were then assembled on the basis of similar arguments. Assignments of ^{1}H and ^{13}C chemical shifts in this linear terpenoid head were verified by comparison with literature values for analogous moieties (Ito et al., 1999).

An *E*-configuration was established for the $\Delta^{10,11}$ olefin of callophycoic acid F (**6**) based on NOEs from Me-25 to H-9 and the lack of an NOE between Me-25 and H-10. An *E*-configuration was proposed at the $\Delta^{14,15}$ olefin based on similar arguments. The carbon skeleton of **6** is not novel, matching that of common tocopherols (Shin and Godber, 1994).

From high-resolution mass spectral data, the molecular formula of callophycoic acid G (**7**) was established as $C_{27}H_{37}O_3Br$ (*m/z* 487.1823 $[M - H]^-$). As for **1-6**, ^{1}H, ^{13}C, COSY, and HMBC data were indicative of a disubstituted benzoic acid moiety linked to a diterpene (Table 2.1; Appendix A). Unlike **1-6**, callophycoic acid G (**7**) presented a

phenolic-OH signal (δ 5.45), which was assigned as the C-19 substituent as for bromophycolides (Kubanek et al., 2006; Kubanek et al., 2005). The possibility of a seven-membered ether ring, as in previous compounds, was thus eliminated.

Elucidation of the decalin system of callophycoic acid G (**7**) commenced with singlets Me-25 (δ 0.87) and Me-26 (δ 0.94), for which all expected two- and three-bond HMBC correlations were observed, thus establishing connectivity along positions C-6—C-7—C-24—C-11—C-10 of the decalin group and supporting bonds between C-7—C-8 and C-11—C-12. COSY correlations were observed between H-24 (δ 1.54) and H-23b (δ 1.72), and between H-22 (δ 2.03, δ 2.38) and H-23 (δ 1.48, δ 1.72), thus establishing C-22—C-23—C-24 connectivity. HMBC correlations from exo-methylenes H-21a (δ 4.68) and H-21b (δ 4.82) to C-22 (δ 37.7) and C-6 (δ 55.6) then supported connection of C-22—C-20—C-6, thus sealing this ring. To seal the second ring of the decalin system of **7**, C-8—C-9—C-10 connectivity was established on the basis of COSY correlations between H-8 (δ 1.38, δ 1.91) and H-9 (δ 2.19, δ 2.27), and between C-9 protons and H-10 (δ 4.32). Assignments in the decalin system were verified by comparison with literature values for analogous moieties (Cavin et al., 2006; West and Faulkner, 2006). The isoprenoid head of **7** was next established with COSY and HMBC correlations, analogously to **1**-**6**.

The relative stereochemistry of callophycoic acid G (**7**) was determined from NOE correlations (Appendix A). Observation of an NOE between H-6 (δ 2.25) and H-24 and between H-24 and H-10 indicated that these protons were positioned on the same face of the decalin ring system. Observation of an NOE between Me-25 and Me-26, but

not between either of these groups and H-6 or H-10, next supported placement of these methyls *cis* on the other face. The absolute stereochemistry was left unassigned.

Callophycoic acid H (**8**) possessed a molecular formula of $C_{27}H_{36}O_3Br_2$ (*m/z* 565.0968 $[M - H]^-$). Comparison of ^1H and ^{13}C chemical shifts (Table 2.1) and 2D correlations (Appendix A) between callophycoic acids G-H (**7-8**) indicated these molecules differed by one bromine atom within the aryl ring, with **8** including a trisubstituted benzoic acid in contrast to the disubstituted moiety of **7**. The substitution pattern of this aryl ring was determined by HMBC correlations from aryl protons and confirmed by comparison of ^{13}C chemical shifts with empirical values (Silverstein and Webster, 1998). Together, callophycoic acids G-H (**7-8**) represent a third novel carbon skeleton.

High-resolution mass spectrometry and ^1H and ^{13}C NMR spectra indicated that callophycol A (**9**) had a molecular formula of $C_{26}H_{35}OBr_4Cl$ (*m/z* 712.9066 $[M - H]^-$), one fewer carbon than **1-8**. With only one oxygen atom, this molecular formula did not support the carboxylic acid functionality observed in **1-8**, suggesting the missing carbon was in this functional group, a hypothesis supported by the absence of a diagnostic carboxylic acid signal in the ^{13}C NMR spectrum for **9** and confirmed by the lack of a characteristic carbonyl stretching absorption in the IR spectrum, as compared to the strong IR absorbance at 1687 cm^{-1} for **1**.

^1H, ^{13}C, and HMBC NMR data were applied in elucidating the dibromophenol of **9** (Table 2.2; Appendix A). HMBC correlations were observed from the aryl hydroxy proton (δ 5.60) to C-1 (δ 149.3), C-2 (δ 110.7), and C-6 (δ 131.3), and the downfield shift of C-1 corresponded with literature values for phenolic carbons (Silverstein and Webster,

1998), establishing C-2—C-1—C-6 connectivity. HMBC correlations from alkyl H-7 (δ 2.73; δ 2.75) to C-1, C-5 (δ 132.1), and C-6 next supported connection of these aryl carbons. HMBC correlations from H-3 (δ 7.39) to C-1, C-4 (δ 112.2), and C-5 and from H-5 (δ 7.13) to C-1, C-3 (δ 131.1), and C-4 then established remaining carbon connectivity within the aryl group. Completion of the aryl framework of **9** left the C-2 and C-4 substituents to be identified as either two bromines or one bromine and one chlorine. Arguments based upon substituent effects on carbon chemical shifts (Silverstein and Webster, 1998) and comparison with data for 2,4-dibromo-6-methylphenol (Maloney and Hecht, 2005) supported assignment of a dibromonated phenol.

For the remaining portions of **9** except for the diterpene head, NMR data were nearly identical with data for **7-8** (Table 2.1; Table 2.2; Appendix A), supporting a decalin system identical to those molecules. At the diterpene head, COSY correlations between H-14a (δ 1.38) and H-15b (δ 2.26) and between H-14b (δ 2.06) and both H-15 multiplets supported C-14—C-15 connection. Further, both H-14 protons showed HMBC correlations to methine C-16 (δ 65.5), establishing the C-15–C-16 linkage, which was verified by a COSY correlation between H-15a (δ 1.68) and H-16 (δ 3.90). The carbon skeleton was then completed by HMBC correlations from Me-18 (δ 1.79) and Me-26 (δ 1.70) to one another, to C-16, and to C-17 (δ 72.7). The bromine atom was then attached to methine C-16 and the chlorine at quaternary C-17 on the basis of ^{13}C chemical shift predictions (Silverstein and Webster, 1998) and empirical data (Suzuki et al., 1993; Wright et al., 1991), which supported assignment of the chlorine at the more deshielded carbon.

NOEs within the decalin system were analogous for **7-9**, supporting the same relative stereochemistries for all of these molecules. However, an additional stereocenter was introduced at C-16 in callophycol A (**9**). Because no NOEs were observed between decalin stereocenters and the stereocenter at C-16, it was left unassigned.

Table 2.2 ^{13}C and ^{1}H NMR spectral data for callophycols A-B (**9-10**) (500 MHz; in $CDCl_3$).

#	**9**		**10**	
	δ ^{13}C	δ ^{1}H	δ ^{13}C	δ ^{1}H
1	149.3	-	149.3	-
2	110.7	-	110.8	-
3	131.1	7.39d (2.2)	131.1	7.39brs
4	112.2	-	112.2	-
5	132.1	7.13d (2.2)	132.1	7.13brs
6	131.3	-	131.3	-
7	24.5	2.73d (2.8) 2.75brs	24.4	2.74brs 2.75brs
8	55.4	2.14m	55.4	2.14m
9	39.9	-	39.9	-
10	40.1	1.35m 1.87m	40.1	1.37m 1.87m
11	31.2	2.18m 2.24m	31.1	2.19m 2.25m
12	63.2	4.15dd (12.4, 4.4)	63.8	4.21dm (10.2)
13	42.0	-	42.1	-
14	38.8	1.38m 2.06m	38.0	1.57m 1.86m
15	28.0	1.68m 2.26m	28.2	1.50m 2.33m
16	65.5	3.90brd (9.8)	72.7	3.91d (10.1)
17	72.7	-	68.3	-
18	33.5	1.79s	33.6	1.92s
19	146.3	-	146.4	-

20	108.8	4.60brs 4.80brs	108.7	4.60brs, 4.80brs
21	37.7	1.95m 2.35dm	37.8	1.96m 2.35m
22	25.2	1.48m 1.67m	25.0	1.47m 1.75m
23	50.7	1.43m	50.1	1.39m
24	15.1	0.86s	15.2	0.86s
25	19.8	0.99s	19.7	0.99s
26	26.6	1.70s	28.3	1.82s
OH	-	5.60brs	-	5.59brs

br=broad; s=singlet; d=doublet; dd=doublet of doublets; m=multiplet

High-resolution mass spectrometry indicated that **9** and **10** shared the $C_{26}H_{35}OBr_4Cl$ molecular formula (*m/z* 712.8889 $[M - H]^-$). Comparison of NMR spectral data for these two molecules indicated differences at C-16 and C-17 (Table 2.2), with the C-16 methine in callophycol B (**10**) being shifted downfield relative to **9** (δ 65.5 in **9** vs. δ 72.7 in **10**), and quaternary C-17 in **10** shifted upfield relative to **9** (δ 72.7 in **9** vs. δ 68.3 in **10**). This supported chlorination at C-16 and bromination at C-17 in **10**. As with **9**, the stereochemistry at C-16 was unassigned for **10**.

In the biosynthesis of callophycoic acids A-H (**1-8**) and callophycols A-B (**9-10**), carbon-carbon bond formation between the aromatic moiety and geranylgeranyl diphospate (GPP) likely occurs by electrophilic aromatic substitution, analogously to the pathway hypothesized for ten bromophycolides (diterpene-benzoate macrolides) previously isolated from *Callophycus serratus*.(Kubanek et al., 2006; Kubanek et al., 2005) Among the bromophycolides and currently presented metabolites, callophycols A-B (**9-10**) are exceptional in the lack of a benzoic acid-based aromatic moiety; the putative shikimate-based 2,4-dibromophenol group of **9-10** was likely introduced during the electrophilic aromatic substitution step of biosynthesis and indicates either a different

biosynthetic pathway for **9-10**, or, more likely, that the enzymes catalyzing this step are flexible in substrate acceptance.

Unlike the bromophycolides, in which electrophilic aromatic substitution was likely followed with esterification to yield 15- and 16-membered lactones, callophycoic acids A-H (**1-8**) maintained their carboxylic acid functional group. LC-MS analysis of the extract from which callophycoic acids A-H (**1-8**) and callophycols A-B (**9-10**) were isolated indicated no presence of bromophycolides, originally isolated from *Callophycus serratus* collected at a different Fijian site. Likewise, LC-MS analysis of the extract containing bromophycolides showed no indication of callophycoic acids or callophycols. This may suggest that different populations of this red alga possess different genotypes, only one of which produces the enzymes necessary for lactonization. Alternatively, environmental differences between the two collection sites may have resulted in production of different metabolites due to induction or related mechanisms. Another possibility is that specimens collected at these two sites actually represent different, closely-related species of red algae, which were morphologically indistinguishable in our hands.

Following electophilic aromatic substitution, the linear diterpene-benzoic acid (in **1-8**) or diterpene-phenol (in **9-10**) likely underwent a series of hydride shifts, addition, and elimination reactions, characteristic of isoprenoid biosynthesis (Herbert, 1989). These reactions resulted in halogenation at electrophilic sites expected for vanadium haloperoxidase-based biosynthetic enzymes previously implicated in terpenoid biosynthesis (Butler and Carter-Franklin, 2004). Callophycoic acid F (**6**) is a probable precursor of callophycoic acids A-E (**1-5**) (Scheme 2.1), while callophycoic acids G-H

(**7-8**) and callophycols A-B (**9-10**) are hypothesized to be formed by an alternative mode of cyclization (Scheme 2.2). The wide diversity of metabolites produced from diterpene-benzoic acid (in **1-8**) or diterpene-phenol (in **9-10**) precursors suggests either the involvement of a diverse array of enzymes or catalytic promiscuity in the enzymatic machinery that biosynthesizes these metabolites.

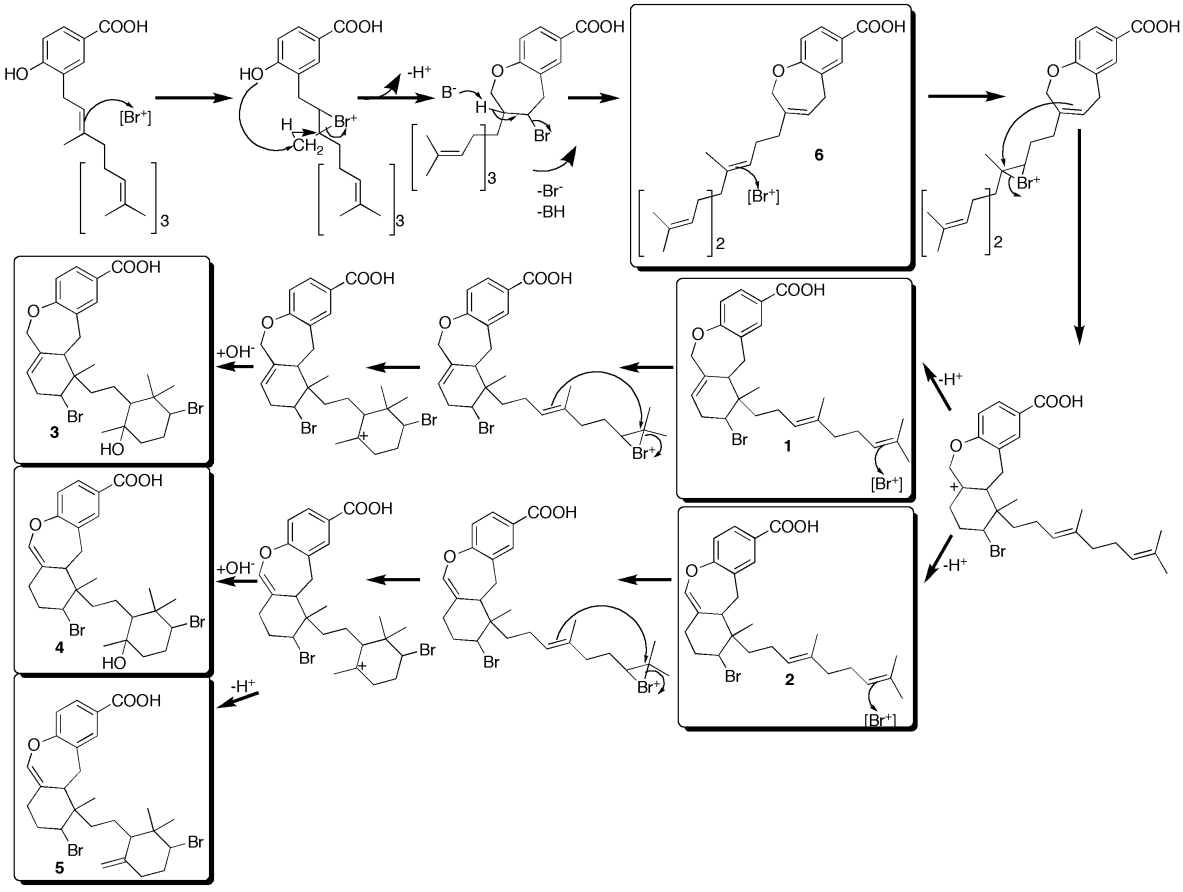

Scheme 2.1. Proposed biosynthesis of callophycoic acids A-F (1-6).

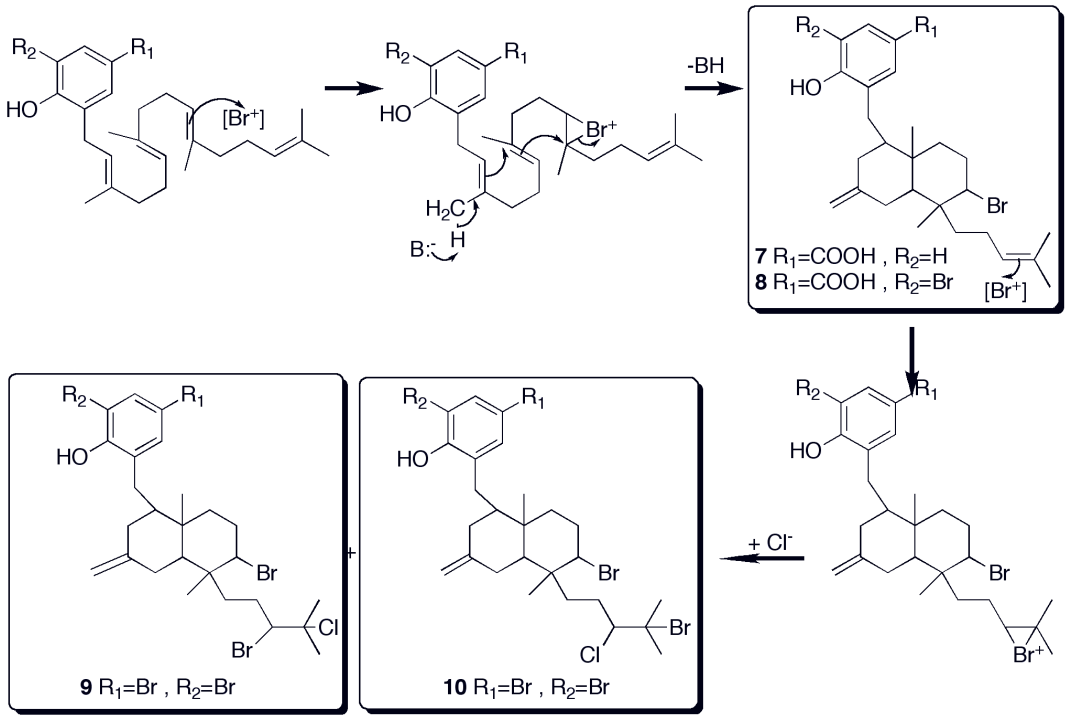

Scheme 2.2 Proposed biosynthesis of callophycoic acids G-H (7-8) and callophycols A-B (9-10).

In addition to the structural novelty of callophycoic acids A-H (**1**-**8**) and callophycols A-B (**9**-**10**), compounds in this group demonstrated modest antibacterial, antimalarial, and anticancer activities (Table 2.3). Antibacterial activity was species-

specific, with regioisomers **1-2** both inhibiting *Enterococcus faecium*, yet inactive against *Staphylococcus aereus.* In contrast, regioisomers **3-4** were more active against *S. aureus* than *E. faecium*.

Table 2.3 Pharmacological activities of callophycoic acids A-H (**1**-**8**) and callophycols A-B (**9**-**10**).

	antibacterial MIC (μM)			anticancer activity	
cmpd	*S. aureus*	*E. faecium*	Antitubercular	IC_{50} (μM)[a]	Antimalarial IC_{50} (μM)
1	>500	16.0	>100	24.5	41.0
2	>500	16.0	>100	24.4	51.5
3	53.6	>100	>100	20.6	58.6
4	26.7	>100	>100	23.2	76.1
5	>500	>100	>100	>25	96.2
6	>600	>100	>100	>25	27.0
7	31.9	63.9	>10	>25	>100
8	27.4	27.4	>50	>25	>100
9	>350	>350	NT	>25	35.7
10	>350	>350	>10	>25	40.4

[a]Mean of 11 cancer cell lines (see Experimental section for details); NT indicates not tested.

To our knowledge, the eight callophycoic acids (**1-8**) presented herein provide the first reports of macroalgal diterpene-benzoic acids, as this class of compounds was previously reported exclusively in terrestrial cyanobacteria (Jaki et al., 2000; Jaki et al., 1999; Prinsep et al., 1996). The two callophycols (**9-10**) represent an even more unique class of compounds, with no previous reports of halogenated diterpene phenols, to our knowledge. Considered together, the 20 bromophycolides, callophycoic acids, and callophycols more than quadruple the number of secondary metabolites previously isolated from members of the algal family Solieriaceae (Graber et al., 1996; Whitfield et al., 1999), and suggest evaluation of additional members of this group may provide further structurally novel bioactive compounds.

Materials and Methods

General Experimental Procedures. NMR spectra were recorded at 500 MHz and 125 MHz for ^{1}H and ^{13}C NMR, respectively, and referenced to residual $CHCl_3$ (7.24 and 77.0 ppm, for ^{1}H and ^{13}C, respectively) for **1-2** and **5-10** and to residual $(CH_3)_2CO$ (2.04 and 29.8 ppm, for ^{1}H and ^{13}C, respectively) for **3-4**.

Biological Material. *Callophycus serratus* (Harvey ex Kutzing 1957) (family Solieriaceae, order Gigartinales, class Rhodophyceae, phylum Rhodophyta) was collected at depths from 9-15 m near Harold's Passage, Astrolobe Reef, Kadavu Province, Fiji (18° 46' 37" S, 178° 27' 74" E). Material was identified by comparison with previously described morphological traits (Littler and M.M., 2003) and frozen at -20 °C until extraction. A voucher specimen is deposited at the University of the South Pacific.

Pharmacological Assays. Bioassay-guided fractionation was directed by a sublethal rotifer ingestion toxicity assay with the freshwater species *Brachionus calyciflorus*, as previously described (Kubanek et al., 2006; Snell, 2005). Isolated compounds were evaluated against a panel of tumor cell lines including breast, colon, lung, prostate, and ovarian cancer cells. Specific cell lines were: BT-549, DU4475, MDA-MD-468, NCI-H446, PC-3, SHP-77, LNCaP-FGC, HCT116, MDA-MB-231, A2780/DDP-S, and Du145. *In vitro* cytotoxicity was tested with the (3-(4,5-dimethylthiazol-2-yl)-5-(3-carboxylmethoxyphenyl)-2-(4-sulfophenyl)-2H-tetrazolium inner salt) MTS dye conversion assay as described previously (Lee et al., 2001). Antibacterial assays were

performed against *Staphylococcus aureus* (ATCC #10537) and *Enterococcus faecium* (ATCC #12952) as previously described (Kubanek et al., 2005). Antifungal assays were performed against *Candida albicans* as previously described (Kubanek et al., 2005).

Antitubercular activity was assessed against *Mycobacterium tuberculosis* strain $H_{37}Rv$ (ATCC 27294) using the alamar blue susceptibility test (MABA) as described previously (Collins and Franzblau, 1997). Compounds **1**-**6** were tested at a maximum concentration of 100 uM, **8** at a maximum concentration of 50 uM, and **7** and **10** at a maximum concentration of 10 uM. The MIC was reported as the lowest concentration of a serial dilution series resulting in ≥90% growth inhibition relative to controls. Antimalarial activity was determined with a SYBR Green based parasite proliferation assay, adapted from Smilkstein (Smilkstein et al., 2004) and Bennett (Bennett et al., 2004). Briefly, *Plasmodium falciparum* parasites (3D7 strain MR4/ATCC, Manassas,VA) were cultured in human O+ erythrocytes as previously described (Trager and Jensen, 1976). Compounds were diluted in complete medium and 40 µl transferred to 96-well assay plates. To this 80 µl of complete media with 3D7 infected erythrocytes were dispensed in order to obtain a 2.5% hematocrit and 0.5% parasitemia in the assay. Uninfected erythrocytes were dispensed into the background wells at the same final hematocrit. Plates were incubated for 72 hours in a low oxygen environment (96% N_2, 3% CO_2, 1% O_2) in a modular incubation chamber. The plates were sealed and placed in a -80^{o}C freezer overnight then thawed, and 120 µl of lysis buffer (20 mM Tris-HCl, pH 7.5, 5mM EDTA, 0.08% Triton X-100, 0.008% saponin with 0.2 µl/ml Sybr Green I) was dispensed into each well and incubated at 37^{o}C in the dark for 6 hours to achieve

maximum signal to noise ratio. The plates were read with a Molecular Devices SpectraMAX Gemini EM at ex: 495 nm, em: 525 nm with 515 nm cut-off.

Isolation. *Callophycus serratus* was exhaustively extracted with water, methanol, and methanol/dichloromethane (1:1 and 1:2). Extracts were combined, filtered, and concentrated *in vacuo*. This crude extract was partitioned between methanol/water (9:1) and petroleum ether. The aqueous fraction was adjusted to methanol/water (3:2) and partitioned against chloroform. This bioactive chloroform extract was fractionated into **1**-**10** by multiple rounds of C_{18} reversed-phase HPLC using gradients of methanol/water and acetonitrile/water with an Agilent Zorbax SB-C_{18} column, followed by normal-phase HPLC using a hexanes/ethyl acetate gradient with an Agilent Zorbax RX-SIL column.

Callophycoic acid A (1): clear crystalline solid (9.8 mg; 0.037% plant dry mass); $[\alpha]^{24}_{D}$ -115º (*c* 0.13 g/100 mL, MeOH); UV (MeOH) λ_{max} (log ε) 258 (3.70) nm; for ^{1}H and ^{13}C NMR data see Table 2.1; for COSY, HMBC, and NOE data, see the Appendix A; HR ESI-MS *m/z* 485.1697 $[M-H]^-$ (calcd for $C_{27}H_{34}O_3Br$, 485.1691).

Callophycoic acid B (2): white amorphous solid (12.0 mg; 0.046% plant dry mass); $[\alpha]^{24}_{D}$ +165º (*c* 0.071 g/100 mL, MeOH); UV (MeOH) λ_{max} (log ε) 260 (3.64) nm; for ^{1}H and ^{13}C NMR data see Table 2.1; for COSY, HMBC, and NOE data, see the Appendix A; HR ESI-MS *m/z* 485.1665 $[M-H]^-$ (calcd for $C_{27}H_{34}O_3Br$, 485.1691).

Callophycoic acid C (3): white amorphous solid (2.5 mg, 0.009% plant dry mass); $[\alpha]^{24}_{D}$ -49º (*c* 0.031 g/100 mL, MeOH); UV (MeOH) λ_{max} (log ε) 258 (4.03) nm; ^{1}H and ^{13}C NMR ($(CD_3)_2CO$, 500 MHz) data see Table 2.1; COSY, HMBC, and NOE data, see Appendix A; HR ESI-MS $[M - H]^-$ *m/z* 581.0895 (calcd for $C_{27}H_{35}O_4Br_2$, 581.0902).

Callophycoic acid D (4): white amorphous solid (1.6 mg, 0.006% plant dry mass); $[\alpha]^{24}_{D}$ +85º (*c* 0.018 g/100 mL, MeOH); UV (MeOH) λ_{max} (log ε) 258 (3.81) nm; ^{1}H and ^{13}C NMR ($(CD_3)_2CO$, 500 MHz) data see Table 2.1; COSY, HMBC, and NOE data, see Appendix A; HR ESI-MS $[M - H]^-$ *m/z* 581.0889 (calcd for $C_{27}H_{35}O_4Br_2$, 581.0902).

Callophycoic acid E (5): white amorphous solid (1.9 mg; 0.007% plant dry mass); $[\alpha]^{24}_{D}$ +117º (*c* 0.031 g/100 mL, MeOH); UV (MeOH) λ_{max} (log ε) 227 (3.70) nm; for ^{1}H and ^{13}C NMR data see Table 2.1; for COSY, HMBC, and NOE data, see the Appendix A; HRESIMS *m/z* 563.0807 $[M-H]^-$ (calcd for $C_{27}H_{33}O_3Br_2$, 563.0800).

Callophycoic acid F (6): white amorphous solid (6.0 mg; 0.023% plant dry mass); $[\alpha]^{24}_{D}$ 0º (*c* 0.034 g/100 mL, MeOH); UV (MeOH) λ_{max} (log ε) 246 (3.08) nm; for ^{1}H and ^{13}C NMR data see Table 2.1; for COSY, HMBC, and NOE data, see the Appendix A; HRESIMS *m/z* 407.2574 $[M-H]^-$ (calcd for $C_{27}H_{35}O_3$, 407.2586).

Callophycoic acid G (7): white amorphous solid (1.0 mg; 0.004% plant dry mass); $[\alpha]^{24}_{D}$ +137º (*c* 0.018 g/100 mL, MeOH); UV (MeOH) λ_{max} (log ε) 258 (3.88) nm; for ^{1}H and ^{13}C NMR data see Table 2.1; for COSY, HMBC, and NOE data, see the Appendix A; HRESIMS *m/z* 487.1823 $[M-H]^-$ (calcd for $C_{27}H_{36}O_3Br$, 487.1853).

Callophycoic acid H (8): white amorphous solid (2.4 mg; 0.009% plant dry mass); $[\alpha]^{24}_{D}$ +99º (*c* 0.024 g/100 mL, MeOH); UV (MeOH) λ_{max} (log ε) 258 (3.72) nm; for ^{1}H and ^{13}C NMR data see Table 2.1; for COSY, HMBC, and NOE data, see the Appendix A; HRESIMS *m/z* 565.0968 $[M-H]^-$ (calcd for $C_{27}H_{35}O_3Br_2$, 565.0958).

Callophycol A (9): white amorphous solid (2.5 mg; 0.009% plant dry mass); $[\alpha]^{24}_{D}$ +75º (*c* 0.029 g/100 mL, MeOH); UV (MeOH) λ_{max} (log ε) 229 (4.11) nm; for ^{1}H and ^{13}C

NMR data see Table 2.2; for COSY, HMBC, and NOE data, see the Appendix A; HRESIMS *m/z* 712.9066 $[M-H]^-$ (calcd for $C_{26}H_{34}OBr_4Cl$, 712.9032).

Callophycol B (10): white amorphous solid (2.2 mg; 0.008% plant dry mass); $[\alpha]^{24}_D$ +110º (*c* 0.018 g/100 mL, MeOH); UV (MeOH) λ_{max} (log ε) 229 (4.04) nm; for ^1H and ^{13}C NMR data see Table 2.2; for COSY, HMBC, and NOE data, see the Appendix A; HRESIMS *m/z* 712.8889 $[M-H]^-$ (calcd for $C_{26}H_{34}OBr_4Cl$, 712.9032)

Works Cited

Bennett, T. N., Paguio, M., Gligorijevic, B., Seudieu, C., Kosar, A. D., Davidson, E., and Roepe, P. D. (2004). Novel, rapid, and inexpensive cell-based quantification of antimalarial drug efficacy. Antimicrobial Agents and Chemotherapy *48*, 1807-1810.

Blunt, J. W., Copp, B. R., Munro, M. H. G., Northcote, P. T., and Prinsep, M. R. (2005). Marine natural products. Natural Product Reports *22*, 15-61.

Butler, A., and Carter-Franklin, J. N. (2004). The role of vanadium bromoperoxidase in the biosynthesis of halogenated marine natural products. Natural Product Reports *21*, 180-188.

Cavin, A. L., Hay, A. E., Marston, A., Stoeckli-Evans, H., Scopelliti, R., Diallo, D., and Hostettmann, K. (2006). Bioactive diterpenes from the fruits of Detarium microcarpum. Journal of Natural Products *69*, 768-773.

Collins, L. A., and Franzblau, S. G. (1997). Microplate Alamar blue assay versus BACTEC 460 system for high-throughput screening of compounds against Mycobacterium tuberculosis and Mycobacterium avium. Antimicrobial Agents and Chemotherapy *41*, 1004-1009.

Graber, M. A., Gerwick, W. H., and Cheney, D. P. (1996). The isolation and characterization of agardhilactone, a novel oxylipin from the marine red alga Agardhiella subulata. Tetrahedron Letters *37*, 4635-4638.

Herbert, R. B., ed. (1989). The Biosynthesis of Secondary Metabolites, 2nd edn (London: Chapman & Hall).

Ito, H., Onoue, S., Miyake, Y., and Yoshida, T. (1999). Iridal-type triterpenoids with ichthyotoxic activity from Belamcanda chinensis. Journal of Natural Products *62*, 89-93.

Jaki, B., Heilmann, J., and Sticher, O. (2000). New antibacterial metabolites from the cyanobacterium Nostoc commune (EAWAG 122b). Journal of Natural Products *63*, 1283-1285.

Jaki, B., Orjala, J., and Sticher, O. (1999). A novel extracellular diterpenoid with antibacterial activity from the cyanobacterium Nostoc commune. Journal of Natural Products *62*, 502-503.

Kubanek, J., Prusak, A. C., Snell, T. W., Giese, R. A., Fairchild, C. R., Aalbersberg, W., and Hay, M. E. (2006). Bromophycolides C-I from the Fijian red alga Callophycus serratus. Journal of Natural Products *69*, 731-735.

Kubanek, J., Prusak, A. C., Snell, T. W., Giese, R. A., Hardcastle, K. I., Fairchild, C. R., Aalbersberg, W., Raventos-Suarez, C., and Hay, M. E. (2005). Antineoplastic diterpene-benzoate macrolides from the Fijian red alga Callophycus serratus. Organic Letters *7*, 5261-5264.

Kuniyoshi, M., Marma, M. S., Higa, T., Bernardinelli, G., and Jefford, C. W. (2001). New bromoterpenes from the red alga Laurencia luzonensis. Journal of Natural Products *64*, 696-700.

Lee, F. Y. F., Borzilleri, R., Fairchild, C. R., Kim, S. H., Long, B. H., Reventos-Suarez, C., Vite, G. D., Rose, W. C., and Kramer, R. A. (2001). BMS-247550: A novel epothilone analog with a mode of action similar to paclitaxel but possessing superior antitumor efficacy. Clinical Cancer Research *7*, 1429-1437.

Littler, D. S., and Littler, M.M. (2003). South Pacific Reef Plants (Washington, D.C.: Offshore Graphics, Inc.).

Maloney, D. J., and Hecht, S. M. (2005). A stereocontrolled synthesis of delta-trans-tocotrienoloic acid. Organic Letters *7*, 4297-4300.

Prinsep, M. R., Thomson, R. A., West, M. L., and Wylie, B. L. (1996). Tolypodiol, an antiinflammatory diterpenoid from the cyanobacterium Tolypothrix nodosa. Journal of Natural Products *59*, 786-788.

Shin, T. S., and Godber, J. S. (1994). Isolation of 4 Tocopherols and 4 Tocotrienols from a Variety of Natural Sources by Semipreparative Highperformance Liquid-Chromatography. Journal of Chromatography A *678*, 49-58.

Silverstein, R. M., and Webster, F. X. (1998). Spectrometric Identification of Organic Compounds, 6 edn (New York: John Wiley & Sons, Inc.).

Smilkstein, M., Sriwilaijaroen, N., Kelly, J. X., Wilairat, P., and Riscoe, M. (2004). Simple and inexpensive fluorescence-based technique for high-throughput antimalarial drug screening. Antimicrobial Agents and Chemotherapy *48*, 1803-1806.

Snell, T. W. (2005). In Small-Scale Freshwater Environment Toxicity Test Methods, C. Blaise, and J. F. Ferard, eds. (Dordrecht: Kluwer).

Suzuki, M., Matsuo, Y., Takeda, S., and Suzuki, T. (1993). Intricatetraol, a Halogenated Triterpene Alcohol from the Red Alga Laurencia-Intricata. Phytochemistry *33*, 651-656.
Trager, W., and Jensen, J. B. (1976). Human Malaria Parasites in Continuous Culture. Science *193*, 673-675.

West, L. M., and Faulkner, D. J. (2006). Hexaprenoid hydroquinones from the sponge Haliclona (aka Adocia) sp. Journal of Natural Products *69*, 1001-1004.

Whitfield, F. B., Helidoniotis, F., Shaw, K. J., and Svoronos, D. (1999). Distribution of bromophenols in species of marine algae from eastern Australia. Journal of Agricultural and Food Chemistry *47*, 2367-2373.

Wright, A. D., Konig, G. M., Sticher, O., and Denys, R. (1991). Five New Monoterpenes from the Marine Red Alga Portieria-Hornemannii. Tetrahedron *47*, 5717-5724.

CHAPTER 3

ANTIMALARIAL NATURAL PRODUCTS FROM THE FIJIAN RED ALGA *CALLOPHYCUS SERRATUS*

Abstract

Bromophycolides J-L (**1-3**) were isolated from extracts of the Fijian red alga *Callophycus serratus* and identified with 1D and 2D NMR spectroscopy and mass spectral analyses. These diterpene-benzoate macrolides represent two novel carbon skeletons and add to ten previously reported bromophycolides (**4-13**) from this alga. Among these 13 bromophycolides, several exhibited activities in the low micromolar range against the malaria parasite *Plasmodium falciparum*.

Introduction

Over 500 million cases of malaria are reported annually, causing one- to three-million deaths worldwide (Snow et al., 2005). Although several antimalarial drugs are currently on the market, resistance to these treatments is on the rise, indicating the urgent need for novel antibiotics (Hyde, 2007). As a recognized source of pharmacologically-active natural products (Blunt et al., 2008; Faulkner, 2000), marine organisms such as macroalgae may offer treatments for malaria and other infectious diseases.

From the red alga *Callophycus serratus*, we previously reported the discovery of 10 bromophycolides, unusual C_{27} diterpene-benzoate macrolides (Kubanek et al., 2006; Kubanek et al., 2005). Exploration of additional *C. serratus* collections then led to discovery of 10 novel callophycoic acids and callophycols, C_{27} diterpene-benzoic acids

and C_{26} diterpene-phenols (Lane et al., 2007). Herein, we report identification of three additional macrolides, bromophycolides J-L (**1**-**3**), representing two novel carbon skeletons as well as one regioisomer of a known bromophycolide, and adding further evidence that this red alga is an abundant source of chemically diverse and biologically active natural products.

Results and Discussion

Following the isolation and identification of ten bromophycolides from *Callophycus serratus* in 2005 (Kubanek et al., 2006; Kubanek et al., 2005), LC-MS evaluation of extracts from a Fijian collection of this red macroalga suggested the presence of over ten as-yet unidentified bromophycolide-like metabolites. Reversed- and normal-phase HPLC yielded three of these unknown metabolites, bromophycolides J-L (**1**-**3**), in quantities sufficient for structure elucidation.

A molecular formula of $C_{28}H_{40}O_5Br_2$ was established for bromophycolide J (**1**), based on a mass spectral parent ion at *m/z* 613.1160, supported by a dibrominated isotopic splitting pattern. Inspection of ^{1}H, ^{13}C, HSQC, HMBC, and COSY NMR spectral data for **1** revealed an aryl group common to all bromophycolides (Table 3.1, Appendix B) (Kubanek et al., 2006; Kubanek et al., 2005). Comparison of spectral data for **1** with bromophycolide A (**4**) supported a bromine-substituted isopropyl group at the diterpene head and established diterpene-aryl connectivity identical to that of **4** (Kubanek et al., 2005).

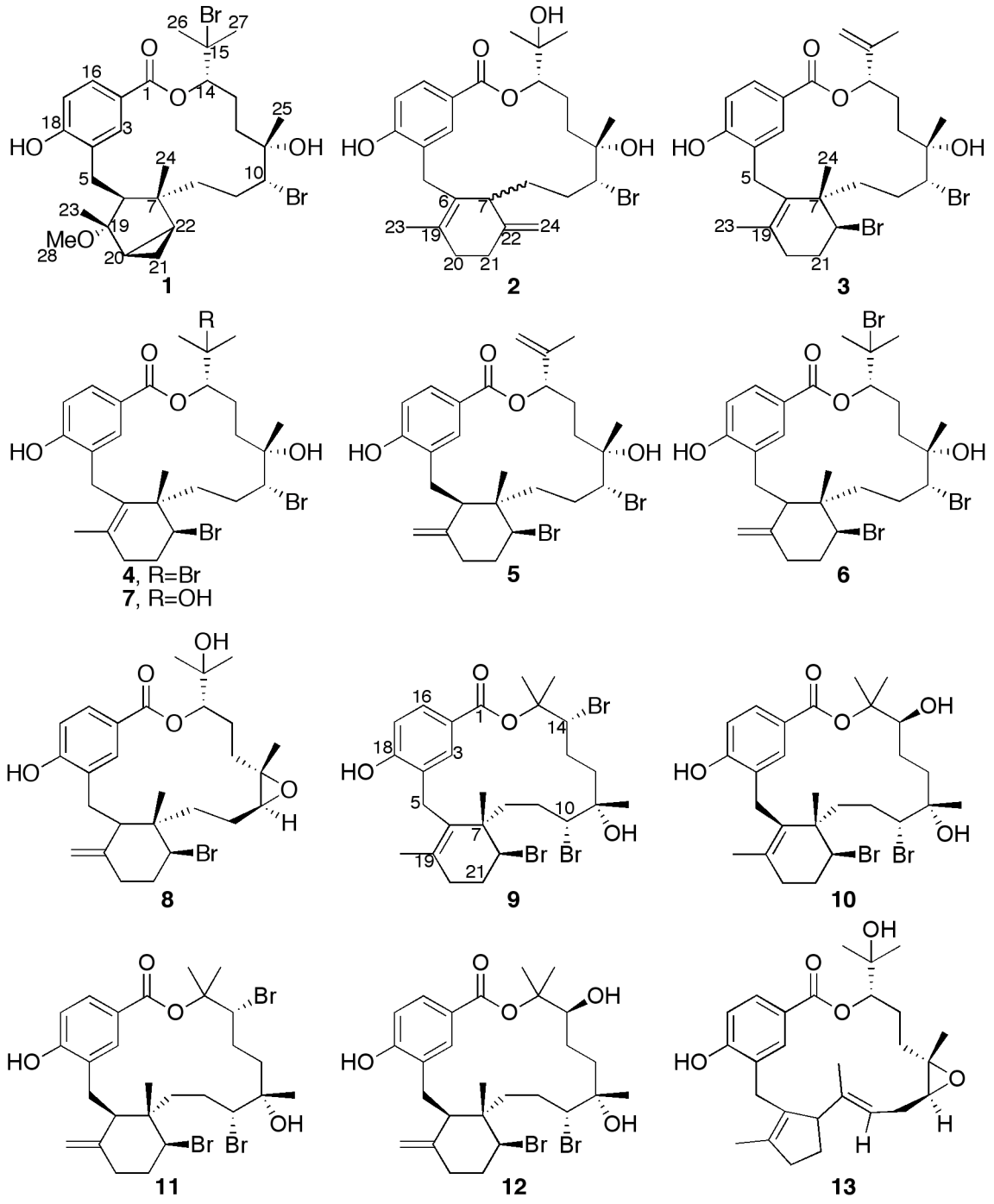

Novel bromphycolides J-L (**1**-**3**) and previously reported bromophycolides A-I and debromophycolide A (**4**-**13**) from *Callophycus serratus*.

Further comparison of NMR spectral data for **1** and **4** revealed substantive differences between these two natural products only in the vicinity of the carbocyclic terpene ring (Kubanek et al., 2005). For **1**, HMBC correlations from Me-23 (δ 1.38) to C-6 (δ 45.5), C-19 (δ 89.8), and C-20 (δ 28.0) established C-6—C-19—C-20 connectivity. Methoxy Me-28 (δ 3.33) also showed an HMBC correlation to C-19, establishing quaternary C-19 as the site of attachment for OMe-28 and Me-23. Observation of HMBC correlations from Me-24 (δ 0.55) to C-6, C-7 (δ 45.8), and C-22 (δ 31.9) established connectivity between these carbons. COSY correlations between H-22 (δ 1.14) and both H-21 protons (δ 0.31, δ 0.42), between H-20 (δ 1.55) and both H-21 protons, and between H-22 and H-20, as well as shielded chemical shifts observed for methylene C-21 (δ 8.5) prompted assignment of a cyclopropyl moiety comprised of C-20, C-21, and C-22, thus establishing a bicyclo(3.1.0) group. HMBC and COSY correlations established connection between this ring system and the benzoate system via C-5, analogous to previously identified metabolites (Kubanek et al., 2006; Kubanek et al., 2005). With a bicyclo(3.1.0) group, **1** provided a carbon skeleton distinct from known *C. serratus* metabolites and novel among synthetic and natural products.

The eight stereocenters within **1** were assigned starting by comparison of ^{1}H-^{1}H scalar couplings and NOE correlations with **4** (Kubanek et al., 2005). Observation of predicted scalar couplings and NOE correlations for **1** prompted assignment of 10*R*, 11*S,* 14*S* stereochemistry as for **4**. Given these identical configurations, it seemed reasonable that C-7 would also be shared, suggesting a 7*R* stereocenter for **1**. Further, the relatively upfield ^{1}H chemical shift observed for Me-24 (δ 0.55) of **1** supported an axial orientation of this group, analogous to **4**. NOE correlations between Me-24 and Me-23 (δ 1.38), not

seen for Me-24 and OMe-28 (δ 3.33), next established an axial orientation for Me-23 and prompted assignment of a 19*S* stereocenter. Observation of an NOE correlation between H-21a (δ 0.31) and Me-23, but not between H-20 (δ 1.55) or H-22 (δ 1.14) and either Me-23 or Me-24, supported assignment of cyclopropyl group C-21 in an axial up position and established 20*R* and 22*S* absolute configurations. Finally, NOE correlations between H-6 (δ 2.59) and H-20 as well as between H-6 and OMe-28, but not between H-6 and either Me-23 or Me-24, established a 6*S* stereocenter. This assignment matched absolute configurations reported for all bromophycolides bearing a stereocenter at this site (e.g., bromophycolide E (**5**)).

The molecular formula of bromophycolide K (**2**) was assigned as $C_{27}H_{37}O_5Br$ from the parent ion observed at *m/z* 519.1767 ([M - H]$^-$). Comparison of ^{1}H, ^{13}C, HSQC, HMBC, and COSY NMR data with known bromophycolides confirmed a 15-membered macrolide framework analogous to **4** (Appendix B) (Kubanek et al., 2006; Kubanek et al., 2005). For **2**, a hydroxy substituent was assigned at C-15 (δ 72.1) on the basis of ^{13}C NMR chemical shift precedents (Kubanek et al., 2006; Kubanek et al., 2005). As with **1**, HMBC and COSY correlations suggested that **2** diverged from other bromophycolides within the cyclohexenyl moiety. Within this group, observation of HMBC correlations from Me-23 (δ 1.91) to C-6 (δ 138.6), C-19 (δ 132.7), and C-20 (δ 36.7) and from H-5a (δ 3.29) to C-7 (δ 50.6) established the tetrasubstituted olefin. COSY correlations from both H-20 protons (δ 2.24, δ 2.37) to both H-21 protons (δ 1.95, δ 2.17) and HMBC correlations from both H-24 protons to C-7 and C-21 (δ 36.0) closed the six-membered ring containing exo- and endocyclic double bonds.

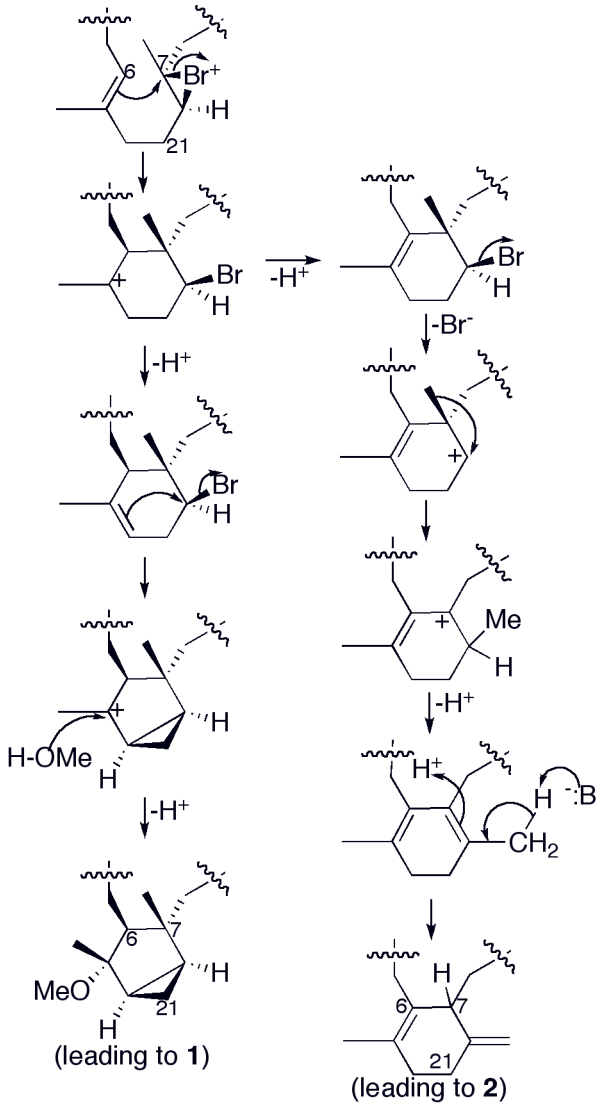

Scheme 3.1 Proposed biosynthesis of diterpene carbocyclic groups within bromophycolides J-K (**1**-**2**). Following carbocation formation, pathways for **1**-**2** diverge from those proposed for previously reported bromophycolides.(Kubanek et al., 2005) ($B:^-$ indicates base.)

Bromophycolide K (**2**) represents another novel carbon skeleton, differing from known bromophycolide structural motifs by a proposed biosynthetic 1,2-methide shift (Scheme 3.1), ultimately resulting in the exo-methylene group at C-24. Both methide and hydride shifts are common in terpene biosynthesis (Herbert, 1989); however, **2** represents

the first bromophycolide exhibiting a rearranged skeleton. The rearranged carbon skeleton observed in the cyclohexenyl group of **2** and the lack of stereocenters near this group prevented stereochemical assignment at C-7.

Bromophycolide L (**3**) exhibited a molecular formula of $C_{27}H_{36}O_4Br_2$ ($[M - H]^-$ *m*/*z* 581.0906), isomeric to known bromophycolide E (**5**) (Kubanek et al., 2006). A combination of 1D and 2D NMR spectral data for **3** supported assignment of a carbon skeleton and most functionalities identical to that of **5**. For **3**, HMBC correlations from Me-23 (δ 1.41) to fully substituted olefinic carbons C-6 (δ 130.8) and C-19 (δ 132.6) as well as to C-20 (δ 32.4) suggested regioisomerization of the exo-methylene group observed for **5**. Finally, 7*S*, 10*R*, 11*S*, 14*S* stereochemistry was proposed for **3**, based on comparison of NOE correlations with **4** and **5** (Appendix B).

Together, bromophycolides J-L (**1**-**3**) represent two novel carbon skeletons plus one regioisomer of previously reported bromophycolide E (**5**). Among 23 known natural products from *C. serratus* (Kubanek et al., 2006; Kubanek et al., 2005; Lane et al., 2007), bromophycolide J (**1**) is unique as the only methoxy-substituted metabolite as well as the only bromophycolide bearing a bicyclo(3.1.0) group. All of these structural features, including stereochemistry, may be accounted for with biosynthetic mechanisms that incorporate the same bromonium intermediate previously suggested for five- and six-membered ring cyclizations in bromophycolides (Scheme 3.1) (Kubanek et al., 2005). A pathway encompassing a bromonium intermediate and including a proposed methide shift is also plausible in biosynthesis of bromophycolide K (**2**), the only known bromophycolide with a rearranged carbon skeleton (Scheme 3.1). The structural novelty

observed among the diterpene carbocyclic rings within these 23 natural products suggests a high biosynthetic flexibility within this group.

Table 3.1 ^{13}C and ^{1}H NMR spectral data for bromophycolides J-L (**1-3**) (500 MHz; in $CDCl_3$).

	1		**2**		**3**	
No.	δ ^{13}C	δ ^{1}H ($J_{H,H}$)	δ ^{13}C	δ ^{1}H ($J_{H,H}$)	δ ^{13}C	δ ^{1}H ($J_{H,H}$)
1	165.6	-	167.6	-	165.3	-
2	121.2	-	122.8	-	122.5	-
3	130.1	8.11 brs	133.3	7.67 d (1.7)	130.6	7.85 brs
4	128.3	-	125.4	-	126.4	-
5	27.1	2.37 d (15.5) 2.69 m	29.4	3.29 d (14.9) 3.64 d (15.0)	28.5	3.24 d (8.8) 3.57 d (17.7)
6	45.5	2.59 m	138.6	-	130.8	-
7	45.8	-	50.6	2.62 d (8.7)	43.4	-
8	42.7	1.21 m 2.62 m	30.0	1.45 m 1.98 m	37.6	1.58 m 1.92 m
9	31.3	1.37 m 1.75 m	31.9	1.44 m 2.20 m	28.8	1.93 m 2.07 m
10	70.5	3.99 d (10.9)	72.0	3.96 m	71.5	3.82 d (8.8)
11	72.5	-	73.3	-	73.4	-
12	35.4	1.50 m 1.58 m	32.6	1.24 m 1.46 m	33.3	1.52 m 1.77 m
13	26.4	2.11 m 2.65 m	23.6	1.83 m 1.94 m	28.6	1.79 m 1.83 m
14	80.5	4.88 d (10.3)	81.5	4.97 dd (2.7, 11.6)	76.3	5.36 d (6.8)
15	66.2	-	72.1	-	142.6	-
16	129.6	7.81 d (8.0)	129.5	7.74 dd (1.8, 8.4)	129.7	7.82 d (8.3)

17	115.5	6.78 d (8.2)	115.9	6.81 d (8.4)	115.2	6.80 d (8.3)
18	157.8	-	159.1	-	157.5	-
19	89.8	-	132.7	-	132.6	-
20	28.0	1.55 m	36.7	2.24 m 2.37 m	32.4	2.13 m 2.26 m
21	8.5	0.31 m 0.42 dd (5.8, 10.0)	36.0	1.95 m 2.17 m	29.9	2.25 m 2.36 m
22	31.9	1.14 m	150.3	-	61.3	4.49 dm
23	19.8	1.38 s	14.1	1.91 s	20.8	1.41 s
24	20.0	0.55 s	108.6	4.46 s 4.66 s	26.0	1.27 s
25	29.0	1.17 s	26.1	1.26 s	30.2	1.26 s
26	31.2	1.80 s	25.6	1.31 s	111.3	4.92 s 4.99 s
27	30.5	1.78 s	26.8	1.31 s	19.2	1.80 s
28	49.9	3.33 s	-	-	-	-
OH	-	6.05 brs	-	5.48 brs	-	5.49 brs

br=broad; s=singlet; d=doublet; dd=doublet of doublets; m=multiplet

Bromophycolides J and L (**1**, **3**) exhibited moderate antibacterial activity against methicillin-resistant *Staphylococcus aureus* (MRSA) and vancomycin-resistant *Enterococcus faecium* (VREF, Table 3.2). More notably, these novel compounds exhibited low micromolar activities against the malaria parasite, *Plasmodium falciparum*, prompting evaluation of antimalarial activities for previously reported bromophycolides A-I and debromophycolide A (**4-13**, Table 3.3). Select bromophycolides possessing both 15- and 16-membered lactone frameworks exhibited potent antimalarial activity, suggesting neither mode of lactonization confers an inherent bioactivity advantage. Furthermore, the macrocycle appears to be essential for activity, seeing as callophycoic

acids and callophycols which lack the macrocycle have a significant decrease in antimalarial activity.

Table 3.2 Antibacterial and anticancer activities of novel bromophycolides J-L (**1**-**3**).

	antibacterial activity			anticancer activity
Cmpd	MRSA IC_{50} (μM)	VREF IC_{50} (μM)	Antitubercular MIC (μM)	IC_{50} (μM)[a]
1	80	66	94	10.3
2	NT	NT	NT	30.6
3	6.7	21	>100	3.1

[a]Mean of 11 cancer cell lines (see Experimental section for details); NT indicates not tested. [b]Using amphotericin B-resistant *Candida albicans*.

Table 3.3 Antimalarial activities of novel (**1**-**3**) and previously reported (**4**-**13**) bromophycolides.

Cmpd	Antimalarial IC_{50} (μM)
1	2.7
2	44
3	0.5
4	0.9
5	10.7
6	0.3
7	55.7
8	18.2
9	4.8
10	13.7
11	0.9
12	2.5
13	>100

Materials and Methods

General experimental procedures. Optical rotation data were collected with a Jasco P-1010 spectropolarimeter, and UV spectra recorded in MeOH using a Spectronic 21D

spectrophotometer. NMR spectra were acquired with a Bruker DRX-500 spectrometer, using a 5 mm broadband probe for ^{1}H, ^{13}C, HSQC, and DEPT-135 NMR experiments and a 5 mm inverse probe for HSQC, HMBC, COSY, and ROESY experiments. All NMR spectra were collected in $CDCl_3$ and referenced to residual $CHCl_3$ (δ 7.24 and 77.0 ppm for ^{1}H and ^{13}C, respectively). High-resolution mass spectral data were acquired using electrospray ionization (ESI) with an Applied Biosystems QSTAR-XL hybrid quadrupole-time-of-flight tandem mass spectrometer and Analyst QS software. LC-MS analyses were completed with a Waters 2695 pump and Alltech Alltima C_{18} reversed-phase column (3 μm, 2.1 × 150 mm) interfaced to a Waters 2996 diode-array UV detector and a Micromass ZQ 2000 ESI mass spectrometer. Semipreparative HPLC was performed using a Waters 1525 or 515 pump with a Waters 2996 diode-array or Waters 2787 dual-wavelength detector. Bromophycolides J-L (**1-3**) were purified using Agilent Zorbax SB-C18 and RX-SIL columns (5 μm, 9.4 × 250 mm). HPLC and Optima grade solvents were used in HPLC and LC-MS experiments, respectively (Fisher Scientific). NMR solvents were obtained from Cambridge Isotope Laboratories.

Biological material. *Callophycus serratus* (Harvey ex Kutzing 1957) (family Solieriaceae, order Gigartinales, class Rhodophyceae, phylum Rhodophyta) was collected from Yanuca in the Fiji Islands (18° 23' 57" S, 177° 57' 59" E). Samples were frozen at – 20° C until extraction. Voucher specimens were identified by comparison with previously described morophological traits,(Littler and M.M., 2003) preserved in aqueous formalin, and deposited at the University of the South Pacific in Suva, Fiji.

Isolation. *Callophycus serratus* was extracted successively with water, methanol, and methanol/dichloromethane (1:1 and 1:2). Extracts were combined, reduced *in vacuo*, and subjected to solvent partitioning between methanol/water (9:1) and petroleum ether. The methanol/water ratio of the aqueous fraction was then adjusted to 6:4 and this fraction partitioned against chloroform. The chloroform fraction was subjected to multiple rounds of reversed-phase C_{18} HPLC with a gradient of acetonitrile/water and methanol/water mobile phases, followed by normal phase silica HPLC with isocratic hexanes/ethyl acetate to yield bromophycolides J-L (**1**-**3**).

Bromophycolide J (1): white amorphous solid (1.0 mg; 0.023 % plant dry mass); $[\alpha]^{23}_{D}$ +35 (*c* 0.057 g/100 mL, MeOH); UV (MeOH) λ_{max} (log ε) 265 (3.78) nm; ^{1}H NMR ($CDCl_3$, 500 MHz) and ^{13}C/DEPT NMR ($CDCl_3$, 125 MHz) data, Table 3.1; NOE, COSY, HMBC NMR data, Appendix B; HRESIMS $[M - H]^-$ *m/z* 613.1160 (calcd for $C_{28}H_{39}O_5Br_2$, 613.1164).

Bromophycolide K (2): white amorphous solid (0.8 mg; 0.018 % plant dry mass); $[\alpha]^{23}_{D}$ +22 (*c* 0.046 g/100 mL, MeOH); UV (MeOH) λ_{max} (log ε) 264 (3.54) nm; ^{1}H NMR ($CDCl_3$, 500 MHz) and ^{13}C/DEPT NMR ($CDCl_3$, 125 MHz) data, Table 3.1; NOE, COSY, HMBC NMR data, Appendix B; HRESIMS $[M - H]^-$ *m/z* 519.1767 (calcd for $C_{27}H_{36}O_5Br$, 519.1746).

Bromophycolide L (3): white amorphous solid (1.8 mg; 0.041 % plant dry mass); $[\alpha]^{23}_{D}$ +68 (*c* 0.10 g/100 mL, MeOH); UV (MeOH) λ_{max} (log ε) 262 (3.66) nm; ^{1}H NMR ($CDCl_3$, 500 MHz) and ^{13}C/DEPT NMR ($CDCl_3$, 125 MHz) data, Table 3.1; NOE,

COSY, HMBC NMR data, Appendix B; HRESIMS $[M - H]^-$ *m/z* 581.0906 (calcd for $C_{27}H_{35}O_4Br_2$, 581.0902).

Works Cited

Blunt, J. W., Copp, B. R., Hu, W. P., Munro, M. H. G., Northcote, P. T., and Prinsep, M. R. (2008). Marine natural products. Natural Product Reports *25*, 35-94.

Faulkner, D. J. (2000). Highlights of marine natural products chemistry (1972-1999). Natural Product Reports *17*, 1-6.

Herbert, R. B., ed. (1989). The Biosynthesis of Secondary Metabolites, 2nd edn (London: Chapman & Hall).

Hyde, J. E. (2007). Drug-resistant malaria - an insight. Febs Journal *274*, 4688-4698.

Kubanek, J., Prusak, A. C., Snell, T. W., Giese, R. A., Fairchild, C. R., Aalbersberg, W., and Hay, M. E. (2006). Bromophycolides C-I from the Fijian red alga Callophycus serratus. Journal of Natural Products *69*, 731-735.

Kubanek, J., Prusak, A. C., Snell, T. W., Giese, R. A., Hardcastle, K. I., Fairchild, C. R., Aalbersberg, W., Raventos-Suarez, C., and Hay, M. E. (2005). Antineoplastic diterpene-benzoate macrolides from the Fijian red alga Callophycus serratus. Organic Letters *7*, 5261-5264.

Lane, A. L., Stout, E. P., Hay, M. E., Prusak, A. C., Hardcastle, K., Fairchild, C. R., Franzblau, S. G., Le Roch, K., Prudhomme, J., Aalbersberg, W., and Kubanek, J. (2007). Callophycoic acids and callophycols from the Fijian red alga *Callophycus serratus*. Journal of Organic Chemistry *72*, 7343-7351.

Littler, D. S., and Littler, M.M. (2003). South Pacific Reef Plants (Washington, D.C.: Offshore Graphics, Inc.).

Snow, R. W., Guerra, C. A., Noor, A. M., Myint, H. Y., and Hay, S. I. (2005). The global distribution of clinical episodes of *Plasmodium falciparum* malaria. Nature *434*, 214-217.

CHAPTER 4

SECONDARY METABOLITE DEFENSES AGAINST PATHOGENS AND BIOFOULERS

Introduction

Competition for space and resources is intense in benthic marine environments (McClintock and Baker 2001). In these habitats, macroalgae constitute a seemingly ideal substrate for growth of microorganisms and other epibionts, presenting these organisms with a living space rich in organic material. Some associations between macroalgae and microbes are mutualistic, benefiting both host and symbiont. For example, algal-associated bacteria may produce metabolites that protect hosts from biofouling (e.g., Boyd et al. 1999; Armstrong et al. 2001), and recent reports have indicated that epibiotic hydroids may enhance growth of the kelp *Macrocystis pyrifera* (Hepburn and Hurd 2005). Other algal associates are clearly detrimental to hosts, as evidenced by reports of algal disease and fouling-associated fitness costs (e.g., D'Antonio 1985; Correa 1997; Ruesink 1998). Red spot disease in the commercially valuable kelp *Laminaria japonica* (Sawabe et al. 1998) is caused by *Pseudoalteromonas bacteriolytica* bacteria; likewise, white rot disease in the kelp *Nereocystis luetkeana* is caused by an *Acinetobacter* sp. bacterium (Andrews 1977). Some bacteria act as secondary pathogens, accelerating disease progression following attack of a primary pathogen (Correa et al. 1994). Fungi can also act as seaweed pathogens, including *Lindra thallasiae*, an Ascomycete, which causes raisin disease in *Sargassum* spp. brown algae and *Thalassia* disease in seagrasses (Kohlmeyer 1971; Andrews 1976; Porter 1986). In addition to bacterial and fungal pathogens, some species of endophytic multicellular algae, cyanobacteria, and amoebae

have been implicated as causes of disease in macroalgae (Andrews 1977; Correa et al. 1993; Correa and Flores 1995).

In addition to pathogens, micro- and macrofoulers negatively impact a variety of macroalgal hosts. Biofouling by the diatom *Isthmia nervosa* is related to declines in growth and reproduction for the red alga *Odonthalia floccose* (Ruesink 1998). Biofoulers may indirectly reduce algal fitness by increasing drag and susceptibility to tissue breakage in turbulent water and by increasing herbivore attraction (Dixon et al. 1981; D'Antonio 1985; Wahl and Hay 1995).

Although pathogens and biofoulers both negatively influence host fitness, there are fundamental differences between these two algal colonizers. Specifically, pathogens must exhibit virulence against hosts while such pathogenesis is absent in biofouling. Chemical defenses against both biofoulers and pathogens are included in this chapter, because each involve relatively long-term intimate associations with host algae, both benefit from association with hosts, and both pose negative fitness effects on hosts.

Despite some reports of algal disease and the seemingly favorable conditions that hosts provide for pathogens and biofoulers, reports of widespread algal destruction remain surprisingly uncommon. This suggests that macroalgae have evolved mechanisms to resist deleterious microorganisms. One strategy is to disrupt colonization or growth of parasites with physical defenses, including production of a mucilaginous covering, outer cell layer shedding, and erosion of the distal ends of blades to remove parasites from macralgal surfaces (Mann 1973; Filion-Myklebust and Norton 1981; Moss 1982; Nylund and Pavia 2005). Algae may also prevent colonization of their tissues through oxidative burst, in which algae respond to microbial challenge through the

release of reactive oxygen species, or by other rapidly activated responses. Another resistance mechanism is the use of secondary metabolites as chemical defenses (e.g., Boyd et al. 1999; Wikstrom and Pavia 2004; Engel et al. 2006; Puglisi et al. 2006). As pathogens and foulers first select, settle, and attach to hosts, algae may prevent tissue damage by harboring secondary metabolites that circumvent this stage. Following parasite attachment, secondary metabolites may inhibit the growth, survival, virulence, or reproduction of these organisms.

Antimicrobial and antifouling chemical defenses have been reviewed previously for macroalgae, marine invertebrates, and other marine organisms (Engel et al. 2002; Steinberg and de Nys 2002; Paul and Puglisi 2004; Dobretsov et al. 2006). Thus, we do not aim to cover the breadth of this area, but instead to explore a few recent studies illustrative of the strategies used by macroalgae to thwart parasites at each stage of the infection or biofouling process. We will focus particular attention on evidence for the role of algal-associated microbes in host chemical defense and on the specificity of antimicrobial secondary metabolites. These two themes are inherently intertwined, as broad-spectrum versus highly targeted antimicrobial defenses could differentially impact the diversity of microbial communities living with macroalgae and, in turn, influence chemical defense profiles of algal-associated microbes.

Defenses against settlement and attachment

Algal chemical defenses that inhibit the settlement and attachment of pathogens or biofoulers represent the first line of defense against microbial challenge. Unlike compounds that function through growth inhibition or lethality, most settlement and

attachment defenses impact microbial behavior, and as a result, may put less selective pressure on microbes to develop resistance (Rasmussen and Givskov 2006).

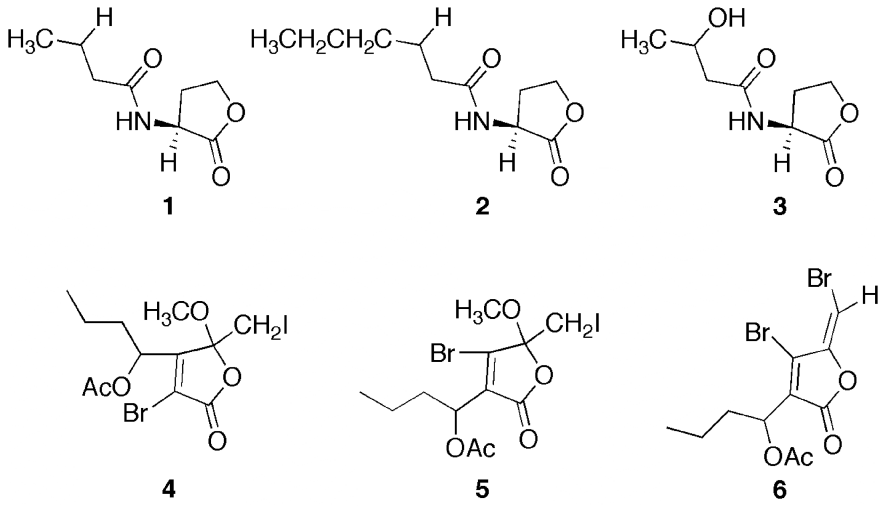

Fig. 4.1 Characteristic acyl homoserine lactones (AHLs) (**1-3**) are structurally similar to representative halogenated furanones (**4-6**) reported from *Delisea pulchra* (de Nys et al. 1993; Gould et al. 2006).

Larval attachment defenses of *Ulva reticulata*

Biofoulers including many species of bryozoans, crustaceans, tunicates, and polychaetes are abundant off the coast of Hong Kong (Harder and Qian 2000). Larvae of these animals attach to abiotic or biotic substrates and remain throughout development. Not all potential hosts are equally affected by biofoulers, suggesting some algae are defended. For example, the green alga *Ulva reticulata* was observed to be unscathed by biofoulers, leading Harder and Qian (2000) to hypothesize that this alga is chemically defended, inhibiting attachment or metamorphosis of biofoulers. In a relatively simple lab-based assay, larvae of the polychaete *Hydroides elegans* or the bryozoan *Bugula neritina* were placed in a Petri dish containing seawater in which *U. reticulata* had been

previously soaked. Both *H. elegans* and *B. neritina* larvae attached to the Petri dish substrate and metamorphosed at a significantly lower rate in seawater conditioned with *U. reticulata* than in control seawater (Harder and Qian 2000; Harder et al. 2004). Although precautions were taken to minimize damage in transferring *U. reticulata* from the field, the stress of collection could have resulted in the release of compounds that might not otherwise be present, potentially confounding results. Furthermore, the lab settlement assay (in still water) could not address whether inhibitory compounds(s) are effective in natural flow regimes, and may have exposed larvae to unnaturally high concentrations of *U. reticulata* exudate.

In an effort to reduce stress to *Ulva reticulata* during generation of anti-settlement cues, exudate was collected in the field by enclosing *U. reticulata* blades in transparent plastic bags for one hour. Lab assays were conducted with the conditioned water, with the results of this experiment further supporting *U. reticulata* deterrence of larval attachment (Harder et al. 2004). Although this experiment provided additional evidence for waterborne algal compounds acting as settlement inhibitors, *U. reticulata* could still have been exposed to unnatural stress while enclosed in the plastic bag; utilizing a gas-permeable but water-impermeable bag to collect exudates may be more appropriate (e.g., Kubanek et al. 2002).

Since the antifouling compounds(s) of *Ulva reticulata* appeared to be effective within the water column surrounding the source plant, these compounds may inhibit larval settlement on nearby macroorganisms as well. If competitors are indeed protected by *U. reticulata* defenses, then natural selection could favor "cheaters," mutant conspecifics which benefit from a neighbor's defenses without paying the costs of

producing the defense (Foster and Kokko 2006). At the same time, local species diversity could increase if undefended heterospecifics are protected by associating with a defended neighbor (e.g., Hay 1986).

Although *Ulva reticulata* lacks significant larval biofouling, it harbors a variety of epibiotic bacterial species. Dobretsov and Qian (2002) evaluated the antifouling effects of seven bacterial species cultured from *U. reticulata* surfaces. The extract of the cell-free supernatant from one *Vibrio* sp. significantly inhibited settlement and metamorphosis of *Hydroides elegans,* but not biofilm-forming bacteria, indicating that settlement inhibitor(s) from *Vibrio* sp. target larval foulers, not other bacteria. However, antibacterial effects of *Vibrio* sp. extracts were addressed solely through disc-diffusion assays, which are poor mimics of natural conditions, as they cannot expose bacteria to natural concentrations of test compounds (Jenkins et al. 1998). Furthermore, bacteria grown in liquid culture may produce different compounds than epiphytic bacteria.

The above discovery suggests that inhibitory compound(s) originally attributed to *Ulva reticulata* might instead be produced by the *Vibrio* sp. symbiont. Thus, Harder et al. (2004) applied bioassay-guided fractionation to isolate defensive compound(s) from (1) *U. reticulata*-conditioned seawater and (2) *Vibrio* sp. culture. Following desalting of crude extracts, ultrafiltration resulted in concentration of active metabolites in the >100 kD molecular weight fraction, suggesting a bioactive protein, polysaccharide, or glycoconjugate from both sources. In both, elimination of bioactivity by β-glucuronidase and α-amylase suggested that the bioactive components contained large polysaccharide units. However, the active fractions were differentially susceptible to proteolytic enzymes, suggesting that *U. reticulata* may be defended from biofoulers by multiple

chemical defenses: glycoprotein(s) from *U. reticulata* and polysaccharide(s) or non-proteinaceous glycoconjugate(s) from *Vibrio* sp. Analogously, extracts from *Pseudoalteromonas* spp. bacteria associated with *U. lactuca* have been reported to inhibit a suite of common biofoulers, although the responsible compound(s) have not been characterized (Egan et al. 2001).

The macromolecular bioactive metabolites from *Ulva reticulata*-conditioned seawater and from *Vibrio* sp. are unique among antifouling compounds characterized to date, since other reported larval-deterrent molecules from macroalgae have included phlorotannins and non-polar terpene alcohols (Schmitt et al. 1995; Lau and Qian 1997; Brock et al. 2007). The apparent lack of proteinaceous antifouling metabolites in the literature may represent a bias in extraction methodology, since most extractions have used solvents that would have denatured or failed to extract high molecular weight, water-soluble proteins.

Through methodological advancements, chemically-mediated relationships among bacterial symbionts, host macroalgae, and biofoulers may be more fully elucidated. Advanced methodology may be especially important in assessing the benefit of defensive metabolite-producing symbionts to host organisms. One possible direction is the application of molecular biology methods to create mutant symbionts for which the genetic ability to produce bioactive secondary metabolites is knocked out. By comparing biofouling of algae harboring symbionts capable of producing defensive metabolites to mutants without this ability, the role of such microbial metabolites may be analyzed in a more ecological context than before. Furthermore, field-deployed mass spectrometry technology has improved greatly in recent years (Short et al. 2006), and such equipment

may in the future be used to determine the natural concentrations and dynamics of some compounds released by marine algae and associated microbes.

Disruption of microbial communication pathways: an effective inhibitor of settlement and attachment

The defense of the red alga *Delisea pulchra* against biofouling is exceptionally well-characterized, and has been previously discussed in a number of excellent reviews (e.g., Steinberg et al. 1997; Rice et al. 1999; Steinberg and de Nys 2002; Paul and Puglisi 2004; de Nys et al. 2006). Thus, only a brief overview and recent developments will be provided herein.

Delisea pulchra produces a variety of structurally-related halogenated furanones (Fig. 4.1), which protect this alga from bacterial settlement and attachment (Kjelleberg et al. 1997; Maximilien et al. 1998). The structures of these furanones resemble acylated homoserine lactones (AHL) (de Nys et al. 1993), which have gained widespread attention as bacterial communication signals that regulate behavior, such as swarming, of many gram-negative bacteria and are important in bacteria-host interactions (Daniels et al. 2004). Manefield et al. (1999) demonstrated that algal furanones effectively inhibit bacterial swarming and subsequent attachment by acting as competitive inhibitors for LuxR, a major transcriptional activator for coordinated bacterial behavior that is activated by AHLs.

With this mechanistic understanding of the biological activity of *Delisea pulchra* furanones, it is possible to predict the bacterial taxa against which this alga is defended. Because gram-negative bacteria rely heavily upon the AHL signaling system (Konaklieva

and Plotkin 2006), it is not surprising that *D. pulchra* exhibits antibiosis against a variety of these microorganisms (Maximilien et al. 1998). Further, furanones also target the autoinducer-2 (AI-2) signaling system, which is present in many genera of gram-positive and gram-negative marine bacteria (Ren et al. 2001; McDougald et al. 2003). This discovery is surprising, given the lack of obvious structural similarity between AI-2 and furanones.

In addition to bacterial inhibition, furanones from *D. pulchra* directly inhibit settlement and attachment of some species of biofouling larvae and zoospores (de Nys et al. 1995; Dworjanyn et al. 2006), demonstrating the broad-spectrum antifouling activity of these molecules. However, the molecular mechanisms by which furanones deter larvae and zoospores are not known.

In contrast to the inhibitory activity of *Delisea pulchra* furanones against some zoospores, recent studies have indicated that AHLs act as chemoattractants to zoospores of the biofouling green algae *Ulva* spp., and are important in zoospore habitat selection in the laboratory (see Chap. 14; Joint et al. 2002; Tait et al. 2005). Analogously, bacteria associated with the red alga *Gracilaria chilensis* produce AHLs or AHL analogs that induce spore liberation and facilitate recruitment of the algal epiphyte *Acrochaetium* sp. to *G. chilensis* hosts in the laboratory (Weinberger et al. 2007). Further investigation of the responses of biofouling algal species to AHLs and related molecules, especially in the field, will yield further insights into the ecological functions of these molecules.

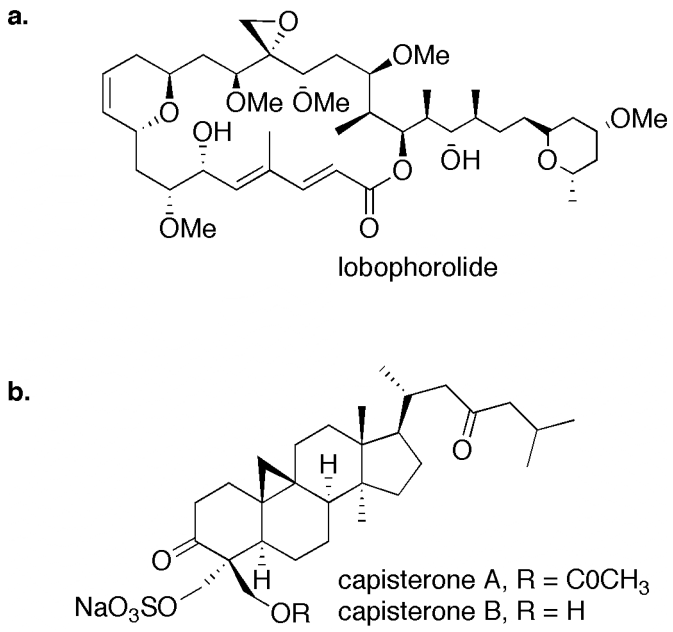

Fig. 4.2 Previously identified macroalgal secondary metabolites that inhibit growth of pathogenic and saprophytic fungi. (a) Lobophorolide was isolated from *Lobophora variegata*, but is likely of cyanobacterial origin (Kubanek et al. 2003). (b) Capisterones A and B were isolated from *Penicillus capitatus* and *P. pyrinformis* (Puglisi et al. 2004).

Lethal and growth inhibitory antimicrobials

The chemical defenses of *Ulva reticulata* and *Delisea pulchra* discussed above illustrate deterrence of potential pathogens and biofoulers during settlement and attachment. Yet, algal hosts may still successfully ward off these organisms even after colonization. Although surveys have suggested antimicrobial and antifouling chemical defenses are widespread among macroalgae and their microbial symbionts (e.g., Boyd et al. 1999; Nylund et al. 2005; Engel et al. 2006; Puglisi et al. 2006), fewer studies have gone on to elucidate the chemical structures of bioactive metabolites (e.g., Jensen et al. 1998; Paul et al. 2006). In the two example cases below, isolation of antimicrobial

compounds was guided by laboratory assays using ecologically-relevant microbes, leading to the characterization of structurally unique natural products.

Lobophorolide: a potent antifungal chemical defense

In a survey of antimicrobial chemical defenses from 55 species of Caribbean seaweeds, extracts from *Lobophora variegata*, a common brown alga, were found to be exceptionally potent in growth inhibition assays using *Lindra thallasiae*, a marine Ascomycete pathogenic to some algal species but not *Lobophora* spp., and *Dendryphiella salina*, a saprophytic marine Deuteromycete (Kubanek et al. 2003). Bioassay-guided fractionation of whole tissue extracts of *L. variegata* resulted in the isolation of lobophorolide, a novel polycyclic macrolide of presumed polyketide origin (Fig. 4.2a). Furthermore, the molecule was present in macroalgal surface extracts at concentrations sufficient for fungal growth inhibition, supporting its role as a chemical defense.

Although lobophorolide bore a novel carbon skeleton, it is largely a structural hybrid of previously identified tolytoxins, scytophycins, and swinholides (Kitagawa et al. 1990; Tsukamoto et al. 1991; Todd et al. 1992; Andrianasolo et al. 2005). Tolytoxin and scytophycins were first isolated from cultures of free-living freshwater and marine cyanobacteria (Carmeli et al. 1990; Carmeli et al. 1993), and more recently tolytoxin-23-acetate was isolated from a cephalaspidean mollusk, although this compound is likely synthesized by cyanobacteria and concentrated via the food web (Nakao et al. 1998). Swinholides have been found in marine sponges of the genus *Theonella* and more recently in free-living *Symploca* and *Geitlerinema* cyanobacteria (Tsukamoto et al. 1991; Todd et al. 1992; Andrianasolo et al. 2005). The true producer of a variety of plant- and

animal-associated polyketides has been debated heavily in the literature (Hildebrand et al. 2004a; Piel 2004). While it is possible that previous researchers have overlooked these pathways in plants and animals, it is more likely that the actual producers of polyketides such as lobophorolide are microbes living in or on host tissues.

Direct evidence for the true producers of some polyketide metabolites has come from culture-independent methods based on the cloning of biosynthetic genes from symbiotic microbes. These efforts have been hindered by the complexity of locating genes of interest within the multitude of microbial genomes generally associated with marine macroorganisms. Despite these difficulties, polyketides of the pederin family, originally attributed to beetles and sponges, were recently determined to be produced by bacterial symbionts (Piel 2002; Piel et al. 2004). Piel (2002) identified the polyketide-producing beetle symbiont as a *Pseudomonas* sp. Using similar cloning techniques, the uncultured γ-proteobacterium "*Candidatus* Endobugula sertula" was identified as the producer of bryostatins, potent anticancer and antipredation polyketides isolated from bryozoans (Davidson et al. 2001; Hildebrand et al. 2004b; Sudek et al. 2007).

Lobophorolide represents another likely example of a chemical defense produced by a microbial symbiont; however, no direct evidence links this molecule to cyanobacteria associated with *Lobophora variegata*. Kubanek et al. (2003) reported observation of a variety of bacteria, including cyanobacteria, on *L. variegata*. The variable but low concentration of lobophorolide in *L. variegata* ($1.2 \pm 0.3 \times 10^{-4}$ % of plant dry mass) also indirectly supported a microbial source, since plant secondary metabolites typically range in concentration from 0.1-10% of dry mass (Paul 1992). It should also be noted, however, that this low abundance could simply represent an

optimized strategy to tune defense concentrations to microbe sensitivity, which ranged 1-2 orders of magnitude below natural concentration. Conclusive evidence of the actual producer of lobophorolide will untimately come only through metagenomic analyses analogous to those applied by Piel (2002), or by future identification of this compound from microbes cultured from *L. variegata*.

Lobophorolide targets a variety of filamentous fungi, including not only ecologically relevant *Linda thalassiae* and *Dendryphiella salina*, but also the human pathogen *Candida albicans*. However, the ecological activity of lobophorolide appears limited to these higher fungi, as this compound did not inhibit growth of the thraustochytrid *Schizochitrium aggregatum* or the bacterium *Pseudoalteromonas bacteriolytica*, known to be pathogenic to selected macroalgae, nor did it deter feeding by herbivorous fishes (Kubanek et al. 2003). Hence, unlike furanones isolated from *Delisea pulchra*, which showed multifunctional biological activity against bacteria and biofoulers, lobophorolide may have evolved as a more targeted, specific defense, albeit one apparently functional against a variety of higher fungi.

Chemical defenses targeted against specific challengers are likely to have quite different implications for algal-associated epibiont communities than defenses that effectively deter all parasites. As it is becoming increasingly clear that a number of antimicrobial natural products isolated from macroorganisms are actually microbial natural products, perhaps antagonistic interactions among microbes originally selected for the evolution of antimicrobial defenses that now protect hosts from microbial parasites. Illustrating the complexity of interaction between microbial competitors on algal surfaces, Franks et al. (2006) demonstrated that algal-associated *Pseudoalteromonas*

tunicata produces secondary metabolites that inhibit fungal colonization thereby giving bacteria a competitive advantage in colonizing algal surfaces. Recently, 16*S* ribosomal RNA sequencing has been applied to evaluate both cultured and uncultured bacterial diversity in nature (Webster et al. 2001; Hentschel et al. 2002), suggesting this methodology may be invaluable in relating algal chemical defense profiles to the diversity of associated microbes.

Antifungal chemical defenses of *Penicillus* spp.

Recent investigations of antimicrobial chemical defenses in green algae of the genus *Penicillus* indicate that, like *Lobophora variegata*, these abundant macroalgae also harbor potent defenses against fungal pathogens. From *P. capitatus*, Puglisi et al. (2004) isolated two novel triterpene sulfate esters, capisterones A and B, with antifungal activity against *Lindra thalassiae* at natural whole-tissue concentrations (Fig. 4.2b). Like lobophorolide, the growth inhibitory activity of capisterones A and B appears limited to higher fungi. Although literature examples of cycloartane class triterpenoids such as capisterones A and B are rare, all marine examples of these molecules have come from algal species such as the red alga *Tricleocarpa fragilis* and the green alga *Tydemania expeditionis* (Govindan et al. 1994; Horgen et al. 2000). This fact, together with biosynthetic studies demonstrating the capacity of algae to produce a variety of isoprenoids (although not these specific triterpenes), suggests that capisterones A and B are produced by *P. capitatus* itself and not by a symbiotic microbe.

More recent investigations by Engel et al. (in prep.) revealed that capisterones are concentrated in the cap filaments of *Penicillus canitatus* and are not present at detectable

levels in their heavily calcified stalks. By combining pulse amplitude modulated (PAM) fluorometry in the field with culture studies and chemical analyses in the lab, Engel et al. (in prep.) demonstrated that photosynthetically active cap filaments harbor low levels of culturable fungi and mean in situ capisterone concentrations of 10 μg/mL. These studies showed a clear positive correlation between photosynthetic activity and in situ capisterone concentrations, as well as a strong negative correlation between fungal abundance on cap filaments and in situ capisterone concentrations. These results imply that healthy, photosynthetically active individuals maintain high capisterone concentrations and are thus more effective at controlling associated fungi. Although surface concentrations of capisterones were not evaluated, the low minimum inhibitory concentration (MIC) of capisterones against cultured fungi (0.1 to 0.7 μg/mL) suggests that natural concentrations are likely sufficient to inhibit fungal infection. Furthermore, capisterones are amphiphilic, possessing a lipophilic terpenoid core and a hydrophilic sulfate group. This may result in aggregation of capisterones at algal surfaces, since the lipophilic portion could interact with algal tissue while the hydrophilic moiety is strongly attracted to surrounding seawater.

Engel et al. (in prep.) also evaluated antifungal chemical defenses of other *Penicillus* species from the tropical Atlantic. Like *P. capitatus*, cap filaments of *P. pyriformis* contained capisterones and closely related natural products at concentrations similar to those found in *P. capitatus*. In contrast, *P. dumetosus* contained only trace amounts of these triterpenoids. All *Penicillus* spp. examined contained indole-3-carboxaldehyde at whole tissue concentrations sufficient to inhibit the algal fungal pathogen *Lindra thalassiae*. Interestingly, this compound has thus far only been reported

as a phytoalexin in terrestrial plants (Tan et al. 2004), produced in response to fungal infection. Future studies will be needed to examine if fungal infection also induces the production of this metabolite in *Penicillus* spp. Induction of macroalgal chemical defenses in response to mesograzers such as amphipods and snails has been reported (Cronin and Hay 1996; Pavia and Toth 2000; Toth and Pavia 2000); however, the induction of antimicrobial defenses has not yet been shown in macroalgae. In investigations of antimicrobial defense induction in terrestrial plants, wounding has been shown to induce chemical defenses (e.g., Kristensen et al. 1999; Aneja and Gianfagna 2001; Rizhsky and Mittler 2001), probably because physical damage is a good proxy for the presence of pathogens. In contrast, Pavia and Toth (2000) demonstrated that physical damage alone was insufficient to induce antiherbivore defense production in algae. Hence, it will be interesting to determine whether wounding induces antimicrobial defenses in marine algae, and such studies are currently underway in our group.

One question that remains to be answered for lobophorolide, capisterones, and indole-3-carboxaldehyde is whether these antimicrobial molecules function by killing susceptible fungi or by slowing their growth and/or reproduction. The isolation of these antifungal natural products was guided using assays testing how fungi grow on agar media containing natural concentrations of macroalgal extracts. Reduced growth on treated agar relative to controls might indicate that a macroalgal chemical defense is lethal to fungi or that it slows fungal growth/reproduction, or a combination of both. Although perhaps not inherently important in assessing the ecological effects of antimicrobial defenses, determination of the mode of inhibition may have important implications for the co-evolution of hosts and parasites. Compounds that inhibit

microbial growth or reproduction could provide selective pressure for the evolution of resistance among microbes, since in cases where the defense is not lethal, small populations of pathogenic microbes might remain associated with algae for substantial periods of time, facilitating the emergence of a resistant phenotype. A competing hypothesis is that lethal compounds could strongly favor the evolution of resistance, since even one mutant resistant cell could rapidly dominate a macroalgal host. By developing ecological assays capable of distinguishing between lethal and growth/reproductive inhibitory effects, it may be possible to address such questions.

Future perspective and conclusions

The studies highlighted above provide a glimpse into the role of secondary metabolites in defending macroalgae against pathogens and biofoulers. These molecules operate at different stages of the infection or fouling process, and demonstrate that multiple strategies can be successful in controlling these organisms. As deterrents to settlement and attachment, molecules such as the polar, high molecular weight compounds from *Ulva reticulata* and an associated *Vibrio* sp. likely defend this alga from biofouling larvae. Furanones from *Delisea pulchra* disrupt bacterial settlement by inhibiting communication pathways necessary for bacterial quorum sensing and settlement. In contrast, chemical defenses including lobophorolide and capisterones defend macroalgae after settlement, by either killing or inhibiting the growth of fungal pathogens.

As illustrated by the cases of an antilarval defense in *Ulva reticulata* produced by a *Vibrio* sp. bacterium and by the likely cyanobacterial origin of lobophorolide, microbial

symbionts probably play an important role in synthesizing chemical defenses for host algal species. Harboring epiphytic or endophytic microbes that produce bioactive secondary metabolites may benefit hosts by eliminating metabolic costs for synthesizing and storing defensive compounds, and may reduce autotoxicity effects. These macroalgal-microbial associations may be mutualistic, although studies are needed to evaluate this hypothesis.

The specificity of most chemical defenses (e.g., Engel et al. 2006; Puglisi et al. 2006) is likely an important contributing factor to the structure of algal-associated microbial communities. Chemical defenses may affect marine communities by promoting some microbes on algal surfaces while deterring others, and by facilitating growth of macroalgae that would otherwise become overgrown by biofoulers. The likely microbial source of many defensive metabolites adds another interesting aspect in addressing the role of natural products in structuring communities. Although no studies to date have provided clear evidence for community consequences of antimicrobial defenses in macroalgae, the synergistic application of natural products chemistry, genetic engineering approaches, and field ecological experimentation may result in an advanced understanding of such relationships.

A better understanding of the dynamics of antimicrobial chemical defense production is also predicted for the future. In the more advanced field of marine plant-herbivore interactions, field experiments have demonstrated increased production of defensive metabolites in response to attack by specific herbivores (e.g., Cronin and Hay 1996; Toth and Pavia 2000). Given the likely costs of antimicrobial defenses, regulation of chemical defenses dependent upon risk of attack is expected to be similarly

advantageous. It is possible the most important chemically-mediated battles are not between microbes and their hosts but instead among microbial species or populations co-occurring on or in a host. Evaluation of such hypotheses is inherently challenging and will necessitate significant methodological advancements and a better understanding of host-pathogen and host-biofouler interactions. Through the synergistic application of improved laboratory and field-based experiments, understanding of secondary metabolite defenses against pathogens and biofoulers will forge ahead.

Works Cited

Andrews JH (1976) The pathology of marine algae. Biol Rev 51: 211-253

Andrews JH (1977) Observations on pathology of seaweeds in Pacific Northwest. Can J Botany 55: 1019-1027

Andrianasolo EH, Gross H, Goeger D, Musafija-Girt M, McPhail KP, Leal RM, Mooberry SL, Gerwick WH (2005) Isolation of swinholide A and related glycosylated derivatives from two field collections of marine cyanobacteria. Org Lett 7: 1375-1378

Aneja M, Gianfagna T (2001) Induction and accumulation of caffeine in young, actively growing leaves of cocoa (*Theobroma cacao* L.) by wounding or infection with Crinipellis perniciosa. Physiol Mol Plant Pathology 59: 13-16

Armstrong E, Yan LM, Boyd KG, Wright PC, Burgess JG (2001) The symbiotic role of marine microbes on living surfaces. Hydrobiologia 461: 37-40

Boyd KG, Adams DR, Burgess JG (1999) Antibacterial and repellent activities of marine bacteria associated with algal surfaces. Biofouling 14: 227-236

Brock E, Nylund GM, Pavia H (2007) Chemical inhibition of barnacle larval settlement by the brown alga *Fucus vesiculosus*. Mar Eco Prog Ser 337: 165-174

Carmeli S, Moore RE, Patterson GML (1990) Tolytoxin and new scytophycins from 3 species of *Scytonema*. J Nat Prod 53: 1533-1542

Carmeli S, Moore RE, Patterson GML, Yoshida WY (1993) Biosynthesis of tolytoxin: origin of the carbons and heteroatoms. Tetrahedron Lett 34: 5571-5574

Correa JA (1997) Infectious diseases of marine algae: current knowledge and approaches. In: Round FE, Chapman DJ (eds) Progress in Phycological Research. Biopress Ltd., Bristol, pp 149-180

Correa JA, Flores V (1995) Whitening, thallus decay and fragmentation in *Gracilaria chilensis* associated with an endophytic amoeba. J Appl Phycol 7: 421-425

Correa JA, Flores V, Garrido J (1994) Green patch disease in *Iridaea laminarioides* (Rhodophyta) caused by *Endophyton* sp. (Chlorophyta). Dis Aquat Organ 19: 203-213

Correa JA, Flores V, Sanchez P (1993) Deformative disease in *Iridaea laminarioides* (Rhodophyta): gall development associated with an endophytic cyanobacterium. J Phycol 29: 853-860

Cronin G, Hay ME (1996) Induction of seaweed chemical defenses by amphipod grazing. Ecology 77: 2287-2301

D'Antonio C (1985) Epiphytes on the rocky intertidal red alga *Rhodomela larix* (Turner) C Agardh: Negative effects on the host and food for herbivores. J Exp Mar Biol Ecol 86: 197-218

Daniels R, Vanderleyden J, Michiels J (2004) Quorum sensing and swarming migration in bacteria. FEMS Microbiol Rev 28: 261-289

Davidson SK, Allen SW, Lim GE, Anderson CM, Haygood MG (2001) Evidence for the biosynthesis of bryostatins by the bacterial symbiont "*Candidatus* Endobugula sertula" of the bryozoan *Bugula neritina*. Appl Environ Microb 67: 4531-4537

de Nys R, Givskov M, Kumar N, Kjelleberg S, Steinberg PD (2006) Furanones. In: Fusetani N, Clare AS (eds) Antifouling Compounds, Berlin Heidelberg, pp 55-86

de Nys R, Steinberg PD, Willemsen P, Dworjanyn SA, Gabelish CL, King RJ (1995) Broad-spectrum effects of secondary metabolites from the red alga *Delisea pulchra* in antifouling assays. Biofouling 8: 259-271

de Nys R, Wright AD, Konig GM, Sticher O (1993) New halogenated furanones from the marine alga *Delisea pulchra* (Cf *Fimbriata*). Tetrahedron 49: 11213-11220

Dixon J, Schroeter SC, Kastendiek J (1981) Effects of the encrusting bryozoan, *Membranipora membranacea*, on the loss of blades and fronds by the giant kelp, *Macrocystis pyrifera* (Laminariales). J Phycol 17: 341-345

Dobretsov S, Dahms HU, Qian PY (2006) Inhibition of biofouling by marine microorganisms and their metabolites. Biofouling 22: 43-54

Dobretsov, S, Qian PY (2002) Effect of bacteria associated with the green alga *Ulva reticulata* on marine micro- and macrofouling. Biofouling 18: 217-228

Dworjanyn SA, de Nys R, Steinberg PD (2006) Chemically mediated antifouling in the red alga *Delisea pulchra*. Mar Eco Prog Ser 318: 153-163

Egan S, James S, Holmstrom C, Kjelleberg S (2001) Inhibition of algal spore germination by the marine bacterium *Pseudoalteromonas tunicata*. Fems Microbiology Ecology 35: 67-73

Engel S, Jensen PR, Fenical W (2002) Chemical ecology of marine microbial defense. J Chem Eco 28: 1971-1985

Engel S, Puglisi MP, Jensen PR, Fenical W (2006) Antimicrobial activities of extracts from tropical Atlantic marine plants against marine pathogens and saprophytes. Mar Bio 149: 991-1002

Engel S, Fenical W Antimicrobial chemical defenses of the green alga *Penicillus capitatus*. *In prep.*

Filion-Myklebust C, Norton TA (1981) Epidermis shedding in the brown seaweed *Ascophyllum nodosum* (L) Lejolis, and its ecological significance. Mar Bio Lett 2: 45-51

Foster KR, Kokko H (2006) Cheating can stabilize cooperation in mutualisms. P Roy Soc B-Biol Sci 273: 2233-2239

Franks A, Egan S, Holmstrom C, James S, Lappin-Scott H, Kjelleberg S (2006) Inhibition of fungal colonization by *Pseudoalteromonas tunicata* provides a competitive advantage during surface colonization. Appl Environ Microb 72: 6079-6087.

Gould TA, Herman J, Krank J, Murphy RC, Churchill MEA (2006) Specificity of acyl-homoserine lactone synthases examined by mass spectrometry. J Bacteriol 188: 773-783

Govindan M, Abbas SA, Schmitz FJ, Lee RH, Papkoff JS, Slate DL (1994) New cycloartanol sulfates from the alga *Tydemania expeditionis*: inhibitors of the protein tyrosine kinase Pp60 (V-Src). J Nat Prod 57: 74-78

Harder T, Dobretsov S, Qian PY (2004) Waterborne polar macromolecules act as algal antifoulants in the seaweed *Ulva reticulata*. Mar Eco Prog Ser 274: 133-141

Harder T, Qian PY (2000) Waterborne compounds from the green seaweed *Ulva reticulata* as inhibitive cues for larval attachment and metamorphosis in the polychaete *Hydroides elegans*. Biofouling 16: 205-214

Hay ME (1986) Associational plant defenses and the maintenance of species diversity: turning competitors into accomplices. Am Nat 128: 617-641

Hentschel U, Hopke J, Horn M, Friedrich AB, Wagner M, Hacker J, Moore BS (2002) Molecular evidence for a uniform microbial community in sponges from different oceans. Appl Environ Microb 68: 4431-4440

Hepburn CD, Hurd CL (2005) Conditional mutualism between the giant kelp *Macrocystis pyrifera* and colonial epifauna. Mar Eco Prog Ser 302: 37-48

Hildebrand M, Waggoner LE, Lim GE, Sharp KH, Ridley CP, Haygood MG (2004a) Approaches to identify, clone, and express symbiont bioactive metabolite genes. Nat Prod Rep 21: 122-142

Hildebrand M, Waggoner LE, Liu HB, Sudek S, Allen S, Anderson C, Sherman DH, Haygood M (2004b) bryA: An unusual modular polyketide synthase gene from the uncultivated bacterial symbiont of the marine bryozoan *Bugula neritina*. Chemistry & Biology 11: 1543-1552

Horgen FD, Sakamoto B, Scheuer PJ (2000) New triterpenoid sulfates from the red alga Tricleocarpa fragilis. J Nat Prod 63: 210-216

Jenkins KM, Jensen PR, Fenical W (1998) Bioassays with marine microorganisms. In: Haynes KF, Millar JG (eds) Methods in Chemical Ecology: Bioassay Methods. Kluwer Academic Publishers, pp 1-37

Jensen PR, Jenkins KM, Porter D, Fenical W (1998) Evidence that a new antibiotic flavone glycoside chemically defends the sea grass Thalassia testudinum against zoosporic fungi. Appl Environ Microb 64: 1490-1496

Joint I, Tait K, Callow ME, Callow JA, Milton D, Williams P, Camara M (2002) Cell-to-cell communication across the prokaryote-eukaryote boundary. Science 298: 1207-1207

Kitagawa I, Kobayashi M, Katori T, Yamashita M, Tanaka J, Doi M, Ishida T (1990) Absolute stereostructure of swinholide A, a potent cytotoxic macrolide from the Okinawan marine sponge *Theonella swinhoei*. J Am Chem Soc 112: 3710-3712

Kjelleberg S, Steinberg P, Givskov M, Gram L, Manefield M, deNys R (1997) Do marine natural products interfere with prokaryotic AHL regulatory systems? Aquat Microb Ecol 13: 85-93

Kohlmeyer J (1971) Fungi from the Sargasso Sea. Mar Bio 8: 344-350

Konaklieva MI, Plotkin BJ (2006) Chemical communication: do we have a quorum? Mini-Rev Med Chem 6: 817-825

Kristensen BK, Bloch H, Rasmussen SK (1999) Barley coleoptile peroxidases. Purification, molecular cloning, and induction by pathogens. Plant Physiol 120: 501-512

Kubanek J, Jensen PR, Keifer PA, Sullards MC, Collins DO, Fenical W (2003) Seaweed resistance to microbial attack: A targeted chemical defense against marine fungi. Proc Natl Acad Sci USA 100: 6916-6921

Kubanek J, Whalen KE, Engel S, Kelly SR, Henkel TP, Fenical W, Pawlik JR (2002) Multiple defensive roles for triterpene glycosides from two Caribbean sponges. Oecologia 131: 125-136

Lau SCK, Qian PY (1997) Phlorotannins and related compounds as larval settlement inhibitors of the tube-building polychaete *Hydroides elegans*. Mar Eco Prog Ser 159: 219-227

Manfield M, de Nys R, Kumar N, Read R, Givskov M, Steinberg P, Kjelleberg SA (1999) Evidence that halogenated furanones from *Delisea pulchra* inhibit acylated homoserine lactone (AHL)-mediated gene expression by displacing the AHL signal from its receptor protein. Microbiology-UK 146: 283-291.

Mann KH (1973) Seaweeds: Their productivity and strategy for growth. Science 182: 975-981

Maximilien R, de Nys R, Holmstrom C, Gram L, Givskov M, Crass K, Kjelleberg S, Steinberg PD (1998) Chemical mediation of bacterial surface colonisation by secondary metabolites from the red alga *Delisea pulchra*. Aquat Microb Eco 15: 233-246

McClintock JB, Baker BJ (2001) Marine Chemical Ecology. CRC Press, Boca Raton, FL

McDougald D, Srinivasan S, Rice SA, Kjelleberg S (2003) Signal-mediated cross-talk regulates stress adaptation in *Vibrio* species. Microbiology-Sgm 149: 1923-1933

Moss BL (1982) The Control of Epiphytes by *Halidrys siliquosa* (L) Lyngb - (Phaeophyta, Cystoseiraceae). Phycologia 21: 185-188

Nakao Y, Yoshida WY, Szabo CM, Baker BJ, Scheuer PJ (1998) More peptides and other diverse constituents of the marine mollusk *Philinopsis speciosa*. J Org Chem 63: 3272-3280

Nylund GM, Cervin G, Hermansson M, Pavia H (2005) Chemical inhibition of bacterial colonization by the red alga *Bonnemaisonia hamifera*. Mar Eco Prog Ser 302: 27-36

Nylund GM, Pavia H (2005) Chemical versus mechanical inhibition of fouling in the red alga *Dilsea carnosa*. Mar Eco Prog Ser 299: 111-121

Paul NA, de Nys R, Steinberg PD (2006) Chemical defence against bacteria in the red alga *Asparagopsis armata*: linking structure with function. Mar Eco Prog Ser 306: 87-101

Paul VJ (1992) Ecological Roles of Marine Natural Products. Comstock, Ithaca, NY

Paul VJ, Puglisi MP (2004) Chemical mediation of interactions among marine organisms. Nat Prod Rep 21: 189-209

Pavia H, Toth GB (2000) Inducible chemical resistance to herbivory in the brown seaweed *Ascophyllum nodosum*. Ecology 81: 3212-3225

Piel J (2002) A polyketide synthase-peptide synthetase gene cluster from an uncultured bacterial symbiont of *Paederus* beetles. Proc Natl Acad Sci USA 99: 14002-14007

Piel J (2004) Metabolites from symbiotic bacteria. Nat Prod Rep 21: 519-538

Piel J, Hui DQ, Wen GP, Butzke D, Platzer M, Fusetani N, Matsunaga S (2004) Antitumor polyketide biosynthesis by an uncultivated bacterial symbiont of the marine sponge *Theonella swinhoei*. Proc Natl Acad Sci USA 101: 16222-16227

Porter D (1986) Mycoses of marine organisms: an overview of pathogenic fungi. Cambridge University Press, New York

Puglisi M, Engel S, Jensen P, Fenical W (2006) Antimicrobial activities of extracts from Indo-Pacific marine plants against marine pathogens and saprophytes. Mar Bio 149: 991-1002

Puglisi MP, Tan LT, Jensen PR, Fenical W (2004) Capisterones A and B from the tropical green alga *Penicillus capitatus*: unexpected anti-fungal defenses targeting the marine pathogen *Lindra thallasiae*. Tetrahedron 60: 7035-7039

Rasmussen TB, Givskov M (2006) Quorum sensing inhibitors: a bargain of effects. Microbiology 152: 895-904

Ren D, Sims JJ, Wood TK (2001) Inhibition of biofilm formation and swarming of *Escherichia coli* by (5*Z*)-4-bromo-5-(bromomethylene)-3-butyl-2(5*H*)-furanone. Environ Micro 3: 731-736

Rice SA, Givskov M, Steinberg P, Kjelleberg S (1999) Bacterial signals and antagonists: the interaction between bacteria and higher organisms. J Mol Microb Biotech 1: 23-31

Rizhsky L, Mittler R (2001) Inducible expression of bacterio-opsin in transgenic tobacco and tomato plants. Plant Mol Biol 46: 313-323

Ruesink JL (1998) Diatom epiphytes on *Odonthalia floccosa*: The importance of extent and timing. J Phycol 34: 29-38

Sawabe T, Makino H, Tatsumi M, Nakano K, Tajima K, Iqbal MM, Yumoto I, Ezura Y, Christen R (1998) *Pseudoalteromonas bacteriolytica* sp. nov., a marine bacterium that is the causative agent of red spot disease of *Laminaria japonica*. Int J System Bacteriol 48: 769-774

Schmitt TM, Hay ME, Lindquist N (1995) Constraints on chemically mediated coevolution: Multiple functions for seaweed secondary metabolites. Ecology 76: 107-123

Short RT, Toler SK, Kibelka GPG, Roa DTR, Bell RJ, Byrne RH (2006) Detection and quantification of chemical plumes using a portable underwater membrane introduction mass spectrometer. Trac-Trend Anal Chem 25: 637-646

Steinberg PD, de Nys R (2002) Chemical mediation of colonization of seaweed surfaces. J Phycol 38: 621-629

Steinberg PD, Schneider R, Kjelleberg S (1997) Chemical defenses of seaweeds against microbial colonization. Biodegradation 8: 211-220

Sudek S, Lopanik NB, Waggoner LE, Hildebrand M, Anderson C, Liu HB, Patel A, Sherman DH, Haygood MG (2007) Identification of the putative bryostatin polyketide synthase gene cluster from "*Candidatus* endobugula sertula", the uncultivated microbial symbiont of the marine bryozoan *Bugula neritina*. Journal of Natural Products 70: 67-74

Tait K, Joint I, Daykin M, Milton DL, Williams P, Camara M (2005) Disruption of quorum sensing in seawater abolishes attraction of zoospores of the green alga Ulva to bacterial biofilms. Environ Microbiol 7: 229-240

Tan JW, Bednarek P, Liu HK, Schneider B, Svatos A, Hahlbrock K (2004) Universally occurring phenylpropanoid and species-specific indolic metabolites in infected and uninfected *Arabidopsis thaliana* roots and leaves. Phytochemistry 65: 691-699

Todd JS, Alvi KA, Crews P (1992) The Isolation of a monomeric carboxylic acid of swinholide A from the Indo-Pacific sponge, *Theonella swinhoei*. Tetrahedron Lett 33: 441-442

Toth GB, Pavia H (2000) Water-borne cues induce chemical defense in a marine alga (*Ascophyllum nodosum*). Proc Natl Acad Sci USA 97: 14418-14420

Tsukamoto S, Ishibashi M, Sasaki T, Kobayashi J (1991) New congeners of swinholides from the Okinawan marine sponge *Theonella* sp. J Chem Soc Perk Trans 1: 3185-3188

Wahl M, Hay ME (1995) Associational resistance and shared doom: Effects of epibiosis on herbivory. Oecologia 102: 329-340

Webster NS, Wilson KJ, Blackall LL, Hill RT (2001) Phylogenetic diversity of bacteria associated with the marine sponge *Rhopaloeides odorabile*. Appl Environ Microb 67: 434-444

Weinberger F, Beltran J, Correa JA, Lion U, Pohnert G, Kumar N, Steinberg P, Kloareg B, Potin P (2007) Spore release in *Acrochaetium* sp (Rhodophyta) is bacterially controlled. Journal of Phycology 43: 235-241

Wikstrom SA, Pavia H (2004) Chemical settlement inhibition versus post-settlement mortality as an explanation for differential fouling of two cogeneric seaweeds. Oecologia 138: 223-230

CHAPTER 5

SURFACE-MEDIATED ANTIFUNGAL CHEMICAL DEFENSES OF A TROPICAL SEAWEED

Abstract

Organism surfaces represent signaling sites for attraction of allies and defense against enemies. However, understanding of these signals has been impeded by methodological limitations that have precluded direct fine-scale evaluation of compounds on native surfaces. Herein, we asked whether natural products from the red macroalga *Callophycus serratus* act in surface-mediated defense against pathogenic microbes. Bromophycolides and callophycoic acids from algal extracts inhibited growth of *Lindra thalassiae*, a marine fungal pathogen. Spatially-resolved and imaging desorption electrospray ionization mass spectrometry (DESI-MS) revealed algal surfaces were largely devoid of bromophycolides, but distinct surface patches and internal tissues contained compounds at concentrations sufficient for fungal inhibition. This represents the first example of natural product imaging on biological surfaces, suggesting the importance of secondary metabolites in localized ecological interactions, and illustrating the potential of DESI-MS in understanding chemically-mediated biological processes.

Introduction

Secondary metabolite cues drive countless biological interactions including mate recognition, competition for space, prey detection, and defense against adversaries including consumers and pathogens (Paul et al., 2006c; Paul and Ritson-Williams, 2008).

As the interface between an organism and its environment, biotic surfaces may represent particularly important sites of chemical signaling (Steinberg et al., 2001). Foulers, pathogens, parasites, and symbionts establish initial physical interaction with hosts via surface contact, and presentation of chemical cues exclusively on host surfaces may afford critical advantages to the organism producing the cue. Compared with maintenance of metabolites throughout tissues, maintaining compounds primarily on outer surfaces where they are most effective could reduce potential autotoxicity and lower costs of compound biosynthesis to the signal producer. Likewise, production of signaling molecules within cells followed by targeted release of compounds onto challenged surfaces may afford substantial benefits. For example, induced release of chemical defenses at sites of microbial challenge could limit infection while decreasing selective pressure for evolution of resistance and reducing the potential for other organisms to utilize these compounds as attractive cues (Karban and Baldwin, 1997; Koricheva, 2002).

Despite the apparent advantages of surface-mediated chemical signaling, our understanding of such processes has been largely impeded by methodological limitations. In the marine realm, numerous genera have been suggested to utilize surface-associated defenses against competitors, foulers, and pathogens (Kelly et al., 2003; Nylund et al., 2005; Nylund et al., 2008; Nylund et al., 2006; Nylund and Pavia, 2003). However, such defenses were often proposed based on inhibitory effects detected in experiments using whole organism extracts (Kelly et al., 2003; Nylund and Pavia, 2003), and it is unclear whether target species actually encountered these chemicals in nature. In more ecologically realistic studies, roles of surface-associated molecules were proposed based

on experiments employing surface extracts or pure compounds tested at their approximate surface concentration (Dworjanyn et al., 1999; Kubanek et al., 2003; Kubanek et al., 2002; Nylund et al., 2008; Nylund et al., 2006; Schmitt et al., 1995). Unfortunately, current extraction-based methodologies are inefficient at extracting compounds associated with biological surfaces and limited to certain groups of molecules. Further, these methods do not allow determination of compound distributions on organismal surfaces at lower than centimeter or millimeter scales. Heterogeneous distributions at the micron-to-millimeter scale may play important, but unexplored, roles in mediating biotic interactions. Such fine-scale interactions may be particularly important in governing relationships, whether beneficial or deleterious, between hosts and microorganisms.

Microbe-borne diseases have caused mass mortality among some marine plant and animal species, and epidemics appear to be on the rise (Harvell et al., 1999). Not all organisms are susceptible to infection, and both internal and surface-associated chemical defenses may account for the observed resistance of some secondary metabolite-rich species to microbial attack (Engel et al., 2002; Lane and Kubanek, 2008). However, antimicrobial chemical defenses have not been widely explored (Engel et al., 2006; Kim et al., 2000; Puglisi et al., 2006). Among marine macroalgae, only a handful of studies have evaluated roles of specific secondary metabolites in defense against deleterious microbes (Jiang et al., 2008; Nylund et al., 2008; Paul et al., 2006b; Puglisi et al., 2004), and even fewer have provided evidence for these molecules in surface-mediated defense (Kubanek et al., 2003; Maximilien et al., 1998; Nylund et al., 2008). Only the 22-membered lactone lobophorolide from the brown alga *Lobophora variegata* (Kubanek et

al., 2003), a poly-brominated 2-heptanone from the red alga *Bonnemaisonia hamifera* (Nylund et al., 2008), and furanones from the red alga *Delisea pulchra* (Maximilien et al., 1998) have been proposed as surface-associated antimicrobial defenses of marine algae.

Recent developments in mass spectrometry offer potential for advanced understanding of these and other chemical signaling processes. The Dorrestein and Gerwick groups recently demonstrated the utility of matrix-assisted laser desorption ionization time-of-flight mass spectrometry (MALDI-TOF MS) for pinpointing secondary metabolite locations within marine microbe-invertebrate assemblages (Esquenazi et al., 2008; Simmons et al., 2008), and this strategy may prove widely applicable in assigning biosynthetic origins and distributions of chemical defenses within tissues or cell types. However, such MALDI-TOF experiments require sample treatments that preclude direct analysis of intact biological surfaces. In contrast, desorption electrospray ionization mass spectrometry (DESI-MS) is promising for evaluation of secondary metabolites on intact surfaces. With DESI-MS, surfaces are maintained at atmospheric pressure in open air and presented with a fine high velocity spray of charged droplets. Biomolecules are desorbed from the surface, potentially without rupturing cell membranes, and delivered as desolvated ions into the mass spectrometer for analysis (Cooks et al., 2006). Like traditional mass spectrometry techniques, DESI-MS offers rapid analyses, low detection limits, and compatibility with molecules ranging from water-soluble to non-polar, and from low (< 100 Da) to high molecular weights (> 100,000 Da) (Takats et al., 2004). The broad applicability of DESI-MS is evidenced by applications including profiling of targeted sites on tissue surfaces for specific phospholipids associated with disease states (Wiseman et al., 2006), analysis

of counterfeit drug molecules on intact pharmaceutical tablets (Nyadong et al., 2007), detection of explosives (Cotte-Rodriguez et al., 2005), and assessment of alkaloid content from terrestrial plant tissue (Talaty et al., 2005). These studies suggest the potential of DESI-MS as a powerful tool in exploring the function of surface-associated natural products in ecological interactions.

On the basis of their cytotoxicity towards biomedical targets, we recently discovered ten bromophycolides, unusual C_{27} diterpene-benzoate macrolides, from a population of the Fijian red alga *Callophycus serratus*. Ten novel callophycoic acids and callophycols, C_{27} diterpene-benzoic acids and C_{26} diterpene-alcohols, were isolated from a different population of the same alga (Kubanek et al., 2006; Kubanek et al., 2005; Lane et al., 2007). In the present study, we merge traditional natural products chemistry and ecological approaches with the capabilities of DESI-MS to provide support for a role of bromophycolides and callophycoic acids as antifungal defenses of whole algae as well as evidence that bromophycolides are presented heterogeneously on algal surfaces where they may interfere with pathogen attack.

Results

Evaluation of whole algal extracts reveals potent antifungal chemical defenses in *Callophycus serratus*.

Chromatographic fractions from extracts of ten separate collections of *C. serratus* were evaluated at natural whole tissue concentrations for growth inhibitory activity against two known pathogens of marine plants: *Lindra thalassiae*, a widely distributed marine Ascomycete reported to infect diverse hosts ranging from brown algae to

seagrasses (Kohlmeyer, 1971; Kohlmeyer and Kohlmeyer, 1979), and *Pseudoalteromonas bacteriolytica*, the bacterium responsible for red spot disease in kelp (Sawabe et al., 1998). Fractions containing either bromophycolides or callophycoic acids/callophycols strongly inhibited growth of *L. thalassiae* relative to no extract controls ($p < 0.0001$ for all fractions), with every fraction inhibiting growth of this fungus by > 95%. Antifungal activities of bromophycolide-containing fractions were not significantly stronger than callophycoic acid/callophycol-containing fractions when each was tested at whole tissue natural concentrations (n=4 bromophycolide fractions, n=6 callophycoic acid/callophycol fractions; $p = 0.12$). None of these fractions were significantly inhibitory towards growth of the pathogenic bacterium *P. bacteriolytica* ($p = 0.32$ for n=4 bromophycolide fractions; $p = 0.29$ for n=6 callophycoic acid/callophycol fractions).

Pure bromophycolides and callophycoic acids are effective antifungal chemical defenses of *C. serratus*.

When natural products within algal extracts were quantified by LC-MS, bromophycolides were found to be associated exclusively with four algal collections, whereas callophycoic acids and callophycols were observed only in the other six collections (Appendix C), consistent with previous reports examining two populations of *Callophycus serratus* (Kubanek et al., 2006; Kubanek et al., 2005; Lane et al., 2007). Algal specimens were collected at a variety of sites in Fiji (Appendix C) and all matched recent morphological descriptions of *C. serratus* (Littler and Littler, 2003), suggesting this macroalga exists as two distinct chemotypes, one containing bromophycolides and the other callophycoic

acids and callophycols. Alternatively, these algae may represent cryptic, closely-related co-occurring species.

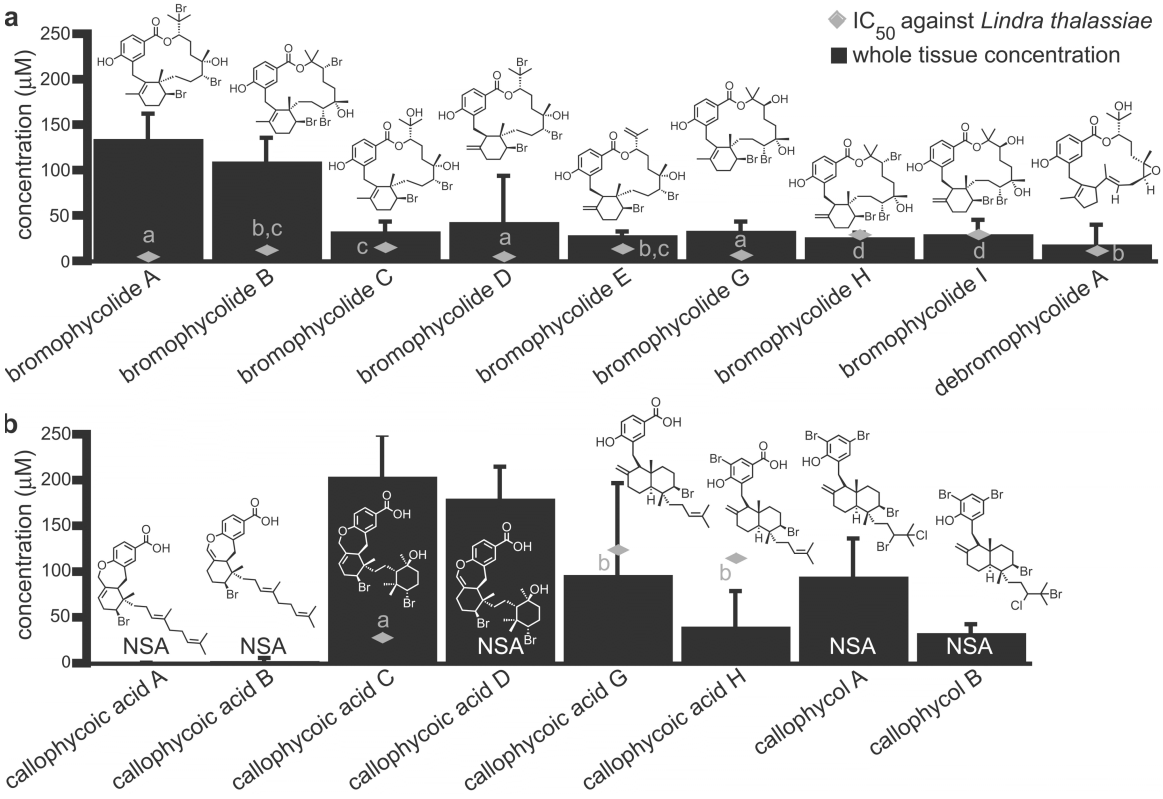

Fig. 5.1 Antifungal IC_{50} values (diamonds) and natural whole tissue concentrations (solid bars) of (a) bromophycolides and (b) callophycoic acids/callophycols. Natural whole tissue concentrations were determined by LC-MS analysis of extracts from (a) four *C. serratus* collections of the bromophycolide chemotype and (b) six collections of the callophycoic acid/callophycol chemotype (Appendix C); error bars denote one standard deviation in metabolite concentration. NSA denotes compounds that were not significantly active at the maximum tested concentration of 300 μM ($p > 0.05$), as determined by one-way ANOVA with Dunnett's post test comparison of treatments vs. controls. Among compounds within each chemotype, different letters indicate treatments differing significantly in antifungal IC_{50} values (F test, $p \leq 0.05$). Bromophycolide F and callophycoic acids E and F were neither detected in these extracts nor evaluated for antifungal activity.

All evaluated natural products from the bromophycolide chemotype of *C. serratus* significantly suppressed growth of the marine pathogenic fungus *L. thalassiae*, with average IC_{50} values for each compound near or below whole tissue natural concentrations (Fig. 5.1a). Among compounds of the callophycoic acid and callophycol chemotype, only callophycoic acids C, G, and H were effective below a concentration of 300 μM, and only callophycoic acids C and G were significantly growth inhibitory near their natural concentration range of 100-200 μM (Fig. 5.1b). The most potent compound evaluated from this chemotype, callophycoic acid C, was 100% inhibitory to *L. thalassiae* at its average natural whole tissue concentration (n=3), and may represent the dominant antifungal defense of this chemotype. The importance of other callophycoic acids and callophycols in antifungal defense cannot be ruled out, however, as these metabolites might interact additively or synergistically in controlling microbial adversaries.

Overall, macrocyclic lactone-based bromophycolides were found to be more potently antifungal than callophycoic acids or callophycols (Fig. 5.1a,b). Evaluation of structure-activity relationships among metabolites from each chemotype suggested the importance of specific functional groups in mediating ecological effects (see Discussion).

DESI-MS reveals heterogeneous distribution of bromophycolides on macroalgal surfaces.

With evidence supporting bromophycolides as potent antifungal chemical defenses of whole algal tissues, we next tested the hypothesis that these metabolites are concentrated on algal surfaces, a potentially advantageous site for control of microbial

infection. Given the strong antifungal activity and high relative abundance of bromophycolides A and B in whole tissues (Fig. 5.1a), these metabolites were selected as model compounds for analysis of chemical defenses on *C. serratus* surfaces.

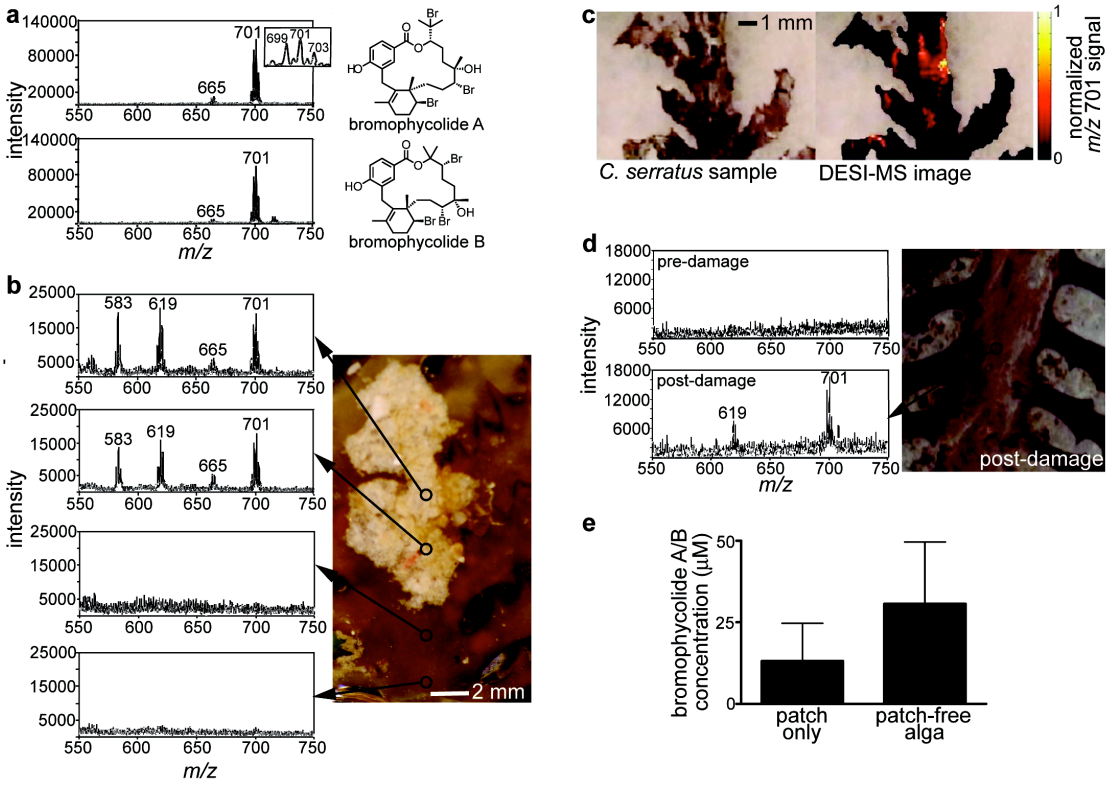

Fig. 5.2 Desorption electrospray ionization mass spectra (DESI-MS) of bromophycolides. (a) Mass spectra of pure bromophycolides A and B deposited on synthetic substrates (1 μL, 1 mg/mL solution). Ion clusters centered around *m/z* 665 and 701 correspond to [bromophycolide A/B - H]$^-$ and [bromophycolide A/B + Cl]$^-$, respectively. (b) Typical spatially-resolved mass spectra of *C. serratus* surface, showing that bromophycolides occur on algal surfaces only in association with light-colored patches (n = 40 sites observed on 6 independent algal samples). Ion clusters centered at 583 and 619 represent [bromophycolide E – H]$^-$ and [bromophycolide E + Cl]$^-$, respectively (Appendix C). (c) Imaging mass spectrum of *C. serratus* surface, indicating that bromophycolide A-B "hot spots" correspond to pale patches. (d) Representative mass spectrum from patch-free algal surface prior to and following mechanical damage (n = 2 damaged samples). (e) LC-MS quantification of combined bromophycolides A

and B from extracts of patches removed from algal surfaces and within whole, patch-free algal tissues.

Negative-mode DESI-MS analysis of pure bromophycolides on synthetic surfaces revealed a limit of detection of 0.9 pmol/mm^2 (signal:noise ratio = 6) for bromophycolide A, supporting the capacity of DESI-MS in assessing this class of secondary metabolites at low concentrations. Mass spectra of isomeric bromophycolides A and B were indistinguishable, each displaying a minor deprotonated ion centered around *m/z* 665 as well as a dominant chloride adduct centered at *m/z* 701 (Fig. 5.2a). Spatially-resolved DESI-MS analyses of sites across algal surfaces revealed these diagnostic bromophycolide A and B signals were associated exclusively with distinct light-colored patches attached to *C. serratus* surfaces (n=6 independent algal samples; Fig. 5.2b), a finding confirmed by imaging DESI-MS analysis (Fig. 5.2c). Additional patch-associated DESI-MS signals centered at *m/z* 583 and 619 were assigned as the $[M-H]^-$ ion and chloride adduct for bromophycolide E, based upon comparison with signals observed for pure standard compounds (Appendix C). Bromophycolide signals were not observed on clean, patch-free algal surface sites (Fig. 5.2b, c). Light microscopy provided evidence for algal cell integrity both before and after analyses (Appendix C), supporting DESI-MS as a general, non-destructive method for analysis of secondary metabolites on intact biological surfaces.

The combined concentration of bromophycolides A and B on patch surfaces was estimated at 36 ± 23 pmol/mm^2 by DESI-MS (n = 3 patches). Evaluation of the antifungal activity against *L. thalassiae* of combined bromophycolides A and B coated on

artificial substrates revealed a mean IC_{50} value of 17 pmol/mm^2 (log IC_{50} = 1.2 ± 0.1 SE), suggesting patch-associated bromophycolides sufficiently inhibit susceptible fungi. Supporting the DESI-MS results, LC-MS quantification of individual bromophycolides A and B within patches removed from algal surfaces revealed concentrations of 8.8 ± 7.6 and 4.3 ± 3.8 μM (± 1 SD), respectively. When tested at these average concentrations, bromophycolides A and B were significantly inhibitory to *L. thalassiae* (n = 3; $p < 0.01$ for bromophycolide A; $p < 0.05$ for bromophycolide B).

Having found surface-associated bromophycolides A and B among unusual patches (Fig. 5.2b, c), we then tested whether these compounds were located internally within algal tissue as well. DESI-MS analysis following physical damage to clean, bromophycolide-free algal surfaces revealed the presence of internal bromophycolides (n=2, Fig. 5.2d). Supporting the DESI-MS results, LC-MS revealed bromophycolides A and B in extracts of patch-free algal fragments (Fig. 5.2e).

Characterization of bromophycolide-containing agal surface patches.

Digital imaging revealed that 4.5 ± 4.3% (± 1 SD) of algal surfaces were covered with bromophycolide-containing light-colored patches (n=10 algal pieces examined). These distinctive patches were observed on both frozen and formalin-preserved algal samples.

Bromophycolide-rich patches were removed from algal surfaces, pulverized, and examined with light and epifluorescence microscopy. Epifluorescence microscopy revealed a variety of structures that stained with 4',6-diamidino-2-phylindole (DAPI; n=5). However, intact fluorescent nuclei were not observed for any structures, despite some structures with sizes suggestive of eukaryotic cells (~10 μm diameter and > 100 μm

length; Appendix C). This may be explained by DAPI staining of inorganic materials as can occur in complex natural mixtures (P.R. Jensen, personal communication). It is also plausible that exposure to high formalin concentrations (10%) during collection and storage of most samples resulted in nuclear lysis.

Patch-associated algal samples were sectioned and analyzed with light microscopy in an effort to further characterize these bromophycolide-rich surface regions. This processing resulted in loss of patches from algal samples, but permitted analysis of algal tissue underlying these patches. A variety of unusual cellular structures were observed (Fig. 5.3). Large-scale algal cell lysis was not observed in these sections. However, potential surface algal cell damage was detected in some sections and could suggest bromophycolides are released at these sites as a result of localized surface damage (Fig. 5.3a).

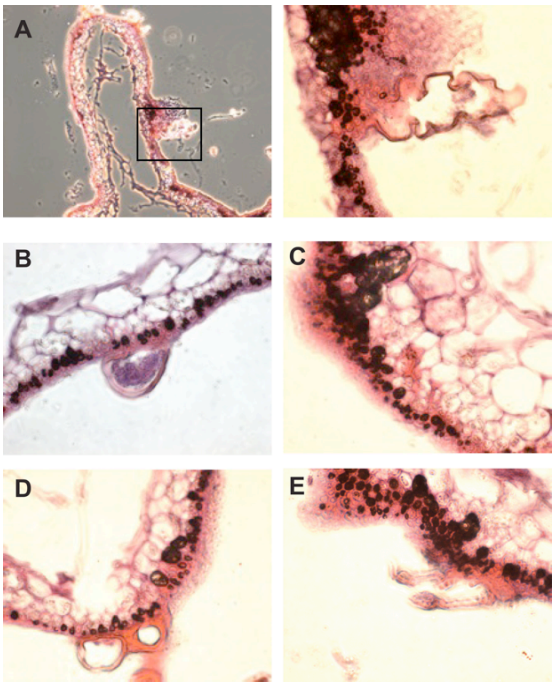

Fig 5.3 Light micrographs of 5 μm sections from *C. serratus* fragments associated with bromophycolide-containing patches. In all cases, sample processing dislodged patches from algal surfaces. (a) (left) 100× magnification of *C. serratus* section for which potential algal surface tissue damage was observed (highlighted with black box). (right) 400× magnification of region highlighted by black box. Large-scale cell damage was not observed; however, unusual protrusions, possibly indicative of localized damage, were noted. (b-d) Typical 400× micrographs of *C. serratus*, illustrating patched regions were not associated with large-scale tissue damage. In all cases, external algal surfaces are pointed downward. Unusual, potential bromophycolide-containing structures were observed in some sections (b, d, e).

Discussion

Antifungal effects of pure *Callophycus serratus* natural products: Structure-activity relationship insights

Collectively, the bromophycolides and callophycoic acids comprise the largest group of antifungal chemical defenses reported to date from marine algae, and offer unprecedented opportunity for understanding which molecular features confer antifungal function in an ecological context. Overall, the macrocyclic lactone-based

bromophycolides were found to be more potently antifungal than callophycoic acids or callophycols (Fig. 5.1a,b). The superior bioactivity of bromophycolides parallels trends in biomedical activities previously reported for these groups of compounds (Kubanek et al., 2006; Kubanek et al., 2005; Lane et al., 2007).

The most abundant 15-membered macrocyclic compound, bromophycolide A, was among the most antifungal, whereas bromophycolide B, the most abundant 16-membered macrolide, was not. Fifteen-membered macrolides bromophycolides A and D and 16-membered macrolide bromophycolide G, the most potent macrolides, did not exhibit significantly different antifungal IC_{50} values ($p = 0.17$-0.50), suggesting that neither macrocyclic cyclization mode (15 vs. 16-membered ring) confers an inherently superior chemical defense function (Fig. 5.1a, Appendix C).

Among bromophycolides of each macrolide framework, specific functional groups significantly impacted antifungal activity. Substitution of the isopropyl bromine (as in bromophycolide A) with a hydroxyl group (as in bromophycolide C) significantly reduced antifungal activity ($p = 0.0038$) among 15-membered macrolides. Dehydrobromination of the isopropyl moiety also led to reduced potency, as illustrated by comparison of activity between bromophycolides D and E ($p = 0.028$). Among 16-membered macrocyclic bromophycolides, the role of bromination in antifungal activity was less clear. Bromophycolide G, with a hydroxyl group near the terpene head, was significantly more antifungal than bromophycolide B, bearing a bromine group ($p < 0.0001$). Among bromophycolides H and I, however, the presence of a bromine vs. hydroxy group at the same position did not significantly affect antifungal activity ($p = 0.96$).

Among callophycoic acids, the relationship between structure and function was more dramatic. Tested up to 300 μM, callophycoic acid D did not significantly suppress *L. thalassiae* (data not shown), whereas callophycoic acid C, a regioisomer differing only in the position of a single olefinic group within the cyclohexene ring, was at least 10× more potent than callophycoic acid D (Fig. 5.1b). The highly substituted cyclohexanol group of callophycoic acid C also appeared important to its activity, as illustrated by the inactivity of callophycoic acid A.

Heterogeneous distribution of bromophycolides on macroalgal surfaces

Spatially-resolved DESI-MS revealed antifungal bromophycolides both within algal tissue and among distinct patches covering only ~5% of algal surfaces (Fig. 5.2b-d), and demonstrated the utility of mass spectrometry in exploring surface-mediated ecological interactions. Further, DESI-MS analysis revealed that bromophycolide concentrations on these surface patches were sufficient to suppress growth of *L. thalassiae* (see Results). These data should be considered semi-quantitative, as previous DESI-MS studies have shown that signal intensity is influenced by surface morphology (Nyadong et al., 2008b); hence, data are truly quantitative only across identical, homogenous surfaces – a feature not inherent in most biological materials. Despite these limitations, with an antifungal IC_{50} value of approximately half the measured concentration of bromophycolides on patches, it is probable that these compounds were present at sufficient levels for inhibition of fungi such as *L. thalassiae* that may encounter this substrate. This assertion was further supported by quantitative LC-MS experiments,

which showed that antifungal bromophycolides were present within patches at concentrations inhibitory to *L. thalassiae* (see Results).

The discovery of bromophycolides among heterogeneous patches on algal surfaces as well as within algal tissues suggests that *C. serratus* maintains these defenses internally and presents compounds only at select surface sites. Analogously, combined fluorescence microscopy- and chemical extraction-based investigations of *Asparagopsis armata* and *Delisea pulchra* revealed secondary metabolites to be found within gland cells of these red algae and released to algal surfaces, although triggers for compound release remain unclear (Dworjanyn et al., 1999; Paul et al., 2006a). In these previous investigations, heterogeneous distribution of compounds on algal surfaces was not observed. However, it is unlikely methods employed in these studies could have detected such small-scale variation.

A number of possibilities may explain the heterogeneous presentation of bromophycolides across *C. serratus* surfaces (Fig. 5.2b-c). One possibility is that bromophycolide-rich sites represent a targeted response to microbial challenge, although light and epifluorescence microscopy did not conclusively support the presence of patch-associated microbes (Appendix C). However, if bromophycolides are indeed effective antimicrobial chemical defenses in nature, one might expect low microbial abundances in bromophycolide-rich areas. It is also plausible that patches are associated with sites of localized algal cell damage from which bromophycolides are either purposefully or fortuitously presented. Light microscopy of patch-associated algal tissues indicated algal cells were predominantly intact (Fig. 5.3; Appendix C). However, the possibility of localized algal cell damage and associated bromophycolide up-regulation and/or release

cannot be fully ruled out. Macroalgae have been reported to up-regulate chemical defenses in response to bites from small grazers (Cronin and Hay, 1996; Pavia and Toth, 2000; Taylor et al., 2002), although it is unclear whether these defenses were induced throughout the alga or exclusively at sites of challenge.

Since the biosynthetic origin of bromophycolides has not yet been evaluated, it is plausible that bromophycolides are not actually algal natural products, instead being produced by a microbial symbiont present within algal tissues and/or distinct surface regions. Recent studies have provided convincing evidence that a number of secondary metabolites originally ascribed to sponges, bryozoans, and other macroorganisms are actually of microbial biosynthetic origin (Piel et al., 2004; Schmidt et al., 2005; Sudek et al., 2007). Further, microbial metabolites such as 2,3-indolinedione from a bacterium associated with crustacean embryos have been shown to defend hosts against pathogen infection (Gil-Turnes et al., 1989). In the case of bromophycolides, however, a microbial origin appears unlikely, given that microorganisms were not obvious within sections of *Callophycus serratus* (Fig. 5.3) and that epifluorescence microscopy revealed no consistently DAPI-stained microbes within bromophycolide-containing surface patches. Further, biosynthesis of terpenoid and shikimate natural products from red algae have been reported extensively (Moore, 2006), suggesting the capacity of macroalgae such as *C. serratus* to produce bromophycolide-like metabolites.

Chemically-mediated interactions between *C. serratus* and associated microbes may be further addressed by cultivation- or genomics-based experiments, and efforts are now underway to culture this macroalga as well as microorganisms associated with bromophycolide-rich algal surface patches. These approaches may permit further

characterization of potential patch-associated microbes and allow the effect of bromophycolides on such microbes to be addressed directly. These experiments may also permit testing of algal cells and alga-associated microbes for bromophycolide biosynthesis, and allow direct evaluation of such microbes for pathogenic, fouling, or symbiotic relationships with marine algae.

Significance

In the present study, evidence was provided that bromophycolides and callophycoic acids act as chemical defenses of the red alga *Callophycus serratus* against the pathogenic marine fungus *Lindra thalassiae*. Together, these compounds represent the largest group of algal antifungal chemical defenses reported to date, adding to only a handful of previously identified antimicrobial chemical defenses from macroalgae (Jiang et al., 2008; Kubanek et al., 2003; Nylund et al., 2008; Paul et al., 2006b; Puglisi et al., 2004). Spatially-resolved and imaging desorption electrospray ionization mass spectrometry (DESI-MS) provided an unprecedented ability to map secondary metabolites to distinct surface sites and revealed that bromophycolides are not homogenously distributed across *C. serratus* surfaces but instead associated with distinct patches. This appears to be among the first direct evidence for sub-millimeter presentation of chemical signals at specific sites on biological surfaces in concentrations sufficient for targeted antifungal defense. The heterogeneous natural product distributions observed in field-collected algal samples potentially represent essential, but until now, largely overlooked aspects of chemical signaling. Given the inherently small scale of marine microbe-host interactions, the imaging mass spectrometry technologies

demonstrated herein have the potential to revolutionize our understanding of these highly elusive biological interactions.

Materials and Methods

Isolation and quantification of *C. serratus* natural products. Bromophycolides, callophycoic acids, and callophycols were isolated from *C. serratus* following previously described procedures, and identified by comparison of ^{1}H NMR spectra and HR ESI-MS data with literature values (Kubanek et al., 2006; Kubanek et al., 2005; Lane et al., 2007). Pure compounds for DESI-MS, LC-MS, and antimicrobial assays were quantified by ^{1}H NMR spectroscopy using 2,5-dimethylfuran (DMFu, Sigma Aldrich) as internal standard (Gerritz and Sefler, 2000). For each natural product, aromatic proton signals were integrated and compared with intensities of two DMFu protons at 5.80 ppm.

For antimicrobial assays with chromatographic fractions and LC-MS quantification of metabolites from whole plant extracts, ten fresh *C. serratus* collections were extracted exhaustively with methanol and methanol/dichloromethane (2:1 and 1:1); extracts were reduced *in vacuo* and subjected to fractionation with HP20ss resin (Supelco). Fractions 1 and 2 were eluted with methanol/water (1:1 and 4:1, respectively), and fraction 3 with methanol followed by acetone. Fraction 3 contained all previously reported bromophyoclides, callophycoic acids, and callophycols.

Quantitative LC-MS was performed for each chromatographic fraction from all *C. serratus* collections applying a gradient mobile phase of acetonitrile/water (1:1 to 19:1), with 0.1% acetic acid throughout. For each natural product, negative-mode ESI-MS selected ion recordings were integrated for 2-3 *m/z* values corresponding to prominent

molecular ion cluster signals, and standard curves prepared by analysis of each compound at 5-7 concentrations (r^2 = 0.95-0.99). Concentrations of individual compounds within chromatographic fractions were calculated by interpolation from standard curve data.

Quantitative LC-MS experiments with patch-only and patch-free algal extracts were completed similarly. Pale patches were removed from algal surfaces by gently scraping with a razor blade, then pulverized and evaluated under light microscopy at 100× and 400× magnification to ensure the absence of algal cells. Underlying algal cells were also evaluated with light microscopy to verify cellular integrity. Three independent groups of 10-15 algal cell-free patches were quantified volumetrically and each individual group extracted in methanol. The absence of surface patches was verified by light microscopy for comparable volumetric quantities of three patch-free samples of whole *C. serratus*, which were then extracted in methanol. LC-MS quantification of bromophycolides A and B in these mixtures was completed as described above.

Antimicrobial assays. Assays with *Lindra thalassiae* (ATCC 56663) were completed as previously described (Kubanek et al., 2003). HP20ss fractions were solubilized in a minimal volume of acetone and incorporated into molten YPM agar (16 g/L granulated agar, 2 g/L yeast extract, 2 g/L peptone, 4 g/L D-mannitol, 250 mg/L of both streptomycin sulfate and penicillin G in 1 L of natural seawater) at concentrations approximating natural whole algal tissue concentrations. For each fraction, three 400 μL subsamples of this mixture were dispensed into sterile 24-well microtiter plates, allowed to solidify, and an aliquot of *L. thalassiae* suspension in sterile seawater added to each

well. Control wells were prepared with YPM agar and acetone but no algal material. Plates were incubated at 28 °C for three days and digital photographs collected for each well. The area calculator feature of ImageJ software (NIH) was applied to determine the percent of each well covered in fungal hyphae. Fungal coverage was averaged over each set of three subsample assays. These average values were pooled across corresponding fractions from other *C. serratus* collections of the same chemotype, and fungal coverage of treatment and control wells compared using one-way ANOVA with Dunnett's post test (Zar, 1998).

Antifungal assays with pure bromophycolides, callophycoic acids, and callophycols were completed as with extract fractions. Individual compounds were incorporated into molten YPM agar at 1:1 serially diluted concentrations ranging from 300 μM to 0.15 μM and n=3 assays completed at each concentration. Significant growth inhibition at the maximum tested concentration was established by comparison of individual treatments with solvent-only controls applying one-way ANOVA with Dunnett's post test (Zar, 1998). For compounds significantly inhibitory ($p \leq 0.05$) at the maximum tested concentration, inhibition data were fit to a sigmoidal dose-response curve; mean log IC_{50} and standard error values were calculated. Reported IC_{50} values were determined by computing the antilog of mean log IC_{50} values; standard errors for IC_{50} values were not determined, as such values are not directly correlated with log IC_{50} standard errors (Motulsky and Christopoulos, 2003). Significant antifungal activity differences among active compounds were analyzed with an F test of the log IC_{50} value for each compound (Motulsky and Christopoulos, 2003).

Antibacterial assays using *Pseudoalteromonas bacteriolytica* (ATCC 700679) were adapted from previously reported methods (Kubanek et al., 2003). A 24 h shake culture of *P. bacteriolytica* was diluted 1:160 in Difco Marine Broth 2216 (BD Biosciences) and 195 μL of this mixture added to duplicate treatment and control wells of a 96-well plate. An equal amount of sterile marine broth was added to blank wells. Five microliters of 40× concentrated HP20ss fractions in DMSO were then dispensed into all treatment and blank wells, giving a final concentration approximating natural whole tissue concentrations in the alga; five microliters of DMSO were added to corresponding control wells. Plates were incubated at 30 °C for 24 h and turbidity measured at a wavelength of 600 nm. We corrected for the natural absorbance of extract fractions by subtracting extract-only sterile blank turbidities from values obtained for treatments. For individual fractions from each *C. serratus* collection, turbidity values from n=2 subsample assays were averaged and these data pooled with corresponding fractions from other *C. serratus* collections of the same chemotype. Turbidities for individual fractions were statically compared with one those obtained for no-extract controls using a one-tailed, unpaired *t*-test (Zar, 1998).

To establish a role of bromophycolides in antifungal defense of algal surfaces, 2:1 bromophycolide A and B solutions were serially diluted (1:1) in ethyl ether and 30 μL aliquots dispensed as evenly as possible over the surface of 400 μL solidified YPM agar blocks (200 mm^2 area) in 24-well microtiter plates, and allowed to air dry. Assuming even distribution of bromophycolides A and B across agar surfaces and negligible absorption of compounds into agar blocks, this corresponded to combined surface concentrations ranging from 340 $pmol/mm^2$ to 1.3 $pmol/mm^2$ (n = 2 assays at each

concentration). Solvent-only control wells were prepared equivalently. Surfaces of treatment and control wells were inoculated with a suspension of *L. thalassiae* in sterile seawater and incubated at 28 °C for 3 days. *L. thalassiae* growth was assessed and the log IC_{50} value computed as before.

DESI-MS analyses. DESI-MS was performed with a custom-built DESI ion source as previously described (Nyadong et al., 2008a). Experiments were performed by subjecting targeted surface sites to a DESI spray solution of 100 μM NH_4Cl (Sigma Aldrich) in 100 % MeOH at a flow rate of 5 μL/min; the DESI spray covered a surface area of approximately 0.25 mm^2. The nebulizer gas pressure was set at 110 psi and the spray solution electrically charged externally to -3 kV. All experiments were performed on an LCQ DECA XP+ ion trap mass spectrometer (Thermo Finnigan, San Jose, CA) operated in negative ion mode. The ion transfer capillary was held at 300 ^oC, and data were collected in full scan mode (*m/z* 550-750) using Xcalibur software version 2.0 (Thermo Finnigan). In all experiments, the instrument was set to collect spectra in automatic gain mode for a maximum ion trap injection time of 200 ms at 2 microscans per spectrum for a total acquisition time of 10 s.

To determine the limit of detection for pure bromophycolide A on a model substrate, serially diluted solutions of this compound in MeOH were deposited on measured areas of polytetrafluoroethylene (PTFE) surfaces. The MeOH was allowed to air dry prior to analysis, giving a surface concentration range of 0.9 fmol/mm^2 to 0.9 pmol/mm^2. The detection limit was recorded as the surface concentration at which S/N = 6.

Algal samples (approx. 1.0-1.5 cm length; 0.2-1.0 cm width), preserved with 10% formalin in seawater, were affixed to PTFE substrates with double-sided tape for DESI-MS analysis and samples kept moist with seawater; no additional sample pretreatment was completed. Algal cell integrity was verified before and after DESI-MS experiments by evaluation under a light microscope at 100× and 400× magnification. For each of six evaluated patch-containing algal samples, 6-8 independent sites were targeted with the DESI spray beam. These sites comprised both patch-covered areas and areas of clean alga representing all surface morphological features.

For DESI-MS experiments comparing bromophycolide levels on the intact surface of clean, patch-free alga with those found within damaged tissue, two intact *C. serratus* pieces (approx. 1.0-1.5 cm length; 0.2-1.0 cm max. width) were first evaluated for bromophycolides by rastering, or continuously bombarding the algal surface with DESI spray while gradually moving the beam along the entire length of the sample. These intact algal pieces were then wounded by scraping with a razor blade and evaluated again at approximately the same sites as before.

Concentrations of bromophycolides A+B on intact patch surfaces were estimated by comparing integrals from chloride adduct DESI-MS signals for individual sites on patches with a standard curve developed by depositing known concentrations of bromophycolides A and B (2:1) on intact patch-free algal surfaces of known surface area ($r^2 = 0.97$, n = 4 standards analyzed in triplicate). Total standard surface concentrations of bromophycolides A and B ranged from 2.4 to 120 pmole/mm^2. The 2:1 ratio of bromophycolides A and B represented a reasonable approximation based on the average 2.2:1 ratio observed by LC-MS for these compounds in extracts from patches.

DESI-MS imaging experiments were conducted with the above-described mass spectrometer, equipped with a joystick and software-controlled motorized microscope xy stage (Prior Scientific, Rockland, MA). The mass spectrometer was operated in automatic gain control (AGC) off mode with trapping time of 40 milliseconds. DESI-MS imaging experiments are similar to standard DESI-MS experiments, except the sample stage is scanned according to a pattern in the xy plane. Chemical images were acquired using a looped stage scanning mode, controlled by LabVIEW automation software (National Instruments Corporation, Austin, TX). In this mode, the xy stage was first moved by a predetermined distance in the x-dimension (orthogonal to the entrance capillary) from left to right and the same distance right to left, followed by a y-dimension step movement in the forward direction. The stage scan speed in both dimensions was set to 80 μm/s and the step size in the y-dimension was set to 200 μm. Mass spectra were collected in continuous full-scan MS mode, over the *m/z* range of 200-800. The electrospray plume was held at a fixed angular position, pointing towards the sampling surface. HPLC grade methanol was used as the imaging DESI electrospray solvent, at a flow rate of 3 μL min^{-1}. The nebulizer gas pressure was set at 110 psi. Mass spectra of each spray impact region were collected and relevant bromophycolide signals were processed and transformed into an image using an in-house written MATLAB user program (version R2008a, MathWorks, Inc. Natick, MA).

Microscopy of bromophycolide-containing surface patches. The percentage of *C. serratus* surfaces covered with distinctive patches was estimated by randomly clipping segments from ten collections of *C. serratus* (approx. 1.0-1.5 cm length; 0.2-1.0 cm

width), digitally photographing under a dissection microscope (~25×), and analyzing images with the area calculator feature of ImageJ software (NIH) to compare the number of pixels covered in distinctive patches to pixels containing clean, patch-free alga. To better understand the nature of these distinctive surface regions, four groups of 2-4 patches were removed from algal surfaces with a razor blade and/or forceps, pulverized, and observed under a light microscope at total magnifications ranging from 100× to 1000×. Testing for autofluorescence, unstained samples were observed with epifluorescence microscopy at FITC and DAPI excitation wavelengths of 490 and 360 nm, respectively. Samples were then stained with DAPI (Porter and Feig, 1980), and again observed at the DAPI excitation wavelength.

Sections of *C. serratus* with attached bromophycolide-containing patches were frozen and sectioned into 5 micron-thick pieces with a microtome. Resulting sections were stained with hematoxylin and eosin and examined by light microscopy at 100× and 400× magnification.

Works Cited

Cooks, R. G., Ouyang, Z., Takats, Z., and Wiseman, J. M. (2006). Ambient mass spectrometry. Science *311*, 1566-1570.

Cotte-Rodriguez, I., Takats, Z., Talaty, N., Chen, H. W., and Cooks, R. G. (2005). Desorption electrospray ionization of explosives on surfaces: Sensitivity and selectivity enhancement by reactive desorption electrospray ionization. Analytical Chemistry *77*, 6755-6764.

Cronin, G., and Hay, M. E. (1996). Induction of seaweed chemical defenses by amphipod grazing. Ecology *77*, 2287-2301.

Dworjanyn, S. A., De Nys, R., and Steinberg, P. D. (1999). Localisation and surface quantification of secondary metabolites in the red alga *Delisea pulchra*. Marine Biology *133*, 727-736.

Engel, S., Jensen, P. R., and Fenical, W. (2002). Chemical ecology of marine microbial defense. Journal of Chemical Ecology *28*, 1971-1985.

Engel, S., Puglisi, M. P., Jensen, P. R., and Fenical, W. (2006). Antimicrobial activities of extracts from tropical Atlantic marine plants against marine pathogens and saprophytes. Marine Biology *149*, 991-1002.

Esquenazi, E., Coates, C., Simmons, L., Gonzalez, D., Gerwick, W. H., and Dorrestein, P. C. (2008). Visualizing the spatial distribution of secondary metabolites produced by marine cyanobacteria and sponges via MALDI-TOF imaging. Molecular Biosystems *4*, 562-570.

Gerritz, S. W., and Sefler, A. M. (2000). 2,5-dimethylfuran (DMFu): An internal standard for the "traceless" quantitation of unknown samples via H-1 NMR. Journal of Combinatorial Chemistry *2*, 39-41.

Gil-Turnes, M. S., Hay, M. E., and Fenical, W. (1989). Symbiotic marine bacteria chemically defend crustacean embryos from a pathogenic fungus. Science *246*, 116-118.

Harvell, C. D., Kim, K., Burkholder, J. M., Colwell, R. R., Epstein, P. R., Grimes, D. J., Hofmann, E. E., Lipp, E. K., Osterhaus, A., Overstreet, R. M*., et al.* (1999). Review: Marine ecology - Emerging marine diseases - Climate links and anthropogenic factors. Science *285*, 1505-1510.

Jiang, R. W., Lane, A. L., Mylacraine, L., Hardcastle, K. I., Fairchild, C. R., Aalbersberg, W., Hay, M. E., and Kubanek, J. (2008). Structures and absolute configurations of sulfate conjugated triterpenoids including an antifungal chemical defense of the marine green alga *Tydemania expeditionis*. Journal of Natural Products *71*, 1616-1619.

Karban, R., and Baldwin, I. T. (1997). Induced Responses to Herbivory (Chicago: University of Chicago Press).

Kelly, S. R., Jensen, P. R., Henkel, T. P., Fenical, W., and Pawlik, J. R. (2003). Effects of Caribbean sponge extracts on bacterial attachment. Aquatic Microbial Ecology *31*, 175-182.

Kim, K., Kim, P. D., Alker, A. P., and Harvell, C. D. (2000). Chemical resistance of gorgonian corals against fungal infections. Marine Biology *137*, 393-401.

Kohlmeyer, J. (1971). Fungi from the Sargasso Sea. Marine Biology *8*, 344-350.

Kohlmeyer, J., and Kohlmeyer, E. (1979). Marine Mycology: The higher fungi (New York: Academic Press).

Koricheva, J. (2002). Meta-analysis of sources of variation in fitness costs of plant antiherbivore defenses. Ecology *83*, 176-190.

Kubanek, J., Jensen, P. R., Keifer, P. A., Sullards, M. C., Collins, D. O., and Fenical, W. (2003). Seaweed resistance to microbial attack: A targeted chemical defense against marine fungi. Proceedings of the National Academy of Sciences of the United States of America *100*, 6916-6921.

Kubanek, J., Prusak, A. C., Snell, T. W., Giese, R. A., Fairchild, C. R., Aalbersberg, W., and Hay, M. E. (2006). Bromophycolides C-I from the Fijian red alga Callophycus serratus. Journal of Natural Products *69*, 731-735.

Kubanek, J., Prusak, A. C., Snell, T. W., Giese, R. A., Hardcastle, K. I., Fairchild, C. R., Aalbersberg, W., Raventos-Suarez, C., and Hay, M. E. (2005). Antineoplastic diterpene-benzoate macrolides from the Fijian red alga Callophycus serratus. Organic Letters *7*, 5261-5264.

Kubanek, J., Whalen, K. E., Engel, S., Kelly, S. R., Henkel, T. P., Fenical, W., and Pawlik, J. R. (2002). Multiple defensive roles for triterpene glycosides from two Caribbean sponges. Oecologia *131*, 125-136.

Lane, A. L., and Kubanek, J. (2008). Secondary metabolite defenses against pathogens and biofoulers, In Algal Chemical Ecology, C. D. Amsler, ed. (Berlin: Springer), pp. 229-243.

Lane, A. L., Stout, E. P., Hay, M. E., Prusak, A. C., Hardcastle, K., Fairchild, C. R., Franzblau, S. G., Le Roch, K., Prudhomme, J., Aalbersberg, W., and Kubanek, J. (2007). Callophycoic acids and callophycols from the Fijian red alga *Callophycus serratus*. Journal of Organic Chemistry *72*, 7343-7351.

Littler, D. S., and Littler, M. M. (2003). South Pacific Reef Plants (Washington, D.C.: Offshore Graphics, Inc.).

Maximilien, R., de Nys, R., Holmstrom, C., Gram, L., Givskov, M., Crass, K., Kjelleberg, S., and Steinberg, P. D. (1998). Chemical mediation of bacterial surface colonisation by secondary metabolites from the red alga *Delisea pulchra*. Aquatic Microbial Ecology *15*, 233-246.

Moore, B. S. (2006). Biosynthesis of marine natural products: macroorganisms (Part B). Natural Product Reports *23*, 615-629.

Motulsky, H. J., and Christopoulos, A. (2003). Fitting models to biological data using linear and nonlinear regression. A practical guide to curve fitting. (San Diego: GraphPad Software, Inc.).

Nyadong, L., Green, M. D., De Jesus, V. R., Newton, P. N., and Fernandez, F. M. (2007). Reactive desorption electrospray ionization linear ion trap mass spectrometry of latest-generation counterfeit antimalarials via noncovalent complex formation. Analytical Chemistry *79*, 2150-2157.

Nyadong, L., Hohenstein, E. G., Johnson, K., Sherrill, C. D., Green, M. D., and Fernandez, F. M. (2008a). Desorption electrospray ionization reactions between host crown ethers and the influenza neuraminidase inhibitor Oseltamivir for the rapid screening of Tamiflu®. The Analyst *In press.*

Nyadong, L., Late, S., Green, M. D., Banga, A., and Fernandez, F. M. (2008b). Direct quantitation of active ingredients in solid artesunate antimalarials by noncovalent complex forming reactive desorption electrospray ionization mass spectrometry. Journal of the American Society for Mass Spectrometry *19*, 380-388.

Nylund, G. M., Cervin, G., Hermansson, M., and Pavia, H. (2005). Chemical inhibition of bacterial colonization by the red alga *Bonnemaisonia hamifera*. Marine Ecology-Progress Series *302*, 27-36.

Nylund, G. M., Cervin, G., Persson, F., Hermansson, M., Steinberg, P. D., and Pavia, H. (2008). Seaweed defence against bacteria: a poly-brominated 2-heptanone from the red alga *Bonnemaisonia hamifera* inhibits bacterial colonisation. Marine Ecology-Progress Series *369*, 39-50.

Nylund, G. M., Gribben, P. E., de Nys, R., Steinberg, P. D., and Pavia, H. (2006). Surface chemistry versus whole-cell extracts: antifouling tests with seaweed metabolites. Marine Ecology-Progress Series *329*, 73-84.

Nylund, G. M., and Pavia, H. (2003). Inhibitory effects of red algal extracts on larval settlement of the barnacle Balanus improvisus. Marine Biology *143*, 875-882.

Paul, N. A., Cole, L., de Nys, R., and Steinberg, P. D. (2006a). Ultrastructure of the gland cells of the red alga *Asparagopsis armata* (Bonnemaisoniaceae). Journal of Phycology *42*, 637-645.

Paul, N. A., de Nys, R., and Steinberg, P. D. (2006b). Chemical defence against bacteria in the red alga *Asparagopsis armata*: linking structure with function. Marine Ecology-Progress Series *306*, 87-101.

Paul, V. J., Puglisi, M. P., and Ritson-Williams, R. (2006c). Marine chemical ecology. Natural Product Reports *23*, 153-180.

Paul, V. J., and Ritson-Williams, R. (2008). Marine chemical ecology. Natural Product Reports *25*, 662-695.

Pavia, H., and Toth, G. B. (2000). Inducible chemical resistance to herbivory in the brown seaweed Ascophyllum nodosum. Ecology *81*, 3212-3225.

Piel, J., Hui, D. Q., Wen, G. P., Butzke, D., Platzer, M., Fusetani, N., and Matsunaga, S. (2004). Antitumor polyketide biosynthesis by an uncultivated bacterial symbiont of the marine sponge Theonella swinhoei. Proceedings of the National Academy of Sciences of the United States of America *101*, 16222-16227.

Porter, K. G., and Feig, Y. S. (1980). The use of DAPI for identifying and counting aquatic microflora. Limnology and Oceanography *25*, 943-948.

Puglisi, M., Engel, S., Jensen, P., and Fenical, W. (2006). Antimicrobial activities of extracts from Indo-Pacific marine plants against marine pathogens and saprophytes. Marine Biology.

Puglisi, M. P., Tan, L. T., Jensen, P. R., and Fenical, W. (2004). Capisterones A and B from the tropical green alga Penicillus capitatus: unexpected anti-fungal defenses targeting the marine pathogen Lindra thallasiae. Tetrahedron *60*, 7035-7039.

Sawabe, T., Makino, H., Tatsumi, M., Nakano, K., Tajima, K., Iqbal, M. M., Yumoto, I., Ezura, Y., and Christen, R. (1998). Pseudoalteromonas bacteriolytica sp. nov., a marine bacterium that is the causative agent of red spot disease of Laminaria japonica. International Journal of Systematic Bacteriology *48*, 769-774.

Schmidt, E. W., Nelson, J. T., Rasko, D. A., Sudek, S., Eisen, J. A., Haygood, M. G., and Ravel, J. (2005). Patellamide A and C biosynthesis by a microcin-like pathway in Prochloron didemni, the cyanobacterial symbiont of Lissoclinum patella. Proceedings of the National Academy of Sciences of the United States of America *102*, 7315-7320.

Schmitt, T. M., Hay, M. E., and Lindquist, N. (1995). Constraints on Chemically Mediated Coevolution - Multiple Functions for Seaweed Secondary Metabolites. Ecology *76*, 107-123.

Simmons, T. L., Coates, R. C., Clark, B. R., Engene, N., Gonzalez, D., Esquenazi, E., Dorrestein, P. C., and Gerwick, W. H. (2008). Biosynthetic origin of natural products isolated from marine microorganism-invertebrate assemblages. Proceedings of the National Academy of Sciences of the United States of America *105*, 4587-4594.

Steinberg, P. D., de Nys, R., and Kjelleberg, S. (2001). Chemical Mediation of Surface Colonization, In Marine Chemical Ecology, J. B. McClintock, and B. J. Baker, eds. (Boca Raton: CRC Press), pp. 355-387.

Sudek, S., Lopanik, N. B., Waggoner, L. E., Hildebrand, M., Anderson, C., Liu, H. B., Patel, A., Sherman, D. H., and Haygood, M. G. (2007). Identification of the putative bryostatin polyketide synthase gene cluster from "Candidatus endobugula sertula", the

uncultivated microbial symbiont of the marine bryozoan Bugula neritina. Journal of Natural Products *70*, 67-74.

Takats, Z., Wiseman, J. M., Gologan, B., and Cooks, R. G. (2004). Mass spectrometry sampling under ambient conditions with desorption electrospray ionization. Science *306*, 471-473.

Talaty, N., Takats, Z., and Cooks, R. G. (2005). Rapid in situ detection of alkaloids in plant tissue under ambient conditions using desorption electrospray ionization. Analyst *130*, 1624-1633.

Taylor, R. B., Sotka, E., and Hay, M. E. (2002). Tissue-specific induction of herbivore resistance: seaweed response to amphipod grazing. Oecologia *132*, 68-76.

Wiseman, J. M., Ifa, D. R., Song, Q. Y., and Cooks, R. G. (2006). Tissue imaging at atmospheric pressure using desorption electrospray ionization (DESI) mass spectrometry. Angewandte Chemie-International Edition *45*, 7188-7192.

Zar, J. H. (1998). Biostatistical Analysis, 4 edn: Prentice Hall).

CHAPTER 6

ECOLOGICAL LEADS FOR NATURAL PRODUCT DISCOVERY: NOVEL SESQUITERPENE HYDROQUINONES FROM A CRUSTOSE RED ALGA

Abstract

Biomedically-motivated marine natural product investigations have yielded structurally-unique compounds with interesting pharmacological properties, but the natural roles of these molecules remain largely unknown. Some of these secondary metabolites may function as antimicrobial chemical defenses. However, defensive roles have been demonstrated for only a few compounds. In the present study, chromatographic fractions from 72 collections of Fijian red macroalgae were evaluated for growth inhibition of three microbial pathogens and saprophytes of marine macrophytes. At least one microbe was suppressed by fraction(s) of all evaluated algae, suggesting that antimicrobial defenses are common among tropical red macroalgae. From these leads, fijioic acids A-B (**1**-**2**), novel sesquiterpene hydroquinones, were isolated from an unidentified crustose red alga, with antibacterial activity against *Pseudoalteromonas bacteriolytica*, a pathogen of marine algae. These compounds included one novel carbon skeleton and illustrated the utility of ecological studies in natural product discovery.

Introduction

Marine organisms including sponges, microbes, and seaweeds are widely recognized sources of structurally novel secondary metabolites (Blunt et al., 2007; Blunt et al., 2008). These natural products have provided promising drug leads, offered targets for synthetic organic chemists, and afforded opportunities for elucidation of unusual

biosynthetic pathways. Secondary metabolite pathways probably evolved as a result of interactions between organisms in their native habitats, but the role of natural products in mediating such interactions remains poorly understood in the vast majority of cases.

Secondary metabolites may play a particularly important role in mediating marine host-microbe interactions (Engel et al., 2002; Lane and Kubanek, 2008). While the majority of microbes may be innocuous or beneficial to hosts, reports of pathogen outbreaks in a variety of marine macroorganisms suggest considerable negative impact of some microbes on coral reef health and thus the potential for selection to resist pathogenic microbes. Among marine plants, coralline lethal orange disease devastated susceptible South Pacific coralline algal populations during the 1990s (Littler and Littler, 1995), red spot disease has impacted commercially valuable kelp populations (Sawabe et al., 1998), a slime mold wasting epidemic destroyed nearly all *Zosteria marina* eelgrass in the North Atlantic during the 1930s (Short et al., 1987), and the pathogenic fungus *Lindra thalassiae* has been reported to cause both raisin disease in the brown algae *Sargassum* spp. and as well as disease in seagrasses (Kohlmeyer, 1971; Porter, 1986). Disease outbreaks affect not only susceptible populations, but can also disturb the structure and function of entire marine communities (Harvell et al., 1999).

Despite the abundance of microbes in marine environments, disease outbreaks appear sporadic and pathogens appear to target specific hosts (Harvell et al., 1999). One possible explanation for this limited disease prevalence is that secondary metabolites defend some species against microbial attack (Engel et al., 2002), but only a handful of studies have investigated this possibility and even fewer have identified specific defensive metabolites. Two previous surveys of macroalgae suggested that antimicrobial

chemical defenses are widespread among marine plants (Engel et al., 2006; Puglisi et al., 2006). Previously reported antimicrobial chemical defenses fall into four classes: halogenated furanones from the red alga *Delisea pulchra* were shown to inhibit colonization of a variety of genera of marine bacteria,(Kjelleberg et al., 1997) a macrocyclic polyketide from the brown alga *Lobophora variegata* was reported to inhibit growth of a pathogenic fungus (Kubanek et al., 2003), a flavone glycoside from the seagrass *Thalassia testudinum* was demonstrated to inhibit a zoosporic fungus (Jensen et al., 1998), and sulfated triterpenes from *Penicillus capitatus* and *Tydemania expeditionis* were reported as growth-inhibitory antifungal agents (Jiang et al., In press.; Puglisi et al., 2004).

Herein, we evaluate antimicrobial chemical defenses for 72 collections of Fijian red macroalgae, providing evidence that chemical defenses represent a wide range of polarities and suggesting these defenses are not broad-spectrum but instead active against specific microbes. Although not commonly investigated as sources of novel natural products, members of the order Cryptonemiales exhibited particularly strong antimicrobial activities in ecological assays. Bioassay-guided fractionation with of extracts from one unidentified species of this group resulted in the discovery of fijioic acids A-B (**1**-**2**), representing one novel carbon skeleton and illustrating the potential of ecology-motivated studies in the discovery of novel natural products.

Results and Discussion

Survey of antimicrobial chemical defenses among Fijian red macroalgae.

Among chromatographic fractions from 72 collections of tropical red macroalgae (Supporting Information), antimicrobial chemical defenses were prevalent against the bacterial pathogen *Pseudoalteromonas bacteriolytica*, known to cause red spot disease in kelp, and the fungal pathogen *Lindra thalassiae*, known to infect phylogenetically distant hosts including *Sargassum* spp. brown algae and seagrasses. For 95% of the 72 algal collections, at least one chromatographic fraction was significantly active against *P. bacteriolytica* at natural whole tissue concentrations; for 75% of collections, at least one fraction was active against *L. thalassiae*. *Dendryphiella salina*, a saprophytic marine fungus, was more resistant to algal chemical defenses, with only 30% of collections exhibiting at least one fraction with significant activity against this saprophyte. This suggests that tropical red algal antimicrobial chemical defenses may be tuned to protect against pathogenic microbes, but not to provide general defense against all microbes. Overall, at least one fraction from all 72 seaweeds exhibited significant activity against one or more microbes. This prevalence of antimicrobial activity suggests that red algae have been selected to deter deleterious microbes via chemical defenses.

All four chromatographic fractions were represented among antimicrobial fractions, suggesting that a variety of secondary metabolite classes of differing polarities afford antimicrobial defense (Fig. 6.1a). Among fractions significantly inhibiting *P. bacteriolytica*, the most polar fractions tended to be more inhibitory than the less polar fractions (Fig. 6.1b). For fungal pathogen *L. thalassiae*, however, this trend was reversed, with the most polar fraction less inhibitory than more lipophilic fractions (Fig.

6.1b). No correlations were observed between antimicrobial potencies for *L. thalassiae* vs. *D. salina*, *L. thalassiae* vs. *P. bacteriolytica*, or *D. salina* vs. *P. bacteriolytica* ($r^2 <$ 0.21). This suggests that algal chemical defenses are not multifunctional against a wide variety of microbial genera, but instead relatively targeted. This specificity may serve an important natural function in warding off deleterious microbes, while leaving commensal or mutualistic microbes unharmed.

The high prevalence of antimicrobial activities observed among chromatographic fractions from several orders of red macroalgae (Appendix D) suggests the potential of ecology-driven studies in the discovery of novel chemistry. A search of the MarineLit database revealed secondary metabolites have been previously reported for only 40% of these evaluated genera (n=20 identified to genus level, excluding as-yet unidentified genera, Supporting Information), suggesting a wealth of ecologically active natural products remain to be identified.

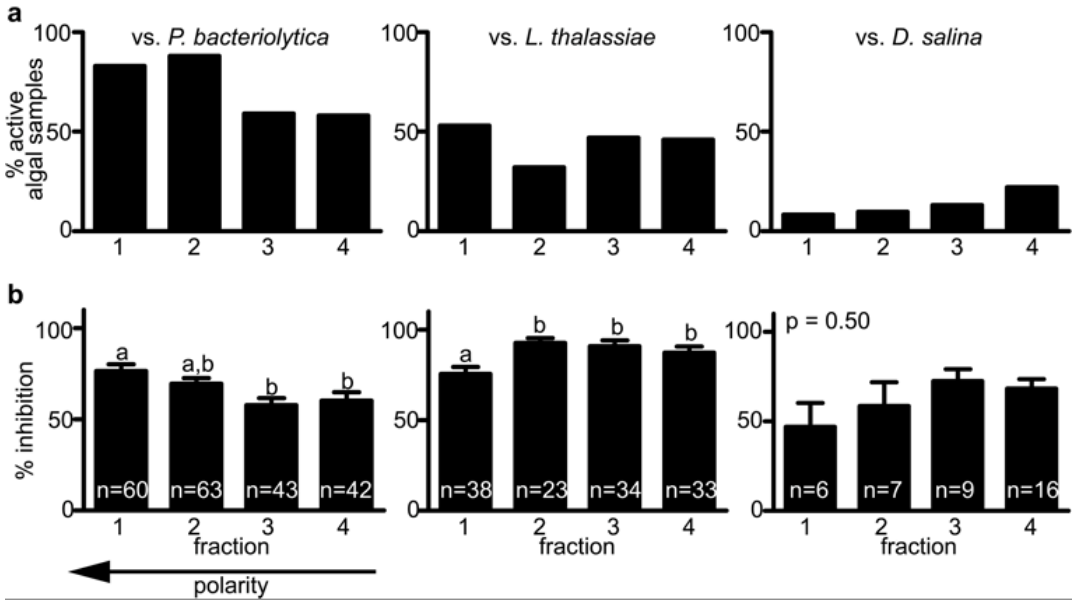

Fig. 6.1 Antimicrobial activities of individual chromatographic fractions from 72 collections of Fijian red macroalgae, against algal pathogenic bacterium *Pseudoalteromonas bacteriolytica*, algal pathogenic fungus *Lindra thalassiae*, and algal saprophyte *Dendryphiella salina*. (a) Frequency of significant antimicrobial activity at natural whole tissue concentrations (n=72). (b) Comparison of inhibitory potency among active fractions at natural whole tissue concentrations. Different letters indicate treatments differing significantly in antimicrobial activity (one-way ANOVA with Tukey post test; bars denote standard error); n represents the number of significantly active fractions compared.

Novel antimicrobial sequiterpene hydroquinones from crustose red alga.

Among chromatographic fractions from 72 collections of Fijian red algae, fraction 2 from an unidentified crustose red alga (Collection ID# G-0109) exhibited particularly potent inhibition of all evaluated microbes and was selected as a candidate for ecology-guided natural product isolation and identification. Guided by growth inhibitory activity against the pathogenic bacterium *Pseudoalteromonas bacteriolytica*, fijioic acids A-B (**1**-**2**) were isolated by reversed-phase HPLC (see Materials and Methods).

Fijioic acid A (**1**) displayed an $[M - H]^-$ molecular ion with *m/z* 449.1309 and a characteristic monobrominated isotopic pattern, supporting a molecular formula of $C_{23}H_{31}O_4Br$. The structure of **1** was established through analyses of 1D and 2D NMR spectral data (Table 6.1, Supporting Information). Assignments within the aromatic group of **1** were established by HMBC correlations from H-5 (δ 6.35) to C-3 (δ 122.6), C-4 (δ 150.1) and C-20 (δ 146.1), and from H-19 (δ 6.31) to aromatic C-4, C-6 (δ 126.6), and C-20. These assignments were confirmed and *para* dihydroxy substitution established by comparison of experimental ^{13}C chemical shifts with empirical and literature values (Silverstein and Webster, 1998; Talpir et al., 1994). HMBC correlations from H-19 to C-2 (δ 44.5), along with correlations from H-2 (δ 3.09) to C-1 (δ 175.3), C-3, C-4, and C-19 (δ 116.6) then established an acetic acid substituent attached at C-3. The connection to the sesquiterpene group was then assigned at C-6 on the basis of HMBC correlations from H-5 to C-7 (δ 30.3) and from both C-7 protons (δ 2.13, δ 2.77) to C-5, C-6, and C-20.

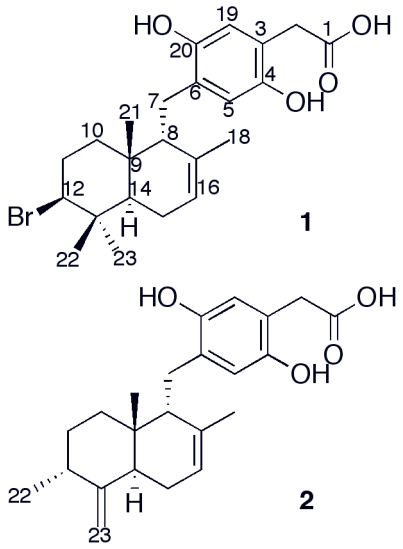

Structures of novel fijioic acids A and B (**1**-**2**).

The bromine-substituted drimane sesquiterpene of **1** was elucidated primarily through analysis of HMBC and COSY data. HMBC correlations from singlet Me-18 (δ 1.49) to C-8 (δ 53.7), C-16 (δ 119.2), and C-17 (δ 136.7) prompted assignment of this methyl group attached to C-17 and established C-8—C-17—C-16 connectivity. HMBC correlations from singlet Me-21 (δ 0.86) to C-8, C-9 (δ 36.4), and C-10 (δ 36.3) next established connectivity between these carbons. COSY correlations between H-10a (δ 0.99) and H-11a (δ 1.93), between H-10b (δ 1.88) and H-11b (δ 2.13), and between both H-11 protons and H-12 (δ 4.20) prompted linkage of C-10—C-11—C-12, with these assignments confirmed by an HMBC correlation from H-11b (δ 2.13) to C-10. A bromine substituent was assigned at C-12 on the basis of downfield ^{13}C and ^{1}H chemical shifts (δ 70.9 and δ 4.20, respectively). HMBC correlations from both Me-22 (δ 0.97) and Me-23 (δ 1.00) to C-12 and quaternary C-13 (δ 39.1) supported C-12—C-13

connectivity, while HMBC correlations from Me-21, Me-22, and Me-23 to C-14 established connectivity between C-9 and C-14, thus sealing this ring. COSY correlations between H-14 (δ 1.64) and both protons at C-15 (δ 1.92, δ 2.06) as well as an HMBC correlation between H-16 and C-15 (δ 25.1) then sealed the second ring, completing the drimane-type skeleton.

Relative stereochemical assignment for fijioic acid A (**1**) commenced with assignment of H-12 (δ 4.20) in an axial position based on a large *J* coupling constant (*J* = 12.5 Hz) observed for this proton (as well as a smaller 3.0 Hz coupling), which supported an axial-axial relationship and 180° dihedral angle between H-12 and a proton at C-11 (Silverstein and Webster, 1998). Observation of a very intense COSY correlation between H-12 and H-11b prompted assignment of H-11b in an axial position on the opposite face of the ring from H-12. NOE correlations between H-12, H-14, and H-10b supported assignment of all of these atoms in axial positions on the same face of the drimane system. NOE correlations were not observed between any of these axial protons and Me-21 or H-11b. However, a strong correlation was noted between Me-21 and a proton at δ 2.13, supporting assignment of Me-21 and H-11b in axial positions on the opposite face of the molecule. These assignments were further established by an NOE correlation observed between H-11b and Me-22, for which an axial position was supported by the upfield carbon chemical shift (δ 17.5) of this methyl relative to equatorial Me-23 (δ 29.9) (Yong et al., 2008). Thus, with axial H-11b, Me-21, and Me-22 assigned on one face of the drimane system and axial H-10b, H-12, and H-14 established on the opposite face, a trans-fused drimane ring configuration was proposed for **1**. The relative stereochemistry at C-8 was then assigned on the basis of NOE and *J*

coupling constant arguments. A 6.2 Hz vicinal coupling observed for H-7b supported a dihedral angle of approximately 30° or 130° between H-7b and H-8. Further, the 5.2 Hz coupling observed for pseudotriplet H-8 suggested gauche relationships between this proton and both H-7a and H-7b. Observation of NOE correlations between H-7b and axial H-10b and between H-8 and axial Me-21 then established relative stereochemistry at C-8.

High-resolution mass spectral data established the molecular formula of fijioic acid B (**2**) as $C_{23}H_{30}O_4$ (*m/z* 369.2080 $[M - H]^-$). Comparison of ^{13}C and ^1H NMR spectral data as well as HMBC and COSY correlations between **1** and **2** indicated these molecules shared an acetic acid-substituted hydroquinone functionality and both possessed a sesquiterpene group attached at aromatic C-6 (Table 6.1, Appendix D). Comparison of molecular formulae for **1** and **2** indicated the loss of a bromine group and gain of an alkene moiety within the sesquitepene portion of **2**. An exo-methylene substituent was assigned at C-13 on the basis of HMBC correlations from singlets H-23a (δ 4.50) and H-23b (δ 4.81) to C-12 (δ 38.5), C-13 (δ 154.5), and C-14 (δ 32.6). HMBC correlations from doublet Me-22 (δ 1.09) to C-11 (δ 30.8), C-12, and C-13 then established attachment of Me-22 to methine C-12. HMBC and COSY correlations supported assignment of the remainder of this decalin-type system identical to that of **1**, and the sesquiterpene skeleton of **2** was verified by comparison with literature values (Talpir et al., 1994).

Table 6.1 ^{13}C and ^{1}H NMR spectral data for **1**-**2** (125 MHz for ^{13}C and 500 MHz for ^{1}H; in DMSO).

	1		**2**	
no.	δ ^{13}C	δ ^{1}H ($J_{H,H}$)	δ ^{13}C	δ ^{1}H ($J_{H,H}$)
1	175.3	-	175.3	-
2	44.5	3.09s	44.5	3.10s
3	122.6	-	122.5	-
4	150.1	-	150.1	-
5	117.8	6.35s	117.5	6.40s
6	126.6	-	126.7	-
7	30.3	2.13m, 2.77dd (6.2, 14.6)	29.4	2.21dd (2.4, 12.2) 2.90dd (7.2, 15.0)
8	53.7	1.78t (5.2)	50.9	1.97m
9	36.4	-	38.4	-
10	36.3	0.99m, 1.88m	29.5	0.68m, 2.06td (2.0, 10.9)
11	30.8	1.93m, 2.13m	28.4	1.28brd (12.7), 1.63m
12	70.9	4.20dd (3.0, 12.5)	38.5	2.53m
13	39.1	-	154.5	-
14	41.8	1.64m	32.6	2.42brt (7.9)
15	25.1	1.92m, 2.06m	25.8	1.90m
16	119.2	5.23s	119.2	5.29s
17	136.7	-	136.7	-
18	23.6	1.49s	23.4	1.60s
19	116.6	6.31s	116.6	6.33s
20	146.1	-	146.1	-
21	21.8	0.86s	19.0	0.65s
22	17.5	0.97s	19.6	1.09d
23	29.9	1.00s	106.8	4.50s, 4.81s
OH	-	8.38brs	-	8.51brs
OH	-	13.39 brs	-	13.37 brs

For fijioic acid B (**2**), NOEs were observed between H-14 and Me-22, but not between H-12 and H-14, supporting assignment of H-14 and H-22 at axial positions on the same face of the drimane-type skeleton. NOEs between H-10b (δ 2.06) and both Me-22 and H-14 completed this series of 1,3-diaxial interactions. Me-21 was then assigned to an axial position on the opposite face based on NOEs observed between Me-21 and H-11b (δ 1.63), but not between Me-21 and H-14 or Me-22. This trans orientation of Me-21 and H-14 corresponded with the trans-fused bicyclic system proposed for **1**. Finally, assignment of the C-8 stereocenter was established analogously to **1**.

The most structurally similar known relatives of fijioic acids A and B (**1**-**2**) are peyssonols A-B, isolated from a Red Sea collection of *Peyssonelia* sp. on the basis of biomedical activity (Talpir et al., 1994). Peyssonol A differs from fijioic acid A (**1**) by substitution with a formyl group instead of an acetic acid group at C-3 on the hydroquinone ring and by a *trans*-fused drimane skeleton in **1** versus a *cis*-fused orientation in peyssonol A. Hence, fijioic acid A (**1**) represents a novel carbon skeleton with one additional carbon relative to peyssonol A. Fijioic acid B (**2**) shares a carbon skeleton with peyssonol B, and differs from this known metabolite in the presence of an acetic acid-substituted hydroquinone versus methyl acetate group at the corresponding position in peyssonol B as well as in regioisomerization of one site of unsaturation in the drimane group. To our knowledge, **1** and **2** represent the first examples of terpene-hydroquinone natural products bearing an acetic acid-substituted hydroquinone.

Ecological and pharmacological activities of sesquiterpene hydroquinones A-B (1-2).

At isolated concentrations, both fijioic acids A-B (**1**-**2**) were effective chemical defenses against the bacterial pathogen *P. bacteriolytica* and the fungal pathogen *L. thalassiae* (Fig. 6.2). Despite significant inhibition of *D. salina* observed for crude extracts, neither of these compounds inhibited growth of this marine saprophyte, suggesting this red alga harbors other defenses against this fungus. While fijioic acids A-B (**1**-**2**) were inhibitory to a marine pathogenic bacterium and fungus, they exhibited only weak inhibition of biomedically relevant fungi and bacteria (Table 6.2). The discovery of fijioic acids A-B (**1**-**2**), together with the high prevalence of antimicrobial activities observed among tropical algal extracts, suggests the potential of ecology-driven studies in the discovery of novel chemistry.

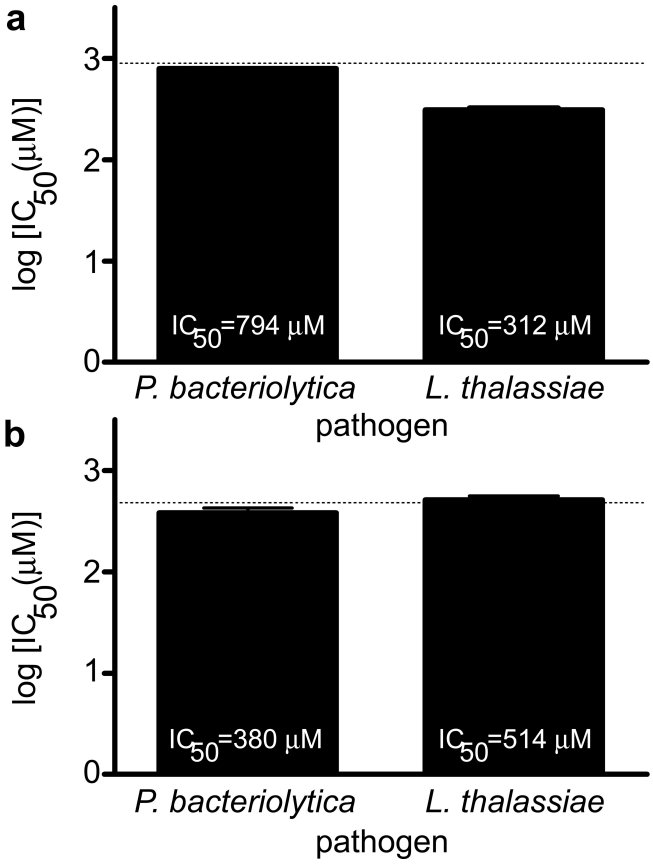

Fig. 6.2 Comparison of log[IC_{50}] growth inhibition values (solid bars) and log[natural concentration] values (dotted line) for (a) **1** and (b) **2** against ecologically relevant pathogens *P. bacterioltyica* and *L. thalassiae* (n = 3 subsample assays at 8-9 concentrations). Bars denote standard error; white text indicates average IC_{50} values.

Table 6.2. Pharmacological activities of **1**-**2**.

	Antibacterial IC_{50} (mM)					**Antifungal MIC (mM)**	
cmpd	**MRSA[a]**	**VREF[b]**	**Antitubercular**	**Anticancer IC_{50} (mM)[c]**	**Antimalarial IC_{50} (mM)**	**WTCA[d]**	**ARCA[e]**
1	>550	>550	>100	55	>100	>550	>550
2	533	230	>100	63	56	>550	>550

[a]Methicillin-resistant *Staphylococcus aureus*; [b]Vancomycin-resistant *Enterococcus faecalis*; [c]Mean of 11 cancer cell lines (see Materials and Methods section for details); [d]Wild-type *Candida albicans*; [e]Amphotericin B-resistant *C. albicans*.

Materials and Methods

General. Semipreparative HPLC was performed with a Waters 1525 or 515 pump and a Waters 2996 diode-array UV detector or a Waters 2487 dual-wavelength absorbance detector. ^{1}H, ^{13}C, DEPT-135, HSQC, HMBC, COSY, NOESY, ROESY, and DPFGSE-NOE NMR experiments were conducted in DMSO with a Bruker DRX-500 instrument using a 5 mm broadband or inverse detection probe, and referenced to residual DMSO (δ 2.49 and δ 39.9 ppm for ^{1}H and ^{13}C, respectively). High resolution mass spectra were acquired using electrospray ionization with an Applied Biosystems QSTAR-XL hybrid quadrupole-time-of-flight tandem mass spectrometer and Analyst QS software. UV spectra were recorded in methanol with a Spectronic 21D spectromphotometer, and optical rotations were measured with a Jasco P-1010 spectropolarimeter. All statistical analyses were completed with either SYSTAT version 9 or GraphPad version 4. HPLC grade solvents were used in semipreparative HPLC (Fisher Scientific Co.), and NMR solvents were obtained from Cambridge Isotope Laboratories.

Algal collection and extraction. Algae were collected at depths of 2 – 20 m from several sites in Fiji. Fijioic acids A-B (**1**-**2**) were isolated from crustose algae collection ID# G-0109. Voucher specimens were identified by comparison with previously described morphological traits,(Littler and M.M., 2003) and deposited at the University of the South Pacific in Suva, Fiji, and Georgia Institute of Technology. Fresh algal material was extracted successively in MeOH (2×) and MeOH/DCM (2:1, 1:1). Extracts were reduced *in vacuo* and subjected to reversed-phase fractionation with HP20ss resin

(Supelco). Fractions 1 and 2 were eluted with MeOH/H_2O (1:1 and 4:1, respectively), fraction 3 with MeOH, and fraction 4 with acetone.

Ecological antimicrobial assays. Chromatographic fractions were evaluated for activity against three ecologically relevant marine microbes (see below). Assays were designed to approximate natural concentrations of metabolites experienced by microbes invading whole algal tissues. All fractions were tested at maximum concentrations volumetrically equivalent to those in the whole alga; fractions corresponding to a 1 mL volume of alga were incorporated into 1 mL of media and inoculated with an evaluated microbe.

Antifungal assays. Antifungal assays were conducted with *Lindra thalassiae* (ATCC 56663), a fungal pathogen of a variety of marine macrophytes, and *Dendryphiella salina*, a fungal saprophyte of marine plants, as previously described.(Kubanek et al., 2003) Chromatographic fractions, at concentrations approximating natural algal tissue concentrations, were each solubilized in a minimal volume of methanol or acetone and incorporated into molten YPM agar (16 g/L granulated agar, 2 g/L yeast extract, 2 g/L peptone, 4 g/L D-mannitol, 250 mg/L of both streptomycin sulfate and penicillin G in 1 L of natural seawater). For each fraction, three 400 μL subsamples of this mixture were dispensed into sterile 24-well microtiter plates, allowed to solidify, and an aliquot of *L. thalassiae* or *D. salina* suspension in sterile seawater added to each well. Control wells were prepared with YPM agar and solvent but no algal material. Plates were incubated at 28 °C for three days and digital photographs collected for each well. The percent of each well covered in fungal hyphae was determined using the area calculator feature of ImageJ

software (NIH), and treatments and controls compared using one-way ANOVA with Dunnett's post test. Antifungal assays with pure **1**-**2** were completed at 1:1 serially diluted concentrations ranging from 900 μM to 3.5 μM, and percent growth inhibition at each concentration was calculated relative to solvent-only controls. Growth inhibition data were fit to a sigmoidal dose-response curve, and mean log IC_{50} and standard error values computed. Reported IC_{50} values were calculated as the antilog of mean log IC_{50} values; standard errors for IC_{50} values were not determined, as such values are not directly correlated with log IC_{50} standard errors and are inherently unrealistic.(Motulsky and Christopoulos, 2003) Antifungal activities of **1**-**2** were statistically compared with an F test of the log IC_{50} value for each compound.

Antibacterial assays. Assays using *Pseudoalteromonas bacteriolytica*, a known marine plant pathogen, were adapted from previous methods.(Kubanek et al., 2003) A 24 h shake culture of this bacterium was diluted 1:160 in Difco Marine Broth 2216 (BD Biosciences) and 195 μL of this mixture added to duplicate treatment and control wells of a 96-well plate. An equal amount of sterile broth was added to blank wells. Five microliters of 40× concentrated chromatographic fractions in DMSO were dispensed into treatment and blank wells, yielding a final concentration approximating that found in whole algal tissues; 5 μL of DMSO were added to corresponding control wells. Plates were incubated for 20 h at 30 °C, and turbidity measured at 600 nm. We corrected for the natural absorbance of chromatographic fractions by subtracting algal-containing sterile blank turbidities from values obtained for treatments. Corrected treatment turbidity values were compared with controls using one-way ANOVA with Dunnett's post-test.

For HPLC fractions and pure compounds from crustose alga ID# G-0109, assays were completed at 1:1 serially diluted concentrations; log IC_{50} values computed and statistically compared analogously to antifungal assays.

Pharmacological assays. Pure sesquiterpene hydroquinones A and B (**1**-**2**) were evaluated for activity against tumor cell lines BT-549, DU4475, MDA-MD-468, NCI-H446, PC-3, SHP-77, LNCaP-FGC, HCT116, MDA-MB-231, A2780/DDP-S, and Du145, representing breast, colon, lung, prostate and ovarian cancer cells. In vitro cytotoxicity was evaluated with the (3-(4,5-dimethylthiazol-2-yl)-5-(3-carboxylmethoxyphenyl)-2-(4-sulfophenyl)-2*H*-tetrazolium inner salt) MTS dye conversion assay as previously described.(Lee et al., 2001) Antimalarial activity was determined with a previously reported SYBR Green based parasite proliferation assay.(Bennett et al., 2004; Smilkstein et al., 2004) Antibacterial assays were performed against methicillin-resistant *Staphylococcus aureus* (ATCC 3747731) and vancomycin-resistant *Enterococcus faecium* (ATCC 3323776), and antifungal assays against both wild type and amphotericin B-resistant *Candida albicans*, using previously reported methods.(Kubanek et al., 2005) Antitubercular activity was assessed against *Mycobacterium tuberculosis* strain H37Rv (ATCC 27294) using the previously described alamar blue susceptibility test (MABA).(Collins and Franzblau, 1997)

Isolation of sesquiterpene hydroquinones A-B. Frozen crustose red alga ID# G-0109 (21.6 mL eq.) was extracted exhaustively in methanol (2×) and methanol/dichloromethane (2:1 and 1:1) and fractionated with HP20ss resin (Supelco),

following the same procedure applied in the algal survey. Fraction 2, with the strongest activity against ecologically-relevant pathogen *P. bacteriolytica*, was subjected to multiple rounds of semipreparative reversed-phase HPLC with an Agilent Zorbax SB-C18 column (5 μm, 9.4 × 250 mm) using methanol:water and acetonitrile:water gradient mobile phases. Antibacterial properties of HPLC fractions were measured with the *P. bacteriolytica* assay described above, and final purification of active compounds **1**-**2** achieved using a Phenomenex Develosil C_{30} column (dimensions) with a methanol:water gradient mobile phase.

Fijioic acid A (1): brown gum; $[\alpha]^{24}_{D}$ 35.0 (*c* 0.343 g/100 mL, MeOH); ^{1}H NMR (DMSO, 500 MHz) and ^{13}C/DEPT NMR (DMSO, 125 MHz) data, Table 6.1; NOE, COSY, HMBC NMR data, Supporting Information; HRESIMS $[M - H]^-$ *m/z* 449.1309 (calcd for $C_{23}H_{30}O_4Br$, 449.1333).

Fijioic acid B (2). brown gum; $[\alpha]^{24}_{D}$ 200.0 (*c* 0.0800 g/100 mL, MeOH); ^{1}H NMR (DMSO, 500 MHz) and ^{13}C/DEPT NMR (DMSO, 125 MHz) data, Table 6.1; NOE, COSY, HMBC NMR data, Supporting Information; HRESIMS $[M - H]^-$ *m/z* 369.2080 (calcd for $C_{23}H_{29}O_4$, 369.2071).

Works Cited

Bennett, T. N., Paguio, M., Gligorijevic, B., Seudieu, C., Kosar, A. D., Davidson, E., and Roepe, P. D. (2004). Novel, rapid, and inexpensive cell-based quantification of antimalarial drug efficacy. Antimicrobial Agents and Chemotherapy *48*, 1807-1810.

Blunt, J. W., Copp, B. R., Hu, W. P., Munro, M. H. G., Northcote, P. T., and Prinsep, M. R. (2007). Marine natural products. Natural Product Reports *24*, 31-86.

Blunt, J. W., Copp, B. R., Hu, W. P., Munro, M. H. G., Northcote, P. T., and Prinsep, M. R. (2008). Marine natural products. Natural Product Reports *25*, 35-94.

Collins, L. A., and Franzblau, S. G. (1997). Microplate Alamar blue assay versus BACTEC 460 system for high-throughput screening of compounds against Mycobacterium tuberculosis and Mycobacterium avium. Antimicrobial Agents and Chemotherapy *41*, 1004-1009.

Engel, S., Jensen, P. R., and Fenical, W. (2002). Chemical ecology of marine microbial defense. Journal of Chemical Ecology *28*, 1971-1985.

Engel, S., Puglisi, M. P., Jensen, P. R., and Fenical, W. (2006). Antimicrobial activities of extracts from tropical Atlantic marine plants against marine pathogens and saprophytes. Marine Biology *149*, 991-1002.

Harvell, C. D., Kim, K., Burkholder, J. M., Colwell, R. R., Epstein, P. R., Grimes, D. J., Hofmann, E. E., Lipp, E. K., Osterhaus, A., Overstreet, R. M.*, et al.* (1999). Emerging marine diseases - Climate links and anthropogenic factors. Science *285*, 1505-1510.

Jensen, P. R., Jenkins, K. M., Porter, D., and Fenical, W. (1998). Evidence that a new antibiotic flavone glycoside chemically defends the sea grass *Thalassia testudinum* against zoosporic fungi. Applied and Environmental Microbiology *64*, 1490-1496.

Jiang, R. W., Lane, A. L., Hay, M. E., Hardcastle, K., and Kubanek, J. (In press.). Molecular structure and absolute configuration of sulfate conjugated triterpenoids: Chemical defenses of the marine green alga *Tydemania expeditionis*. Journal of Natural Products.

Kjelleberg, S., Steinberg, P., Givskov, M., Gram, L., Manefield, M., and deNys, R. (1997). Do marine natural products interfere with prokaryotic AHL regulatory systems? Aquatic Microbial Ecology *13*, 85-93.

Kohlmeyer, J. (1971). Fungi from the Sargasso Sea. Marine Biology *8*, 344-350.

Kubanek, J., Jensen, P. R., Keifer, P. A., Sullards, M. C., Collins, D. O., and Fenical, W. (2003). Seaweed resistance to microbial attack: A targeted chemical defense against marine fungi. Proceedings of the National Academy of Sciences of the United States of America *100*, 6916-6921.

Kubanek, J., Prusak, A. C., Snell, T. W., Giese, R. A., Hardcastle, K. I., Fairchild, C. R., Aalbersberg, W., Raventos-Suarez, C., and Hay, M. E. (2005). Antineoplastic diterpene-benzoate macrolides from the Fijian red alga Callophycus serratus. Organic Letters *7*, 5261-5264.

Lane, A. L., and Kubanek, J. (2008). Secondary metabolite defenses against pathogens and biofoulers, In Algal Chemical Ecology, C. D. Amsler, ed. (Berlin: Springer), pp. 229-243.

Lee, F. Y. F., Borzilleri, R., Fairchild, C. R., Kim, S. H., Long, B. H., Reventos-Suarez, C., Vite, G. D., Rose, W. C., and Kramer, R. A. (2001). BMS-247550: A novel epothilone analog with a mode of action similar to paclitaxel but possessing superior antitumor efficacy. Clinical Cancer Research *7*, 1429-1437.

Littler, D. S., and Littler, M.M. (2003). South Pacific Reef Plants (Washington, D.C.: Offshore Graphics, Inc.).

Littler, M. M., and Littler, D. S. (1995). Impact of Clod Pathogen on Pacific Coral Reefs. Science *267*, 1356-1360.

Motulsky, H. J., and Christopoulos, A. (2003). Fitting models to biological data using linear and nonlinear regression. A practical guide to curve fitting. (San Diego: GraphPad Software, Inc.).

Porter, D. (1986). Mycoses of marine organisms: An overview of pathogenic fungi (New York: Cambridge University Press).

Puglisi, M., Engel, S., Jensen, P., and Fenical, W. (2006). Antimicrobial activities of extracts from Indo-Pacific marine plants against marine pathogens and saprophytes. Marine Biology.

Puglisi, M. P., Tan, L. T., Jensen, P. R., and Fenical, W. (2004). Capisterones A and B from the tropical green alga Penicillus capitatus: unexpected anti-fungal defenses targeting the marine pathogen Lindra thallasiae. Tetrahedron *60*, 7035-7039.

Sawabe, T., Makino, H., Tatsumi, M., Nakano, K., Tajima, K., Iqbal, M. M., Yumoto, I., Ezura, Y., and Christen, R. (1998). Pseudoalteromonas bacteriolytica sp. nov., a marine bacterium that is the causative agent of red spot disease of Laminaria japonica. International Journal of Systematic Bacteriology *48*, 769-774.

Short, F. T., Muehlstein, L. K., and Porter, D. (1987). Eelgrass wasting disease - Cause and recurrence of a marine epidemic. Biological Bulletin *173*, 557-562.

Silverstein, R. M., and Webster, F. X. (1998). Spectrometric Identification of Organic Compounds, 6th edn (New York: John Wiley & Sons, Inc.).

Smilkstein, M., Sriwilaijaroen, N., Kelly, J. X., Wilairat, P., and Riscoe, M. (2004). Simple and inexpensive fluorescence-based technique for high-throughput antimalarial drug screening. Antimicrobial Agents and Chemotherapy *48*, 1803-1806.

Talpir, R., Rudi, A., Kashman, Y., Loya, Y., and Hizi, A. (1994). Three new sesquiterpene hydroquinones from marine origin. Tetrahedron *50*, 4179-4184.

Yong, K. W. L., Jankam, A., Hooper, J. N. A., Suksamrarn, A., and Garson, M. J. (2008). Stereochemical evaluation of sesquiterpene quinones from two sponges of the genus Dactylospongia and the implication for enantioselective processes in marine terpene biosynthesis. Tetrahedron *64*, 6341-6348.

CHAPTER 7

STRUCTURE-ACTIVITY RELATIONSHIP OF CHEMICAL DEFENSES FROM THE FRESHWATER PLANT *MICRANTHEMUM UMBROSUM*

Abstract

Vascular plants produce a variety of molecules of phenylpropanoid biosynthetic origin, including lignoids. Recent investigations indicated that in freshwater plants, some of these natural products function as chemical defenses against generalist consumers such as crayfish. Certain structural features are shared among several of these anti-herbivore compounds, including phenolic, methoxy, methylenedioxy, and lactone functional groups. To test the relative importance of various functional groups in contributing to the feeding deterrence of phenylpropanoid-based natural products, we compared the feeding behavior of crayfish offered artificial diets containing analogs of elemicin (**1**) and β-apopicropodophyllin (**2**), chemical defenses of the freshwater macrophyte *Micranthemum umbrosum*. Both allyl and methoxy moieties of **1** contributed to feeding deterrence. Disruption of the lactone moiety of **2** reduced its deterrence. Finally, feeding assays testing effects of **1** and **2** at multiple concentrations established that these two natural products interact additively in deterring crayfish feeding.

Introduction

Phenylpropanoid-derived natural products, biosynthesized via the shikimate pathway, are widespread among vascular plants (Lewis and Davin, 1999) and have been shown to exhibit antimitotic, antiviral, insect antifeedant, and root growth inhibition properties (Loike and Horwitz, 1976; Elakovich and Stevens, 1985; Gnabre et al., 1995;

Harmatha and Nawrot, 2002). Most biological studies related to phenylpropanoid-based natural products have focused on their potential application in medicine and agriculture. A smaller number of ecological studies have indicated that some of these metabolites function as chemical defenses against co-occurring herbivores. Among freshwater macrophytes, 11 shikimate-derived natural products (10 lignoids and one monomeric phenylpropanoid) and one potential shikimate metabolite (a *p*-hydroxybenzyl ester) have been shown to deter herbivory by generalist crayfish (Bolser et al., 1998; Wilson et al., 1999; Kubanek et al., 2000, 2001; Parker et al., 2006), whose feeding behavior can dramatically affect macrophyte distribution and abundance (Lodge, 1991) (Fig. 7.1a). In these studies, isolation of deterrent natural products was guided by feeding assays such that structurally-related but non-deterrent compounds were not identified. A comparison of structural features for deterrent and non-deterrent metabolites of the same biosynthetic class has therefore not been possible, preventing rigorous analysis of the structural basis for chemical defense.

It is expected that there exists a definable relationship between the structure of phenylpropanoid-based plant natural products and feeding deterrence, when considering a population or species of herbivores. From assessment of a group of deterrent lignoids possessing a common carbon skeleton, Kubanek et al. (2000) suggested that increased aryl hydroxylation may be associated with increased deterrence. By strategic manipulation of the molecular structures of natural products, quantification of biological activities, and statistical analyses to test for differences, insights may be gained into the precise nature of this structure-activity relationship. Such studies have commonly been used to explore the pharmacological (e.g., Lee et al., 1999; Zhang et al., 2004) and

agricultural (e.g., Kim and Mullin, 2003; Morimoto et al., 2003) activities of natural products. However, few studies have investigated such relationships in an ecological context (but see Assmann et al., 2000; Lindel et al., 2000; Silva and Trigo, 2002), and no previous studies have evaluated this for phenylpropanoid-derived molecules. Such studies could lead to testable hypotheses regarding mechanisms of chemoreception and other physiological responses. Structure-activity relationship studies may also provide insights into the evolution of chemical defenses: if herbivore pressure is intense and chemical defenses carry significant costs, one might predict that plants evolved pathways to produce the most deterrent compounds, suggesting that natural products should have greater deterrent potency than unnatural, but structurally-related compounds, and that concentrations of chemical defenses within plants are likely to be adequate, but not excessive, for deterring herbivores.

In the current study, we selected elemicin (**1**) and β-apopicropodophyllin (**2**) (Fig. 7.1a), phenylpropanoid-based chemical defenses of the freshwater plant *Micranthemum umbrosum* (Parker et al., 2006), as model structures for the evaluation of structure-activity relationships among freshwater plant chemical defenses. We obtained eight analogs of **1** and **2** by semi-synthesis or from commercial sources, and from feeding assay data using the crayfish *Procambarus acutus* we generated dose-response curves to quantify deterrent potency and to predict structural requirements for deterrence. Additionally, we compared the deterrent potencies of **1** and **2**, and evaluated the interaction (additive, antagonistic, or synergistic) between **1** and **2** in the chemical defense of the freshwater plant *M. umbrosum*.

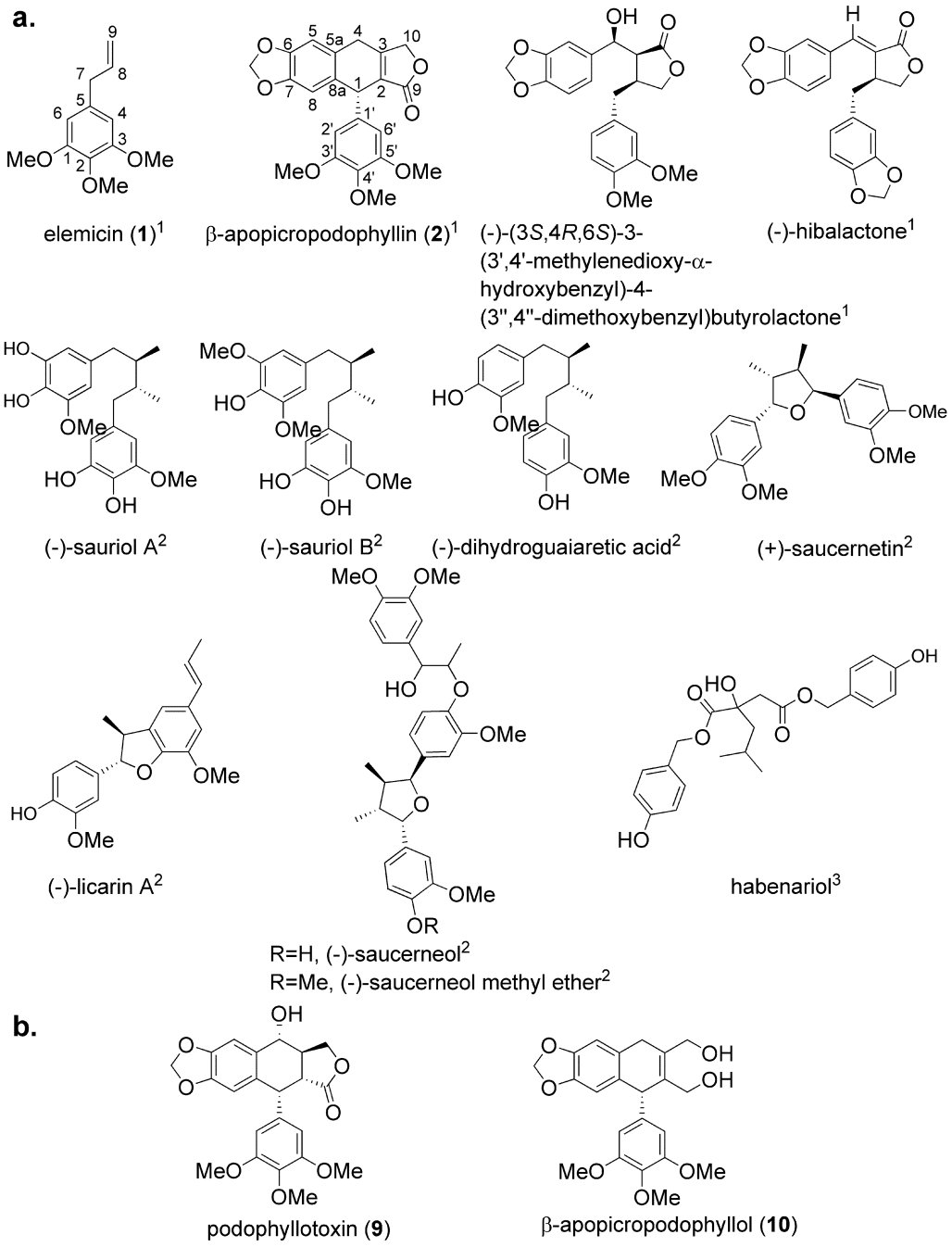

Fig 7.1 (a) Freshwater plant shikimate-derived metabolites previously demonstrated to deter crayfish feeding. [1]Parker et al., 2006 ; [2]Kubanek et al., 2000, 2001 ; [3]Bolser et al., 1998; Wilson et al., 1999. (b) Analogs of β-apopicropodophyllin (**2**) for which crayfish feeding deterrence was assessed in the current study.

Results and discussion

Feeding deterrence of natural products elemicin (1) vs. β-apopicropodophyllin (2)

Comparison of $\log EC_{50}$ values for the feeding deterrence of the phenylpropanoid elemicin (**1**) and the lignoid β-apopicropodophyllin (**2**) against the crayfish *Procambarus acutus* indicated that **2** is approximately 750 times more deterrent than **1** ($p < 0.0001$; Fig. 7.2). Consistent with this finding, in an investigation of the insect feeding deterrence activity of compounds belonging to these two structural groups, Harmatha and Nawrot (2002) reported that lignoids were generally more bioactive than phenylpropanoid monomers.

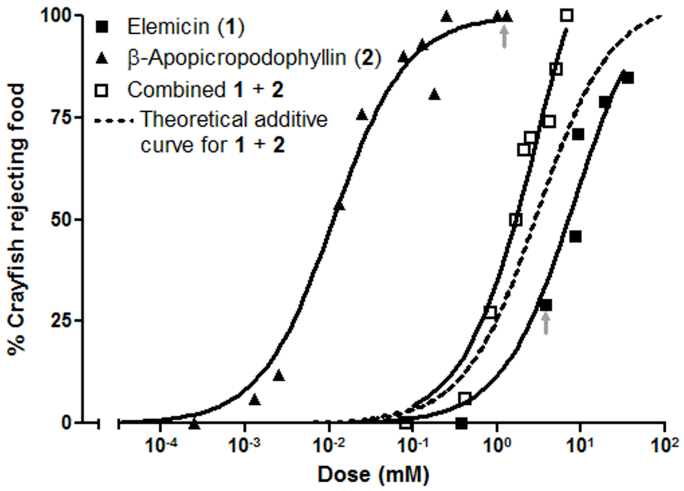

Fig. 7.2 Effect of compound concentration on crayfish feeding behavior for *Micranthemum umbrosum* natural products elemicin (**1**) and β-apopicropodophyllin (**2**), and effect of combined doses of **1** and **2**; n = 13-24 crayfish for each data point. Grey arrows denote natural concentrations of **1** and **2** in *M. umbrosum* from Parker et al. (2006). In determining the effect of combined doses, **1** and **2** were added to artificial diets in 1:1 molar ratios of the EC_{50} values for each compound. The theoretical additive curve was calculated from best fit dose response curves developed individually for **1** and **2**.

According to optimal defense theory (Rhoades and Cates, 1976), if natural products evolved to fulfill a specific ecological function such as chemical defense, one would expect natural concentrations of these defenses to approximately match the sensitivity of potential consumers, in order to minimize costs associated with chemical defense. The experimental EC_{50} for elemicin (**1**), 8.3 mM (Fig. 7.2), was found to be similar to its natural concentration of 3.2 mM (Parker et al., 2006). In contrast, the natural concentration of β-apopicropodophyllin (**2**), 0.96 mM (Parker et al., 2006), was nearly 100 times greater than its experimental EC_{50} value, 0.011 mM (Fig. 7.2). These data suggest that **2** is more important than **1** in deterring crayfish from feeding on *Micranthemum umbrosum*, and may indicate that both metabolites serve multiple ecological functions, as natural concentrations of the combined compounds is greater than that required for feeding deterrence, or that metabolite concentrations are not optimally tuned to herbivore sensitivity.

Interaction between elemicin (1) and β-apopicropodophyllin (2) in the chemical defense of Micranthemum umbrosum

Previous studies have indicated that some phenylpropanoids and lignoids interact synergistically in the deterrence of agricultural pests (Yamashita and Matsui, 1961). Alternatively, antagonistic or additive effects could occur. When **1** and **2** were investigated for combined effects in deterring crayfish feeding, the experimental $\log EC_{50}$ value for the combined compounds was not significantly different from the value

obtained from a theoretical additive curve (F test, $p = 0.73$; Fig. 7.2), leading us to reject the hypothesis that these two natural products behave synergistically or antagonistically in deterring crayfish feeding.

Structure-activity relationship of elemicin (1) analogs

At 12× the natural molar concentration of elemicin (**1**), allylbenzene (**3**) was not significantly deterrent to crayfish (Fisher's exact test, $p > 0.99$; Fig. 5.3), indicating that substituents on the allylbenzene scaffold are necessary for feeding deterrence. In contrast, dimethoxy-substituted methyl eugenol (**4**) was the most deterrent of compounds tested within this group, with an EC_{50} value 87% less than that of **1** (F test, $p < 0.001$; Fig. 7.3). The greater potency of **4** relative to trimethoxy-substituted **1** indicates that the third methoxy substituent on the phenyl ring of **1** undermines deterrence, which may indicate that steric hindrance of the bulkier **1** alters the interaction with a *Procambarus acutus* chemoreceptor. Although crustacean receptors for detecting plant chemical defenses have not yet been identified, it seems likely that taste or odorant chemoreceptors are involved, given the quick response time (seconds) and lack of apparent injury to crayfish rejecting chemically-defended foods which might be expected if a deterrent caused a non-receptor-mediated effect such as burning (Lane and Kubanek, pers. observ.). The enhanced activity (relative to **1**) of dimethoxy-substituted **4**, a metabolite previously isolated from other vascular plants (e.g. Mata et al., 2004), also indicates that *Micranthemum umbrosum* has not evolved to produce the metabolite most deterrent to this particular herbivore.

In addition to the number of aryl methoxy groups affecting deterrence, the identity of substituents also appeared to play an important role. The presence of a hydroxy group *para* to the allyl substituent as in eugenol (**5**) and methoxyeugenol (**6**), instead of a methoxy group as in elemicin (**1**) and methyl eugenol (**4**), was associated with substantially reduced deterrent potency for trisubstituted benzenes **4** vs. **5** (F test, $p < 0.001$; Fig. 7.3), and marginally reduced deterrent potency for tetrasubstituted benzenes **1** vs. **6** ($p = 0.17$; Fig. 7.3). Both hydroxy and methoxy substituents may function as hydrogen bond acceptors in interactions with crayfish chemoreceptors, whereas a hydroxy substituent can also act as a hydrogen bond donor, which could potentially affect deterrent potency by altering the orientation in which a ligand interacts with a chemoreceptor. Alternatively, the bulkier, more hydrophobic methoxy substituent in the *para* position of **4** may enhance deterrence (relative to **5**) via a better steric fit and/or stronger van der Waals attractive forces within the chemoreceptor binding site. The current finding, that aryl hydroxy groups are associated with weaker crayfish deterrence than are aryl methoxy groups among monomeric phenylpropanoids, is contrary to the suggestion of Kubanek et al. (2000) regarding the crayfish deterrence among a group of lignans.

Eugenol (**5**) was previously demonstrated to cause paralysis in crayfish placed in an aqueous solution of this compound (Ozeki, 1975). Given the structural similarity of elemicin (**1**) and **5**, it is possible that **1** may also be toxic at certain concentrations; however, we did not observe incapacitation or mortality of *Procambarus acutus* during or after feeding assays. This may indicate that toxicity is diminished when consumed as part of a diet rather than absorbed from surrounding water. If **1** or **5** is indeed toxic at

high doses or following repeated consumption of plants containing these metabolites, this may have favored evolution of chemoreception in consumers such as *P. acutus*, in order to identify and avoid consuming toxic foods.

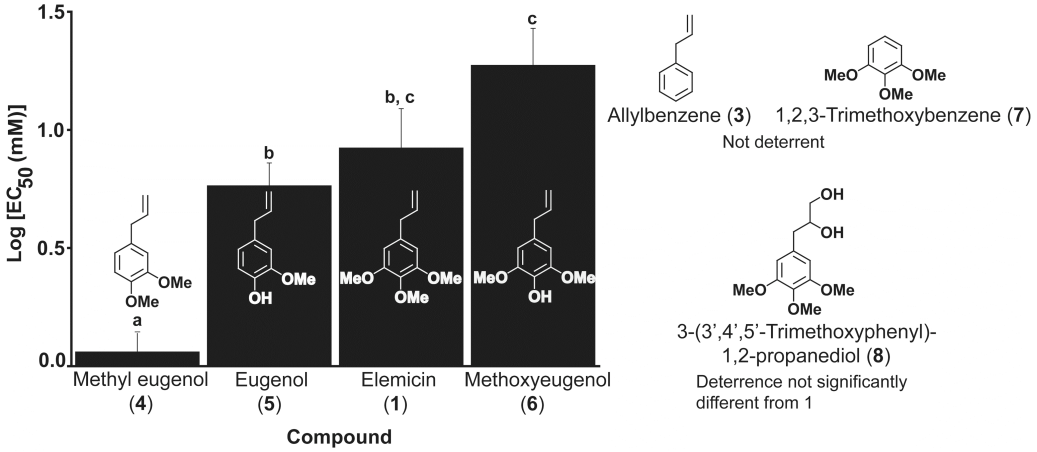

Fig. 7.3 Comparison of crayfish feeding deterrence of elemicin (**1**) and analogs. Different letters indicate treatments differing significantly in feeding deterrence from each other (F-test, $p \leq 0.05$); bars represent standard error. Replacement of methoxy groups with hydroxy groups resulted in decreased potency, as seen in **4** vs. **5** and **1** vs. **6**. Increased substitution with hydroxy and methoxy groups was also associated with decreased activity. Dose response curves were used to calculate EC_{50} values for **1** (Fig. 7.2) and **4**-**6** (data not shown). For **3** and **7**, EC_{50} values could not be calculated because these compounds were not deterrent at any concentration tested (see text). For **8**, an EC_{50} value could not be calculated because low synthetic yield prohibited testing at sufficient concentrations (see text).

Supporting the hypothesis that the allyl group at C-5 of elemicin (**1**) is important in feeding deterrence, 1,2,3-trimethoxybenzene (**7**) was palatable at 38 mM, 12× the natural molar concentration of **1** (Fisher's exact test $p = 0.23$). 3-(3',4',5'-Trimethoxyphenyl-1,2-propanediol (**8**), synthesized from **1**, was significantly deterrent at

the three concentrations at which it was tested, spanning 2.9-8.4 mM (Fisher's exact test, $p = 0.0006$-0.05). Due to limited yield of synthetic product, a full dose-response curve could not be established for **8**. However, comparison of the deterrence of **1** and **8** at 3.8 mM indicated that potency did not appear to differ significantly between these two compounds (Fisher's exact test, $p > 0.99$). Thus, conversion of the allyl substituent to a diol did not appear to reduce bioactivity, despite the enhanced bulkiness, polarity, and hydrogen bonding capacity of this group relative to the allyl substituent of **1**. Although the lack of deterrence of trimethoxybenzene (**7**) indicated that a non-hydrogen substituent was essential at C-5 for deterrence, it appears that the *Procambarus acutus* chemoreceptor for **1** is not highly specific for the C-5 substituent.

Structure-activity relationship of β-apopicropodophyllin (2) analogs

A number of structural features may be expected to influence the bioactivity of β-apopicropodophyllin (**2**), including the unsaturated lactone, trimethoxyphenyl group, methylenedioxy moiety, and stereochemistry at C-1. We focused on the role of the lactone moiety in crayfish feeding behavior, as this group was most amenable to synthetic modification and has been demonstrated to affect bioactivity in pharmacological studies of analogous lignoids including podophyllotoxin (**9**) (Loike and Horwitz, 1976; Brewer et al., 1979).

Podophyllotoxin (**9**) was marginally less deterrent than β-apopicropodophyllin (**2**) (F test, $p = 0.07$; Table 7.1), which may have resulted from different lactone conformations, from the lack of the C-2-C-3 unsaturation in **9**, or from the presence of a hydroxy at C-4 in **9**. Whereas **2** was significantly deterrent at 1% of its natural molar

concentration (Fisher's exact test, $p = 0.001$) and nearly 100% deterrent at its natural concentration ($p < 0.0001$; Fig. 7.2), disruption of the lactone by reduction to the diol β-apopicropodophyllol (**10**) resulted in a complete lack of deterrence for **10** at either of these concentrations ($p > 0.99$ for both concentrations); **10** was significantly less potent than **2** (Fisher's exact test, $p < 0.001$ for comparison of deterrence of **2** and **10** at both concentrations). Feeding assays at higher concentrations were not feasible for **10**, due to insufficient synthetic product yields. This conversion of the lactone ring in **2** to a diol moiety in **10**, while retaining the C2-C3 unsaturation, may have resulted in loss of activity by a diminished capacity of the more polar diol to bind with hydrophobic regions of the chemoreceptor, or by increased conformational flexibility which could disrupt orientation of hydrogen bonding or dipole-dipole interacting groups between a receptor and ligand.

Table 7.1 Comparison of crayfish feeding deterrence for β-apopicropodophyllin (**2**) and analogs. Dose response curves were used to calculate EC_{50} values for **2** (Fig. 7.2) and **9** (data not shown).

Analog	**Log [EC_{50} (mM)] ± Standard Error**	**EC_{50} (mM)**
β-Apopicropodophyllin (**2**)	-1.95 ± 0.08[a]	0.011
Podophyllotoxin (**9**)	-1.70 ± 0.07[a]	0.020
β-apopicropodophyllin (**10**)	(Non-deterrent at all concentrations tested)	
[a]LogEC_{50} values for **2** and **9** differ marginally (F-test, $p = 0.07$)		

The role of the methylenedioxy moiety of β-apopicropodophyllin (**2**) in crayfish feeding deterrence remains unclear, as attempts at selective synthetic modification of this group were unsuccessful (data not shown). Kubanek et al. (2000) reported a series of seven antifeedant lignoids that did not possess methylenedioxy groups, indicating that these groups are not essential for crayfish feeding deterrence among lignoids (although different, albeit congeneric, species of crayfish were used in Kubanek et al. (2000) vs. the current study). In contrast, methylenedioxy moieties have been suggested to be important in the effectiveness of insect feeding deterrents (Harmatha and Nawrot, 2002).

Conclusions

Previous investigations aimed at elucidating the molecular structural requirements for ecological function have made assessments on the basis of one or a few feeding assay data points (e.g., Assmann et al., 2000; Kubanek et al., 2000; Lindel et al., 2000), making it difficult to quantitatively compare the sensitivity of consumers to chemical cues in their food. To our knowledge, this study marks the first aquatic chemical ecology investigation in which structure-activity relationships were evaluated through the use of dose response curves and represents the first investigation of the structure-activity relationship of plant feeding deterrents against a freshwater herbivore.

Comparison of dose response curves for two *Micranthemum umbrosum* natural products, elemicin (**1**) and β-apopicropodophyllin (**2**), and eight analogs (**3-10**) of these natural products indicated that the allyl and methoxy moieties of **1** influenced crayfish feeding behavior, as did the lactone moiety of **2**. The 12-member collection of natural products previously reported to deter crayfish feeding includes some molecules with none

of these functionalities (Wilson et al., 1999; Kubanek et al. 2000), suggesting that several different chemoreceptive mechanisms are likely involved in crayfish feeding deterrence and/or that crayfish species or populations differ in their responses. Studies of interactions between these molecules and individual herbivore chemoreceptors and manipulation of chemoreception physiology will be necessary to develop further understanding regarding receptor-ligand interactions involving chemical defense.

Materials and Methods

General experimental procedures. Fisher Scientific ACS grade solvents were used for extractions, flash column chromatography, and chemical transformations; Fisher Scientific HPLC grade solvents were used for HPLC. Compounds **3-7**, **9**, and chemicals for synthetic modifications were purchased from Sigma Aldrich (St. Louis, MO, USA). HPLC analyses were conducted with Zorbax RX-SIL (Agilent Technologies) semi-preparative normal phase columns using a Waters HPLC system (Waters 515 pump; Waters 2487 dual wavelength absorbance detector) with UV absorbance monitored at 220 and 254 nm. ^{1}H, ^{13}C, and two-dimensional inverse-detected NMR spectral data (COSY, HMQC, HMBC) were acquired with a Bruker DRX-500 MHz spectrometer. All NMR experiments were conducted using $CDCl_3$ and referenced to residual $CHCl_3$ (7.24 and 77.0 ppm, for ^{1}H and ^{13}C, respectively). High and low resolution electron impact (EI) mass spectra were collected with a VG Instruments 70SE spectrometer.

Isolation of plant chemical defenses (1-2). Whole *Micranthemum umbrosum* plants were collected in June, 2003, from ponds at the Owens and Williams Fish Hatchery

(Hawkinsville, GA, USA) and were frozen until extraction. A voucher specimen is stored at the Georgia Institute of Technology. Plant material was shredded in MeOH and extracted successively with MeOH (2×), Me_2CO (2×), and CH_2Cl_2 (2×). Extracts were combined, filtered, and concentrated *in vacuo*. This crude extract was partitioned between petroleum ether and MeOH/H_2O (9:1); the MeOH/H_2O (9:1) portion was further partitioned between MeOH/H_2O (3:2) and $CHCl_3$. TLC R_f values of authentic samples of **1** and **2** were compared with values for compounds in liquid-liquid partition fractions, in order to identify fractions containing these natural products.

β-Apopicropodophyllin (**2**) was found exclusively in the $CHCl_3$ fraction, and so this fraction was further separated by flash column chromatography on silica with gradient elution of hexanes/EtOAc (9:1) to EtOAc. Finally, **2** was purified by normal phase silica HPLC with CH_2Cl_2/Me_2CO (49:1) as the mobile phase. Elemicin (**1**) was found in both the $CHCl_3$ and hexanes fractions following liquid-liquid partitioning. Both fractions were separated by flash column chromatography as described above for **2**, except that the hexane-soluble portion was subjected to a gradient mobile phase of hexanes to EtOAc. Finally, **1** was purified by normal phase silica HPLC using a hexanes/EtOAc (49:1) mobile phase. The structures of **1** and **2** were determined by spectroscopic analysis and verified by comparison with lit. values (Gensler et al., 1970; Achenbach and Frey, 1992). Elemicin (**1**): ^{1}H NMR (500 MHz, $CDCl_3$): δ 6.41 (2H, *s*, H-4 and H-6), 5.95 (1H, *m*, H-8), 5.12 (1H, *m,* H-9), 5.08 (1H, *m*, H-9), 3.85 (6H, *s*, OMe-1 and -3), 3.82 (3H, *s*, OMe-2), 3.32 (2H, *d*, J = 6.5 Hz, H-7). ^{13}C NMR (125 MHz, $CDCl_3$): δ 153.1 (C-1 and C-3), 137.2 (C-8), 136.2 (C-5), 135.8 (C-2), 116.0 (C-9), 105.3 (C-4 and C-6), 60.8 (OCH_3-2), 56.1 (OCH_3-1,3), 40.5 (C-7). EI (*m/z*): [M^+]

calculated for $C_{12}H_{16}O_3$, 208.10994; found 208.10856. β-Apopicropodophyllin (**2**): ^{1}H-NMR (500 MHz, $CDCl_3$): δ 6.70 (1H, *s*, H-5), 6.62 (1H, *s*, H-8), 6.39 (2H, *s*, H-2' and H-6'), 5.93 (1H, *d*, *J* = 4.5 Hz, OCH_2O), 5.90 (1H, *d*, *J* = 4.5 Hz, OCH_2O), 4.87 (1H, *m*, H-10,), 4.82 (1H, *m*, H-1), 4.80 (1H, *m*, H-10), 3.82 (1H, *dd*, *J* = 2.5, 27.9 Hz, H-4), 3.79 (3H, *s*, OMe-4'), 3.78 (6H, *s*, OMe-3',5'), 3.64 (1H, *dd*, *J* = 3.5, 27.9 Hz, H-4). ^{13}C NMR (125 MHz, $CDCl_3$): δ 172.2 (C-9), 157.3 (C-3), 153.2 (C-3' and C-5'), 147.2 (C-4'), 147.0 (C-6), 138.6 (C-7), 136.9 (C-1'), 129.6 (C-5a), 128.1 (C-2), 123.7 (C-8a), 109.5 (C-8), 107.7 (C-5), 105.5 (C-2',6'), 101.3 (OCH_2O), 71.0 (C-10), 60.7 (OCH_3-4'), 56.1 (OCH_3-3',5'), 42.7 (C-1), 29.2 (C-4). EI (*m/z*): [M^+] calculated for $C_{22}H_{20}O_7$, 396.12090; found 396.12071.

Oxidation of elemicin (1) to 3-(3',4',5'-trimethoxyphenyl)-1,2-propanediol (8). A solution of $KMnO_4$ (0.050 mmol) in deionized H_2O (780 μl) was added to an ice-bath cooled solution of **1** (0.070 mmol) in EtOH/H_2O (2:1) and stirred for 3 minutes. The reaction mixture was filtered and then partitioned into Et_2O and aq. layers; TLC indicated presence of the diol product in the aq. layer. The aq. layer was extracted with *n*-BuOH (2 × 15 ml). The *n*-BuOH extract was concentrated *in vacuo* and **8** was purified by normal phase silica HPLC with a mobile phase of hexanes/EtOAc (3:7). The structure of **8** (0.011 mmol; 20% yield) was determined by spectral analysis and verified by comparison with previous data (Dong et al., 1989; Gonzalez et al., 1991). ^{1}H-NMR (500 MHz, $CDCl_3$): δ 6.43 (2H, *s*, H-2' and H-6'), 3.94 (1H, *m*, H-2), 3.84 (6H, *s*, OMe-3'and -5'), 3.81 (3H, *s*, OMe- 4'), 3.70 (1H, *dd*, *J* = 11.5, 2.5 Hz, H-1), 3.49 (1H, *dd*, *J* = 11.5, 6.5 Hz, H-1), 2.74 (1H, *dd*, *J* = 13.5, 4.3 Hz, H-3); 2.67 (1H, *dd*, *J* = 13.5, 8.7 Hz, H-3). ^{13}C-

NMR (125 MHz, $CDCl_3$): δ 153.6 (C-3' and C-5'), 137.0 (C-1'), 133.6 (C-4'), 106.4 (C-2' and C-6'), 73.2 (C-2), 66.4 (C-1), 61.1 (OMe-4'), 56.4 (OMe-3' and -5'), 40.4 (C-3). EI (*m/z*): [M^+] calculated for $C_{12}H_{18}O_5$, 242.11542; found 242.11564.

Reduction of β-apopicropodophyllin (2) to β-apopicropodophyllol (10). A soln. of **2** (0.010 mmol) in CH_2Cl_2 (100 μl) was added to dry Et_2O (5 ml) suspension of $LiAlH_4$ (0.025 mmol) and stirred 15 h at room temp. (Anjanamurthy and Rai, 1987). Aq. HCl (2M, 15 ml) were then added, and the mixture was stirred for 30 min. The Et_2O layer was washed with deionized H_2O (2 × 15 ml) and dried over dry Na_2SO_4. Et_2O was removed *in vacuo*, and **10** was purified as a white powder by normal phase silica HPLC with CH_2Cl_2/EtOAc (7:3) as mobile phase. Compound **10** (0.0047 mmol, 47% yield) was identified by spectral analysis and comparison with published data (Anjanamurthy and Rai, 1987). ^{1}H-NMR (500 MHz, $CDCl_3$): δ 6.63 (1H, *s*, H-5), 6.51 (1H, *s*, H-8), 6.38 (2H, *s*, H-2' and H-6'), 5.88 (1H, *d*, *J* = 1.5 Hz, OCH_2O), 5.84 (1H, *d*, *J* = 1.5 Hz, OCH_2O), 4.53 (1H, *m*, H-1), 4.33 (2H, *m*, H-10), 4.26 (1H, *dd*, *J* = 12.0, 2.5 Hz, H-9), 4.10 (1H, *dd*, *J* = 12.0, 7.8 Hz, H-9), 3.78 (6H, *s*, OMe-3'and -5'), 3.76 (3H, *s,* OMe-4'), 3.72 (1H, *dd*, *J* = 21.5, 4.2 Hz, H-4), 3.53 (1H, *dd*, *J* = 21.5, 3.6 Hz, H-4); ^{13}C-NMR (125 MHz, $CDCl_3$): δ 153.2 (C-3'and C-5'), 146.1-146.0 (C-4' and C-6), 140.5 (C-7), 136.4 (C-1'), 135.3 (C-2), 134.1 (C-3), 130.2 (C-5a), 125.4 (C-8a), 107.8 (C-8), 107.1 (C-5), 104.7 (C-2' and C-6'), 100.5 (OCH_2O), 62.4 (C-10), 61.0 (C-9), 60.6 (OMe-4'), 55.8 (OMe-3' and -5'), 50.0 (C-1), 33.6 (C-4). EI (*m/z*): [M^+] calculated for $C_{22}H_{24}O_7$, 400.15220; found 400.15173.

Bioasssays and statistical methods. Feeding assays were conducted using the omnivorous crayfish, *Procambarus acutus*, collected from the wetlands in the Chattahoochee National Recreation Area (Atlanta, GA, USA) in 2003 and 2004, and identified by comparison of morphological traits (Hobbs, 1981). Crayfish were housed individually in 12.5 × 12.5 cm chambers of a recirculating water table at 23 ˚C and maintained on a diet of commercial trout food pellets.

Assays were completed following procedures described in Parker et al. (2006). Artificial food for each feeding assay was prepared by suspending 100 mg of a 1:1 mixture of freeze-dried, ground broccoli and lettuce in Me_2CO, to which was added the test compound (natural product or synthetic analog) dissolved in Me_2CO. The mixture was shaken and the Me_2CO removed by rotary evaporation. This test food powder was then mixed with 30 mg of sodium alginate in 1 mL of deionized H_2O, and dispensed through a syringe into a 0.10 M aq. soln. of $CaCl_2$. Test food was allowed to solidify in this solution for 1 min, then rinsed with deionized H_2O, and cut into test food pellets ca. 3 mm in length. Test compound concentrations were recorded as millimoles of compound per ml of food mixture. Control food pellets were prepared in the same way, including the use of Me_2CO as solvent, but without the addition of test compounds. Feeding assays were conducted by first feeding a crayfish a control food pellet to confirm that the crayfish was not already satiated, and if that control pellet was consumed, then offering the crayfish a test food pellet. If the crayfish consumed the test food pellet, it was considered accepted. Test food pellets were considered rejected if a crayfish took the pellet into its mouth cavity twice and rejected it each time, in which case, a second control pellet was offered to verify the crayfish did not reject the test food pellet due to

satiation. Feeding deterrence was recorded as the frequency of 14-23 crayfish rejecting a test food pellet, but accepting both control pellets; crayfish that refused control pellets were not included in the analysis. A Fisher's exact test was applied to test for significance of feeding deterrence data for each compound at individual concentrations. A Fisher's exact test was also used to compare deterrence of two different compounds at equal molar concentrations (Zar, 1998).

Dose-response curves were constructed using data from 5-11 feeding assays for each test compound, by plotting the frequency of crayfish rejecting a test food pellet against the log of the concentration of the test compound in food pellets. These data were fit to a sigmoidal dose response curve with a Hill slope of 1; this Hill slope provided the largest R^2 goodness of fit value for all data sets. Differences among dose response curves for different test compounds were analyzed by an F-test of the $\log EC_{50}$ values for each compound using GraphPad Prism version 4 (Motulsky, 1995). For compounds which were not significantly deterrent at any tested concentration, the $\log EC_{50}$ could not be calculated. The highest concentration tested was 38 mM (12× the natural concentration of **1**) for analogs of **1**, and 1.3 mM (1.4× the natural concentration of **2**) for analogs of **2**. One compound, 3-(3',4',5'-trimethoxyphenyl)-1,2-propanediol (**8**) was synthesized in limited yield and so was tested only up to the EC_{50} of **1** (8.3 mM).

The interaction of natural products **1** and **2** in affecting crayfish feeding behavior was assessed using feeding assays incorporating these compounds at nine different concentrations representing 1:1 ratios of experimentally determined EC_{50} values for the two compounds (Luszczki and Czuczwar, 2003). The resulting feeding response curve was compared to a theoretical additive curve, developed on the basis of best fit dose

response curves developed individually for **1** and **2** (Tallarida et al., 1997). An F-test was applied to test for significant difference between $\log EC_{50}$ values associated with the theoretical additive curve vs. the observed plot (using GraphPad Prism version 4).

Works Cited

Achenbach, H., Frey, D., 1992. Cycloartanes and other terpenoids and phenylpropanoids from *Monocylanthus vignei.* Phytochemistry. 31: 4263-4274.

Anjanamurthy, C., Rai, K. M. L., 1987. Synthesis of podophyllotoxin and related analogs. Part 3. Synthesis of β-apopicropodophyllin analogues with modified lactone ring. Indian J. Chem. 26B, 131-135.

Assmann, M., Lichte, E., Pawlik, J. R., Kock, M., 2000. Chemical defenses of the Caribbean sponges *Agelas wiedenmayeri* and *Agelas conifera*. Mar. Ecol. Prog. Ser. 207, 255-262.

Bolser, R. C., Hay, M. E., Lindquist, N., Fenical, W., Wilson, D., 1998. Chemical defenses of freshwater macrophytes against crayfish herbivory. J. Chem. Ecol. 24, 1639-1658.

Brewer, C. F., Loike, J. D., Horwitz, S. B., Sternlicht, H., Gensler, W. J., 1979. Conformational analysis of podophyllotoxin and its congeners. Structure-activity relationship in microtubule assembly. J. Med. Chem. 22, 215-221.

Dong, X., Mondranondra, I. O., Che, C. T., Fong, H. H. S., Farnsworth, N. R., 1989. Kmeriol and other aromatic constituents of *Kmeria duperreana*. Pharm. Res. 6, 637-640.

Elakovich, S. D., Stevens, K. L., 1985. Phytotoxic properties of nordihydroguaiaretic acid, a lignan from *Larrea tridentata* (Creosote bush). J. Chem. Ecol. 11, 27-33.

Gensler, W.J., Ahmed, Q.A., Muljiani, Z., Gatsonis, C.D., 1971. Ultraviolet irradiation of α-apopicropodophyllin. J. Am. Chem. Soc. 93: 2515-2522.

Gnabre, J. N., Brady, J. N., Clanton, D. J., Ito, Y., Dittmer, J., Bates, R. B., Huang, R. C. C., 1995. Inhibition of human immunodeficiency virus type 1 transcription and replication by DNA sequence-selective plant lignans. Proc. Nat. Acad. Sci. USA 92, 11239-11243.

Gonzalez, A. G., Barrera, J. B., Arancibia, L., Diaz, J. G., De Paz, P. P., 1991. Two phenylpropanoids from *Todaroa aurea* subsp. *suaveolens*. Phytochemistry. 30, 4189-4190.

Harmatha, J., Nawrot, J., 2002. Insect feeding deterrent activity of lignans and related phenylpropanoids with a methylenedioxyphenyl (piperonyl) structure moiety. Entomol. Exp. Appl. 104, 51-60.

Hobbs, H. H., 1981. The Crayfishes of Georgia. Smithsonian Institution Press, Washington, D.C.

Kim, J. H., Mullin, C. A., 2003. Antifeedant effects of proteinase inhibitors on feeding behaviors of adult western corn rootworm (*Diabrotica virgifera virgifera*). J. Chem. Ecol. 29, 795-810.

Kubanek, J., Fenical, W., Hay, M. E., Brown, P. J., Lindquist, N., 2000. Two antifeedant lignans from the freshwater macrophyte *Saururus cernuus*. Phytochemistry. 54, 281-287.

Kubanek, J., Hay, M. E., Brown, P. J., Lindquist, N., Fenical, W., 2001. Lignoid chemical defenses in the freshwater macrophyte *Saururus cernuus*. Chemoecology. 11, 1-8.

Lee, I. S., Jung, K. Y., Oh, S. R., Park, S. H., Ahn, K. S., Lee, H. K., 1999. Structure-activity relationships of lignans from *Schisandra chinensis* as platelet activating factor antagonists. Biol. Pharm. Bull. 22, 265-267.

Lewis, N. G., Davin, L. B., 1999. Lignans: biosynthesis and function. In: Barton, D.H.R., Sir, Nakanishi, K., Meth-Cohn, O. (Eds.), Comprehensive Natural Products Chemistry, Vol. 1. Elsevier, Amsterdam, pp. 639-712.

Lindel, T., Hoffmann, H., Hochgurtel, M., Pawlik, J. R., 2000. Structure-activity relationship of inhibition of fish feeding by sponge-derived and synthetic pyrrole-imidazole alkaloids. J. Chem. Ecol. 26, 1477-1496.

Lodge, D. M., 1991. Herbivory on fresh water macrophytes. Aquatic Bot. 41, 195-224.

Loike, J. D., Horwitz, S. B., 1976. Effects of podophyllotoxin and VP-16-213 on microtubule assembly *in vitro* and nucleoside transport in HeLa-cells. Biochemistry. 15, 5435-5443.

Luszczki, J. J., Czuczwar, S. J., 2003. Isobolographic and subthreshold methods in the detection of interactions between oxcarbazepine and conventional antiepileptics - a comparative study. Epilepsy Res. 56, 27-42.

Mata, R., Morales, I., Perez, O., Rivero-Cruz, I., Acevedo, L., Enriquez-Mendoza, I., Bye, R., Franzblau, S., Timmermann, B., 2004. Antimycobacterial compounds from *Piper sanctum*. J. Nat. Prod. 67, 1961-1968.

Morimoto, M., Tanimoto, K., Nakano, S., Ozaki, T., Nakano, A., Komai, K., 2003. Insect antifeedant activity of flavones and chromones against *Spodoptera litura*. J. Agric. Food Chem. 51, 389-393.

Motulsky, H., 1995. Intuitive Biostatistics. Oxford Univ. Press.

Ozeki, M., 1975. Effects of eugenol on nerve and muscle in crayfish. Comp. Biochem. Physiol. 50C, 183-191.

Parker, J. D., Collins, D., Kubanek, J., Sullards, M. C., Bostwick, D., Hay, M. E., 2006. Chemical defenses promote persistence of the aquatic plant *Micranthemum umbrosum*. J. Chem. Ecol.

Rhoades, D.F., Cates, R.G., 1976. Toward a general theory of plant antiherbivore chemistry. In: Wallace, J.W., Nansel, R.L. (Eds.), Recent Advances in Phytochemistry, Vol 10. Plenum Press, NY, pp 168-213.

Silva, K. L., Trigo, J. R., 2002. Structure-activity relationships of pyrrolizidine alkaloids in insect chemical defense against the orb-weaving spider *Nephila clavipes*. J. Chem. Ecol. 28, 657-668.

Tallarida, R. J., Kimmel, H. L., Holtzman, S. G., 1997. Theory and statistics of detecting synergism between two active drugs: cocaine and buprenorphine. Psychopharmacology. 133, 378-382.

Wilson, D. M., Fenical, W., Hay, M., Lindquist, N., Bolser, R., 1999. Habenariol, a freshwater feeding deterrent from the aquatic orchid *Habenaria repens* (Orchidaceae). Phytochemistry. 50, 1333-1336.

Yamashita, K., Matsui, M., 1961. Studies on phenolic lactones. Synergistic activities of phenolic lactones. Agric. Biol. Chem. 25, 141-143.

Zar, J. H., 1998. Biostatistical Analysis: Prentice Hall.

Zhang, H.Z., Kasibhatla, S., Wang, Y., Herich, J., Guastella, J., Tseng, B., Drewe, J., Cai, S.X., 2004. Discovery, characterization, and SAR of gambogic acid as a potent apoptosis inducer by a HTS assay. Bioorg. Med. Chem. 12, 309-317.

APPENDIX A

SUPPORTING INFORMATION: CALLOPHYCOIC ACIDS AND CALLOPHYCOLS FROM THE FIJIAN RED ALGA *CALLOPHYCUS SERRATUS*

General Experimental Procedures. NMR spectra were recorded at 500 MHz and 125 MHz for ^{1}H and ^{13}C NMR, respectively, and referenced to residual $CHCl_3$ (7.24 and 77.0 ppm, for ^{1}H and ^{13}C, respectively) for **1**-**2** and **5**-**10** and to residual $(CH_3)_2CO$ (2.04 and 29.8 ppm, for ^{1}H and ^{13}C, respectively) for **3**-**4**.

Table A.1: COSY correlations for callophycoic acids A-H (**1-8**) and callophycols A-B (**9-10**). For diastereotopic protons with dissimilar chemical shifts, the proton whose chemical shift is listed first in Tables 1-2 of the main article is termed "a" and the other is "b". "NA" (not applicable) indicates that no proton signal exists for that position.

^{1}H at position #:	**COSY correlations observed between protons listed on far left and those below:**									
	1	**2**	**3**	**4**	**5**	**6**	**7**	**8**	**9**	**10**
3	5a, 5b	5b	17	17	-	5	-	5, 17	5	-
5a	3, 5b, 6	5b, 6	5b, 6	5b, 6	5b, 6	3	3, 5b, 6	3, 6	3, 7a, 7b	7a, 7b
5b	3, 5a, 6	3, 5a, 6	5a, 6	5a, 6	5a, 6	NA	3, 5a, 6	NA	NA	NA
6	5a, 5b, 20b, 22	5a, 5b, 20	5a, 5b, 22	5a, 5b	5a, 5b, 20	5, 8, 24	5a, 5b, 21a, 21b	3, 21a, 21b	NA	NA
7a	NA	NA	NA	NA	NA	NA	NA	NA	5, 8	5, 8
7b	NA	NA	NA	NA	NA	NA	NA	NA	5, 8	5, 8
8a	10, 25	10	8b, 9a, 9b	8b, 9a, 9b	8b, 9a, 9b	6, 24	8b, 9a, 9b	8b, 9a, 9b	7a, 7b, 10a, 10b, 20a, 20b	7a, 7b, 10a, 10b, 20a, 20b
8b	10, 25	-	8a, 9a, 9b	8a, 9a, 9b	8a, 9a, 9b	-	8a, 9a, 9b	8a, 9a, 9b	NA	NA
9a	10	10	8a, 8b, 9b, 10	8a, 8b, 9b, 10	8a, 8b, 9b, 10	10	8a, 8b, 9b, 10	8a, 8b, 9b, 10	NA	NA
9b	10	10	8a, 8b, 9a, 10	8a, 8b, 9a, 10	8a, 8b, 9a	NA	8a, 8b, 9a, 10	8a, 8b, 9a, 10	NA	NA
10a	8a, 8b, 9a, 9b, 12a, 12b, 26	8a, 9a, 9b, 12a, 12b, 26	9a, 9b	9a, 9b	9a, 26a	9	9a, 9b	9a, 9b	8, 10b	8, 10b, 24
10b	NA	NA	NA	NA	NA	NA	NA	NA	8, 10a, 11b	8, 10a, 23, 24
11a	NA	NA	NA	NA	NA	NA	NA	NA	11b, 12	11b, 12
11b	NA	NA	NA	NA	NA	NA	NA	NA	10b, 11a, 12	11a, 12
12a	10, 14a, 26	10, 14	12b, 13a, 13b	12b, 13	12b, 13a, 13b	14	12b, 13a	12b, 13a, 13b	11a, 11b	11a, 11b
12b	10, 14a	10, 14	12a, 13a, 13b	12a, 13	12a, 13b	NA	12a, 13a	12a, 13a, 13b	NA	NA
13a	14	14	12a, 12b, 13b, 14	12a, 12b, 14	12a, 13b, 14	14	12a, 12b, 13b, 14	12a, 12b, 13b, 14	NA	NA
13b	14	14	12a, 12b, 13a, 14	NA	12a, 12b, 13a, 14	NA	13a, 14	12a, 12b, 13a, 14	NA	NA
14a	12a,	12a,	13a,	13	13a,	12, 13,	13a,	13a,	14b,	14b,

	12b, 13a, 13b, 16, 27	12b, 13a, 13b, 16, 27	13b		13b	26	13b, 27	13b, 27	15b	15b
14b	NA	NA	NA	NA	NA	NA	NA	NA	14a, 15a, 15b, 23	14a, 15a, 23
15a	NA	NA	NA	NA	NA	NA	NA	NA	14b, 15b, 16	14b, 15b, 16
15b	NA	NA	NA	NA	NA	NA	NA	NA	14a, 14b, 15a	14a, 15a, 16, 18, 26
16	14, 27	14	-	-	27	18	-	14a	15a, 26	15a, 15b
17	18	18	3, 18	3, 18	18	18	18	3	NA	NA
18	17	17	17	17	17	16, 17, 20	17	NA	-	15b
20a	20b, 22	6, 22	20b	-	6, 22a	18	NA	NA	8, 20b	8, 20b, 21a
20b	6, 20a, 22	NA	20a	NA	NA	NA	NA	NA	8, 20a	8, 20a, 21a
21a	NA	NA	NA	NA	NA	22	6, 21b, 22a	6, 21b, 22	21b, 22a, 22b	20a, 20b, 22a, 22b
21b	NA	NA	NA	NA	NA	NA	6, 21a, 22a	6, 21a, 22	21a, 22a	22a
22a	6, 20a, 20b, 23a, 23b	20, 24	6, 23a, 23b	23a, 23b	20, 22a, 23	21	21a, 21b, 22b, 23a, 23b	21a, 21b, 22b, 23a, 23b	21a, 21b, 22b	21a, 21b
22b	NA	24	NA	-	22a, 24	NA	22a, 23a, 23b	21a, 21b, 22a, 23a, 23b	21a, 22a, 23	21a, 23
23a	22, 23b, 24	24	22, 23b, 24	22, 23b, 24	22a, 24	NA	22a, 22b, 23b	22a, 22b, 23b	14b, 22b	10b, 14b, 22b, 25
23b	22, 23a, 24	24	22, 23a, 24	22, 23a, 24	NA	NA	22a, 22b, 23a, 24	22a, 22b, 23a, 24	NA	NA
24	23a, 23b	22a, 22b, 23a, 23b	23a, 23b	23a, 23b	22b, 23	6, 8	23b	23b	-	10a
25	8a, 8b	-	-	-	-	10	-	-	-	23
26a	10, 12a	10	-	-	10, 26b	14	-	-	16	15b

26b	NA	NA	NA	NA	26a	NA	NA	NA	NA	NA
27	14, 16	14	-	-	16	18	14	14	NA	NA

Table A.2: HMBC correlations for callophycoic acids A-H (**1-8**) and callophycols A-B (**9-10**). For diastereotopic protons with dissimilar chemical shifts, the proton whose chemical shift is listed first in Tables 1-2 of the main article is termed "a" and the other is "b". "NA" (not applicable) indicates that no proton signal exists for that position.

^{1}H at position #:	HMBC correlations observed between protons listed on far left and carbons at positions listed below:									
	1	**2**	**3**	**4**	**5**	**6**	**7**	**8**	**9**	**10**
3	1, 2, 17, 18, 19	1, 5, 17, 19	1, 5, 17, 19	1, 5, 17, 19	1, 5, 17, 19	1, 5, 21, 23	1, 5, 17, 19	1, 5, 17, 19	1, 4, 5	1, 4, 5
5a	3, 4, 6, 7, 19, 21	4, 6, 7, 19, 21	3, 4, 6, 19, 21	3, 4, 6, 19, 21	6, 19, 21	3, 4, 6, 7, 23	4, 19, 20	4, 6, 19, 20	1, 3, 4, 6, 7	1, 3, 4, 7
5b	3, 4, 6, 7, 19, 21	4, 6, 7, 19, 21	4, 6, 21	3, 4, 6, 19, 21	4, 6, 19, 21	NA	3, 4, 19, 20	NA	NA	NA
6	4, 5, 7, 21, 22, 25	5, 7, 20, 21, 25	4, 5, 7, 21	5, 7	7, 21	4, 5, 8, 24	-	20	NA	NA
7a	NA	NA	NA	NA	NA	NA	NA	NA	1, 5, 6, 8, 9, 19	1, 5, 6, 8, 9, 19
7b	NA	NA	NA	NA	NA	NA	NA	NA	1, 5, 6, 8, 9, 19	1, 5, 6, 8, 9, 19
8a	7, 9, 24, 25	6, 7, 9, 10, 11, 24	7, 9, 24	7, 9, 10	-	7	10	-	6, 7, 9, 10, 19, 20, 24	7, 9, 19, 20, 24
8b	7, 9, 10, 25	6, 7	7, 24	9, 10, 24	7, 24	10	-	-	NA	NA
9a	7, 8, 10, 11, 26	10	8, 10, 11	8, 10	-	-	-	-	NA	NA
9b	8, 11	10, 11	8, 10, 11	8	-	-	-	-	NA	NA
10a	8, 9, 12, 26	9, 12, 26	9, 11, 15, 16	9, 11, 15, 26	8, 11, 15, 26	8, 9, 12, 25	-	-	8, 9, 11, 12, 24	-
10b	NA	NA	NA	NA	NA	NA	NA	NA	9, 11, 12, 23, 24	-
11a	NA	NA	NA	NA	NA	NA	NA	NA	9, 10, 12, 13	-
11b	NA	NA	NA	NA	NA	NA	NA	NA	9, 10, 12, 13	-
12a	10, 11, 13, 14, 26	10, 11, 13, 26	11, 13, 26	11	-	11, 13, 14	-	-	11, 13, 25	10, 11, 13, 25
12b	NA	NA	11, 13, 26	10	13, 14	NA	-	-	NA	NA
13a	11, 14	11, 12, 14, 15	14	11, 12	-	14	-	-	NA	NA

13b	11, 12, 14, 15	NA	14	NA	11, 15	NA	-	-	NA	NA
14a	12, 16, 27	13, 16, 27	13, 16, 27	16, 27	12, 13	12, 13, 26	-	-	16, 25	15
14b	NA	NA	NA	NA	NA	NA	NA	NA	13, 15, 16	-
15a	NA	NA	NA	NA	NA	NA	NA	NA	-	-
15b	NA	NA	NA	NA	NA	NA	NA	NA	13	-
16	12, 14, 15, 27	14, 15, 27	10, 14, 15, 27	10, 14, 15, 27	10, 14, 15, 27	17, 18	14, 15, 27	14, 15, 27	14, 17, 18, 26	14, 15, 17
17	1, 3, 19	1, 3, 19	1, 3, 19	3, 19	1, 3, 19	16, 18	1, 3, 19	1, 3, 19	NA	NA
18	1, 2, 4, 19	2, 4, 19	2, 4, 19	2, 4, 19	2, 4, 19	16, 17, 27	2, 4, 19	NA	16, 17, 26	16, 17, 26
20a	6, 19, 21, 22	6, 19, 21, 22	6, 19, 21, 22	6, 19, 21, 22	6, 19, 21, 22	18, 19, 27	NA	NA	8, 21	8, 21
20b	6, 19, 21, 22	NA	19, 21, 22	NA	NA	NA	NA	NA	8, 21	8, 21
21a	NA	NA	NA	NA	NA	1, 3, 23	6, 22	6, 22	19, 20, 22	19, 20
21b	NA	NA	NA	NA	NA	NA	6, 22	6, 22	-	-
22a	6, 20, 23, 24	20, 21	-	6, 20, 21, 23	-	2, 4, 23	-	-	9, 21, 23	21, 23
22b	NA	6, 24	NA	NA	24	NA	-	-	-	-
23a	21, 22, 24, 25	7, 24	7, 21, 22, 24	7, 21, 22, 24	22	NA	-	-	8, 9, 10, 12, 13, 22, 24	9, 13, 22, 25
23b	7, 21, 22, 24	7, 21, 24	7, 21, 22, 24	21	NA	NA	-	-	NA	NA
24	7, 8, 23, 25	6, 7, 23, 25	7, 23, 25	23	25	6, 7, 8, 23	11, 23	11, 23	8, 9, 10, 23	8, 9, 10, 23
25	5, 6, 7, 8, 9, 24	6, 7, 8, 24	6, 7, 8, 24	6, 7, 8, 24	6, 7, 8, 24	10, 11, 12	6, 7, 8, 24	6, 7, 8, 24	12, 13, 14, 23	12, 13, 14, 15, 23
26a	10, 11, 12	10, 11, 12	10, 11, 12	10, 11, 12	10, 12	14, 15, 16	10, 11, 12, 24	10, 11, 12, 24	16, 17, 18	16, 17, 18
26b	NA	NA	NA	NA	10, 12	NA	NA	NA	NA	NA
27	14, 15, 16	14, 15, 16	10, 14, 15, 16	10, 14, 15, 16	10, 14, 15, 16	18, 19, 20	14, 15, 16	14, 15, 16	NA	NA
OH	NA	NA	-	-	NA	NA	-	-	1, 2, 6	1, 2, 6

Table A.3: Observed NOEs from NOESY and ROESY NMR experiments, for callophycoic acids A-H (**1-8**) and callophycols A-B (**9-10**). For diastereotopic protons with dissimilar chemical shifts, the proton whose chemical shift is listed first in Tables 1-2 of the main article is termed "a" and the other is "b". Only NOEs important to determinations of stereochemistry are listed.

^{1}H at position #:	NOE observed between protons listed on far left and protons at positions listed below:									
	1	**2**	**3**	**4**	**5**	**6**	**7**	**8**	**9**	**10**
5a	25	25	25	25	25		25	25		
5b	25	25	25	25	25		25			
6	24	24	9b, 24	9b, 24	24	8a, 8b	24	24		
7a									24	24
7b									24	24
8a			10, 16, 25	10, 16, 25	25	6			23	23
8b	24	24	10, 25	10, 25	25	6				
9a			16, 24, 27	16, 24, 27	16	25				
9b	26	26	6, 26	6, 26						
10	12a	12a	8a, 8b, 12a, 14, 16	8a, 8b, 12a, 14, 16	14, 16	12	24	24		
12a	10	10	10, 14	10, 14		10			14a, 14b, 23	14a, 14b, 23
12b			26	26						
14a			10, 12a, 16	10, 12a, 16	10, 16	16			12	12
14b									12	12
16			8a, 9a, 10, 14	8a, 9a, 10, 14	9a, 10, 14	14				
18										
20a	22	22b	22	22	22b					
20b	22									
22a	20a, 20b		20	20						
22b		20			20					
23									8, 12	8, 12
24	6, 8b	6, 8b	6, 9a	6, 9a	6		6, 10	6, 10	7a, 7b, 25	7a, 7b, 25
25	5a, 5b	5a, 5b	5a, 5b, 8a, 8b, 12b	5a, 5b, 8a, 8b	5a, 5b, 8a, 8b	9	5a, 5b, 26	5, 26	24	24
26	9b	9b	9b, 12b, 27	9b, 12b, 27			25	25		
27			9a, 26	9a, 26						

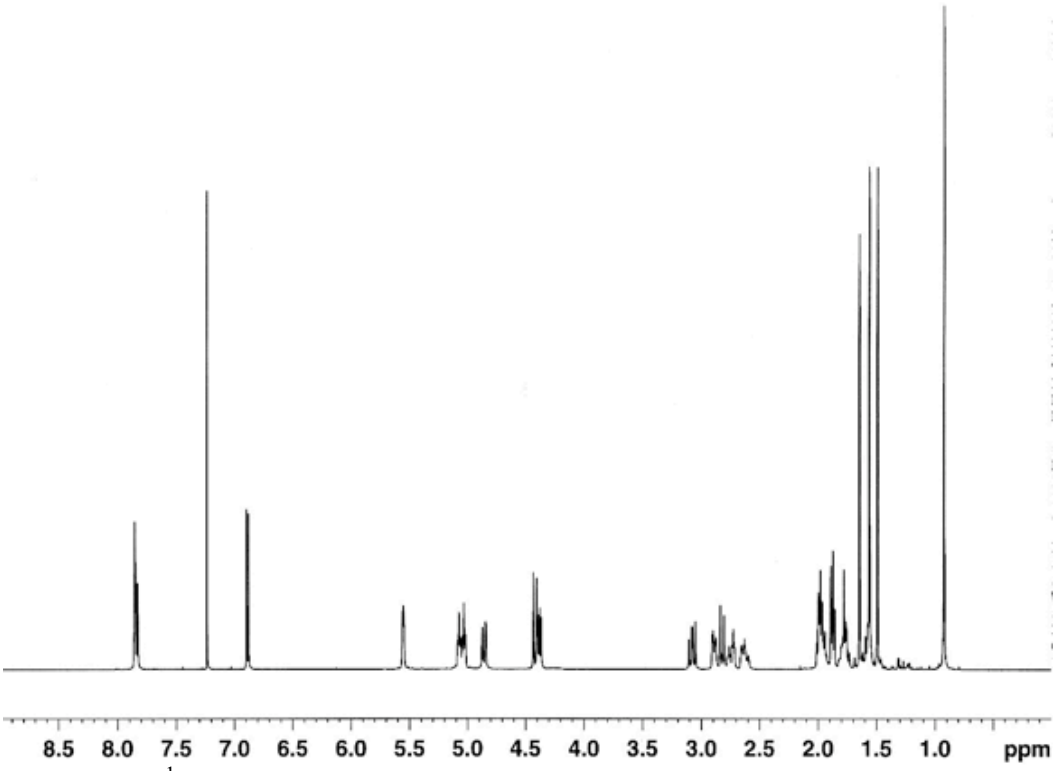

Figure A.1 ^{1}H NMR spectrum of callophycoic acid A (**1**) (500 MHz; $CDCl_3$)

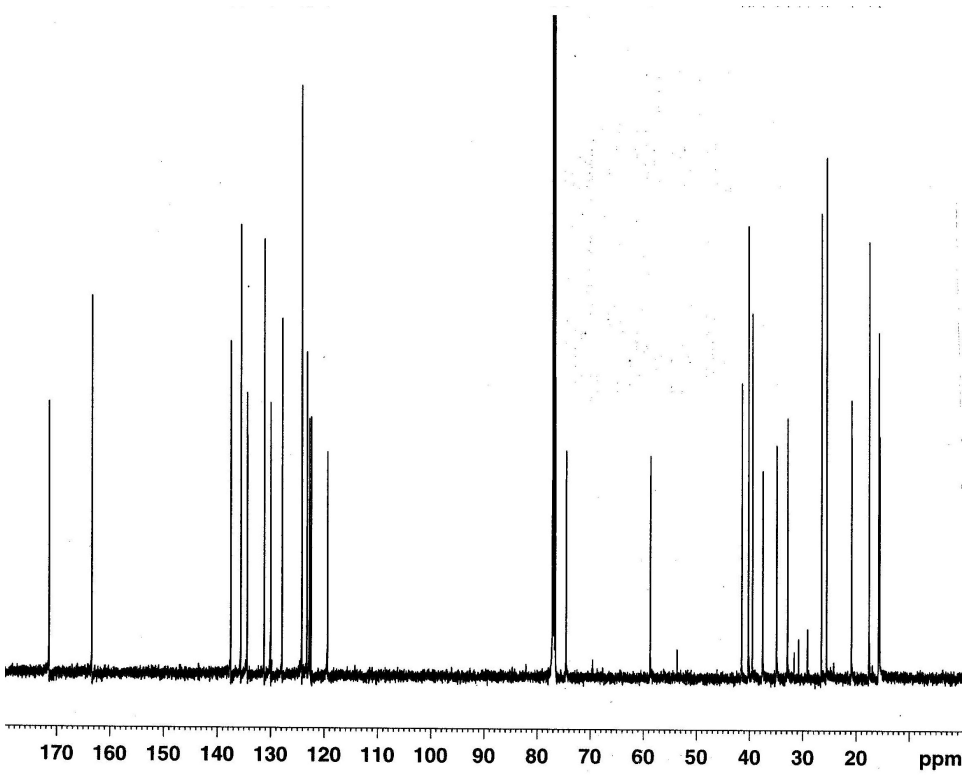

Figure A.2 ^{13}C NMR spectrum of callophycoic acid A (**1**) (125 MHz; $CDCl_3$)

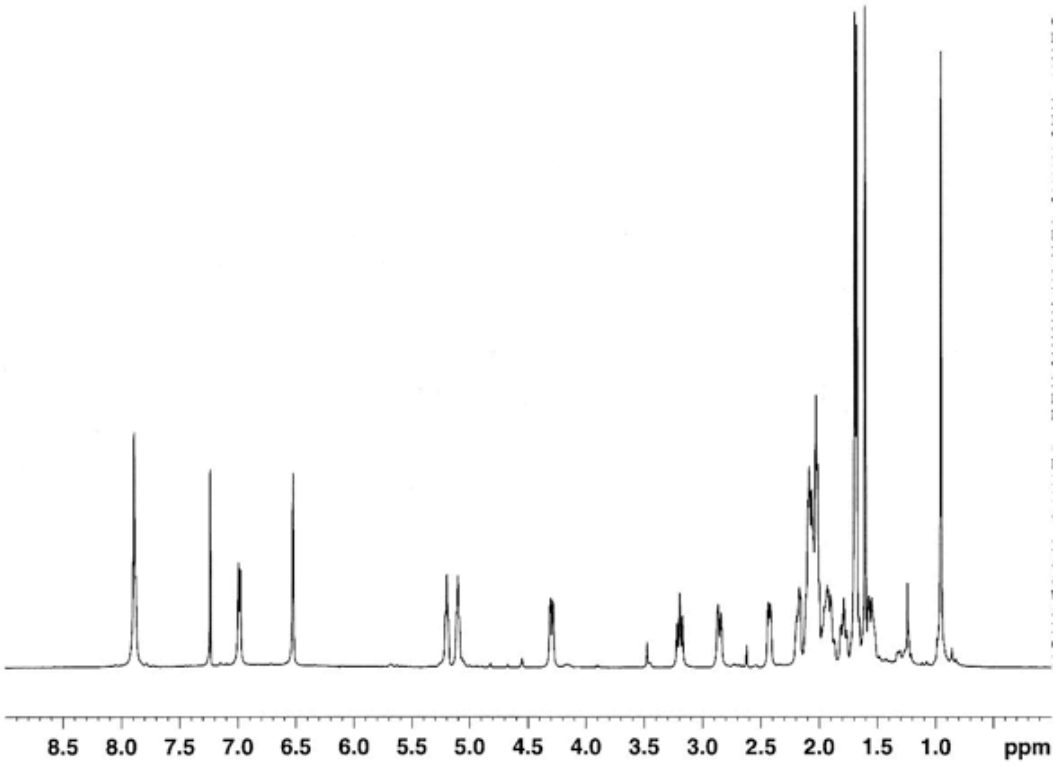

Figure A.3 ^{1}H NMR spectrum of callophycoic acid B (**2**) (500 MHz; $CDCl_3$)

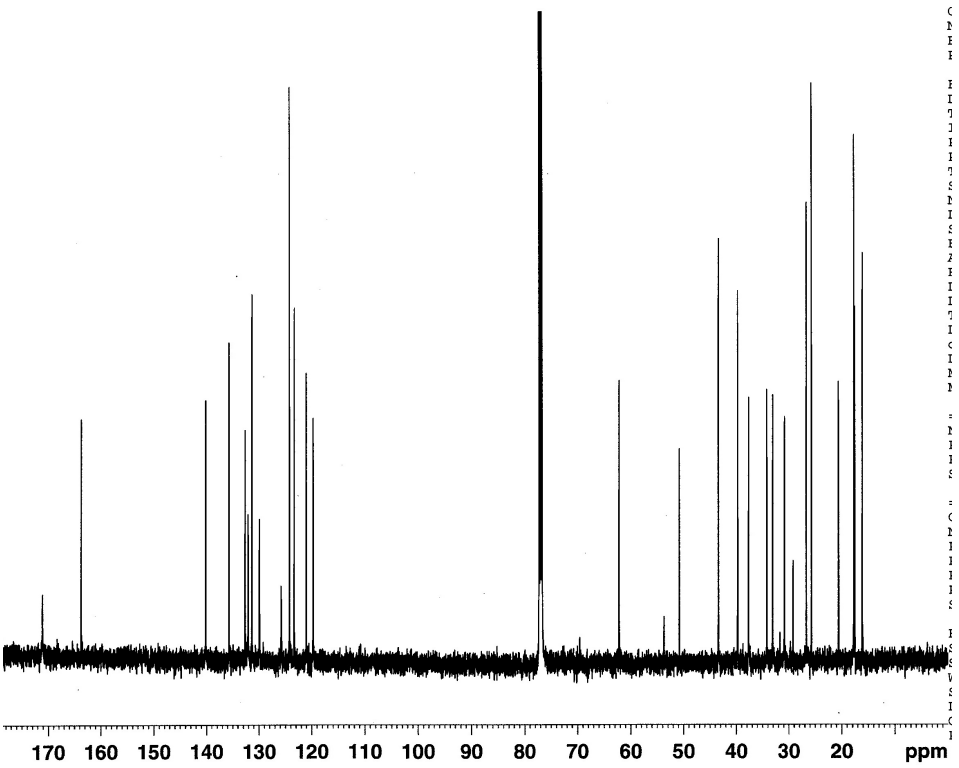

Figure A.4 ^{13}C NMR spectrum of callophycoic acid B (**2**) (125 MHz; $CDCl_3$)

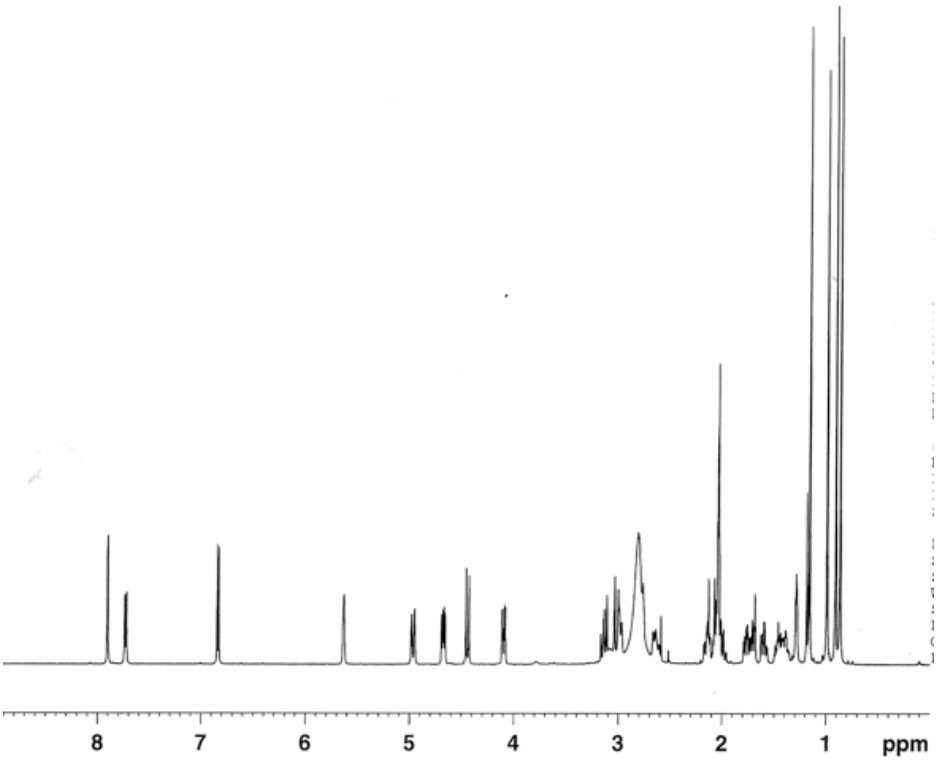

Figure A.5 ^{1}H NMR spectrum of callophycoic acid C (**3**) (500 MHz; $(CD_3)_2CO$)

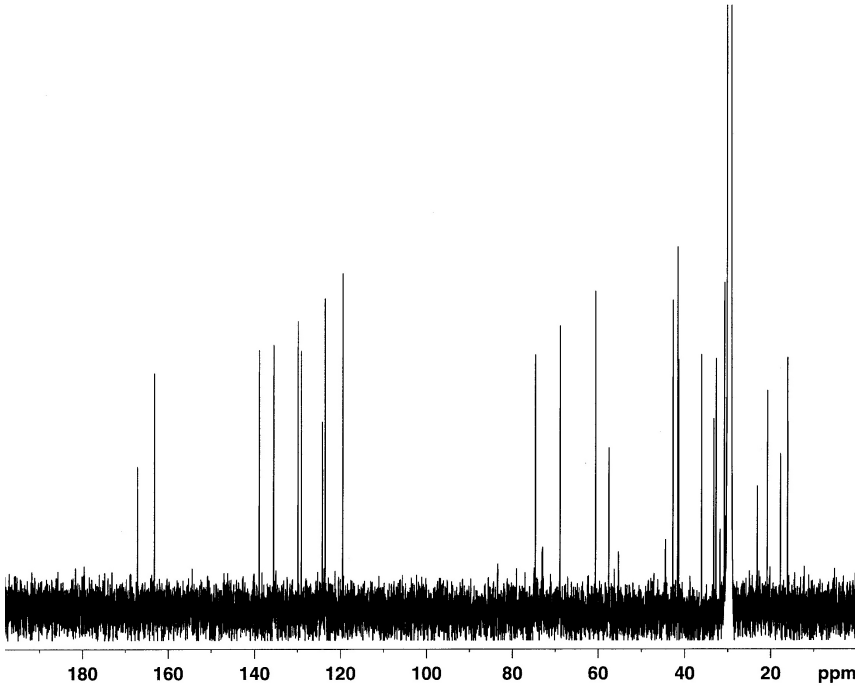

Figure A.6 ^{13}C NMR spectrum of callophycoic acid C (**3**) (125 MHz; $(CD_3)_2C$ O)

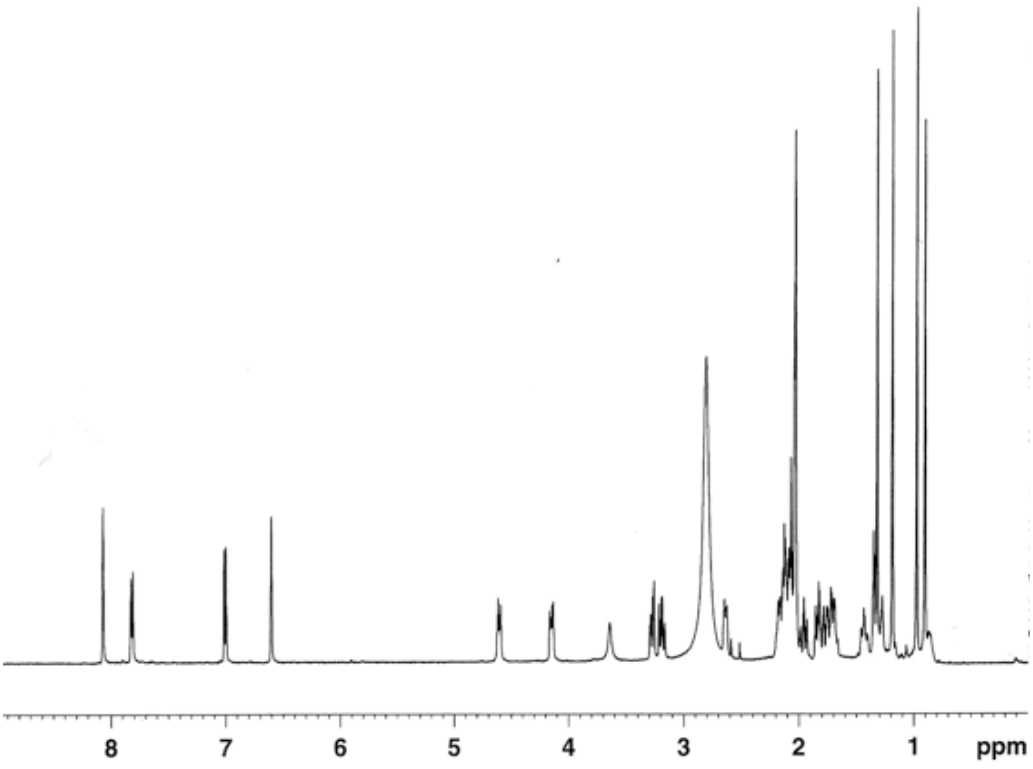

Figure A.7 ^{1}H NMR spectrum of callophycoic acid D (**4**) (500 MHz; $(CD_3)_2CO$)

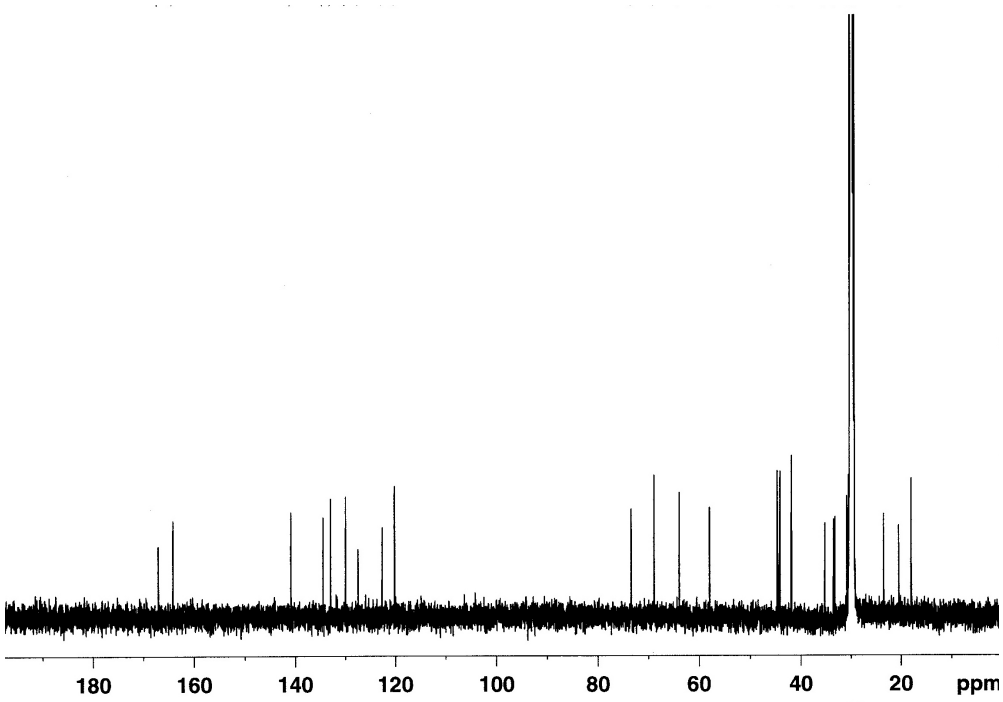

Figure A.8 ^{13}C NMR spectrum of callophycoic acid D (**4**) (125 MHz; $(CD_3)_2CO$)

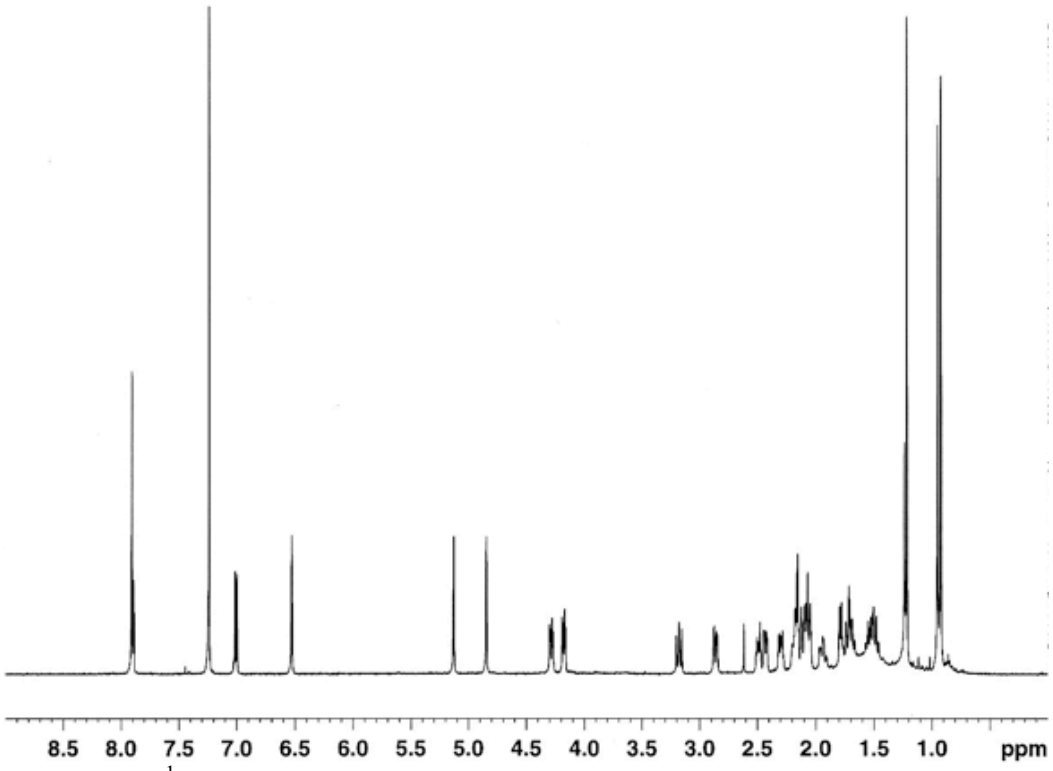

Figure A.9 ^{1}H NMR spectrum of callophycoic acid E (**5**) (500 MHz; $CDCl_3$)

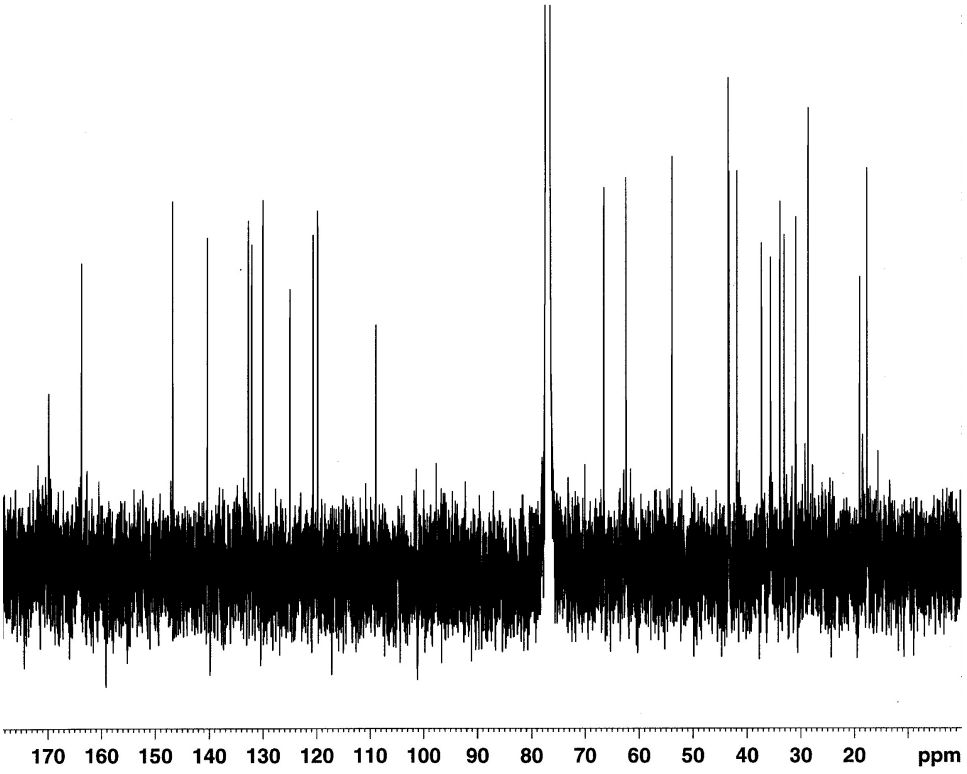

Figure A.10 ^{13}C NMR spectrum of callophycoic acid E (**5**) (125 MHz; $CDCl_3$)

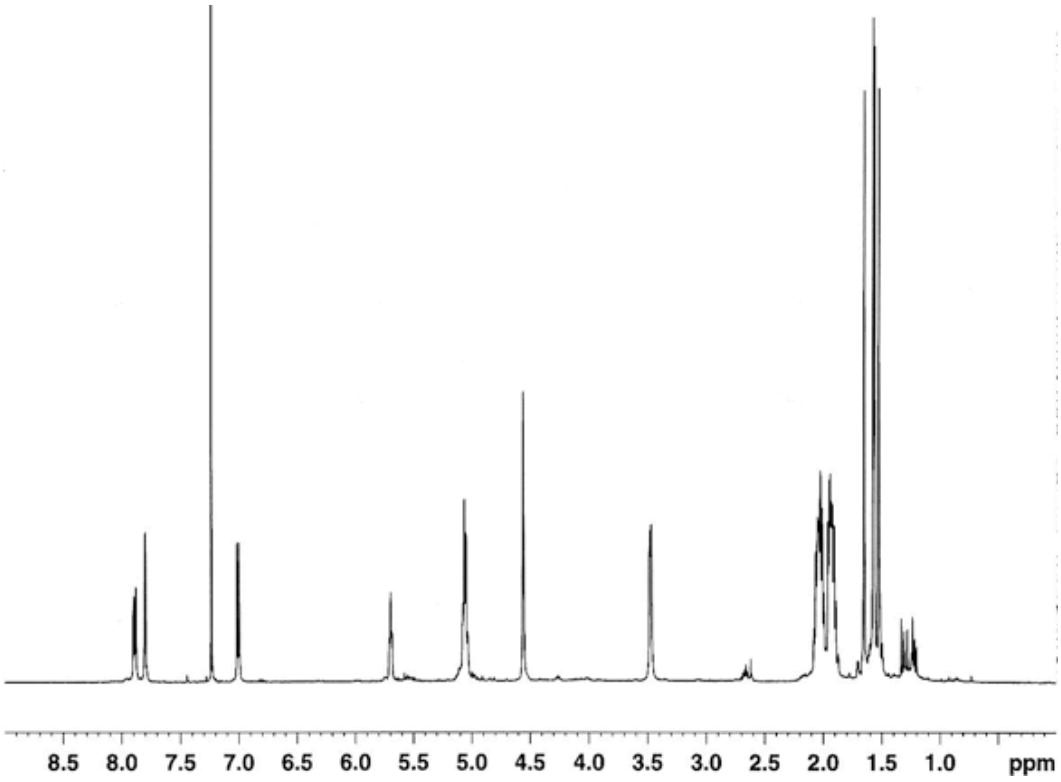

Figure A.11 ^{1}H NMR spectrum of callophycoic acid F (**6**) (500 MHz; $CDCl_3$)

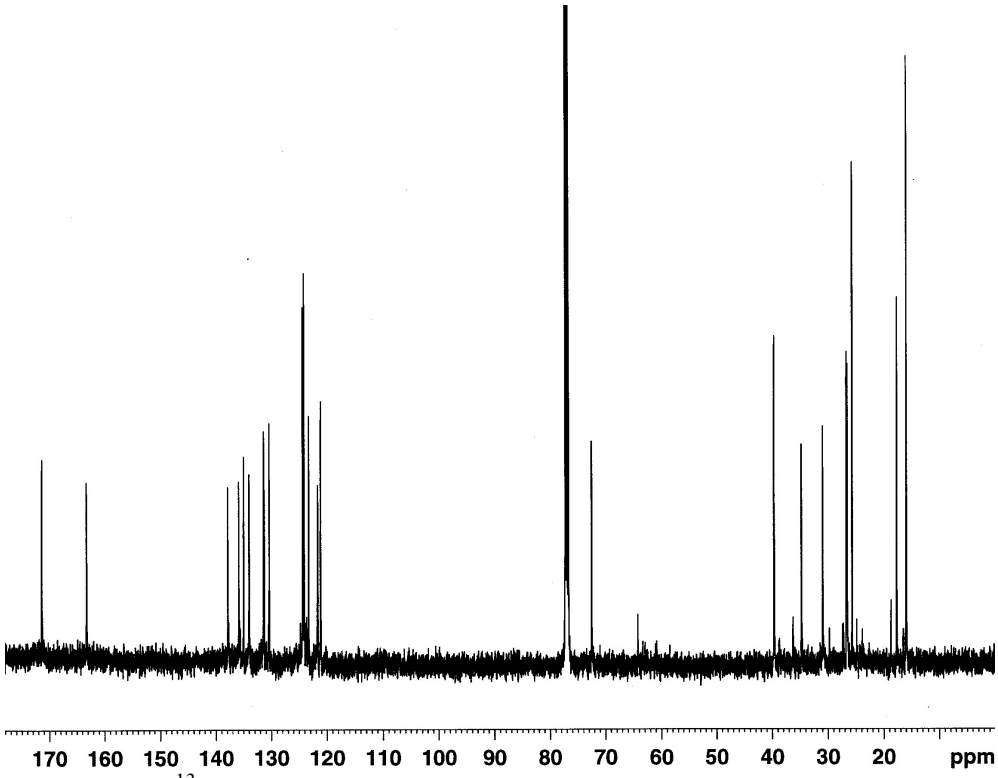

Figure A.12 ^{13}C NMR spectrum of callophycoic acid F (**6**) (125 MHz; $CDCl_3$)

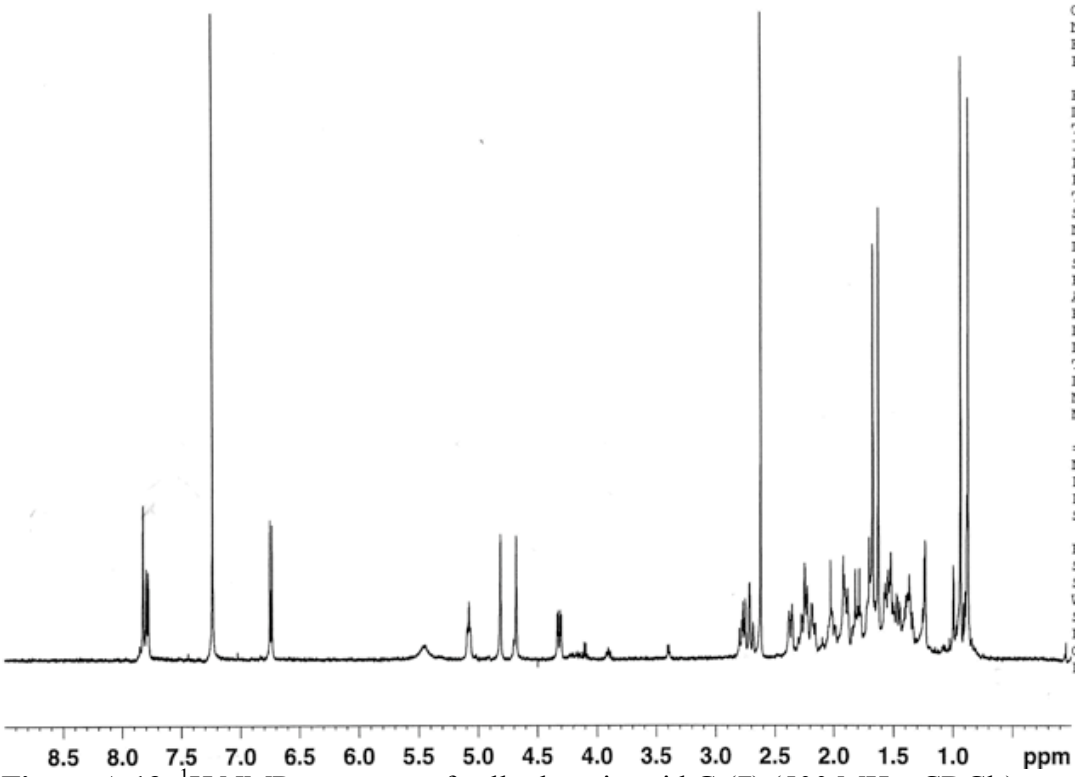

Figure A.13 ^{1}H NMR spectrum of callophycoic acid G (**7**) (500 MHz; $CDCl_3$)

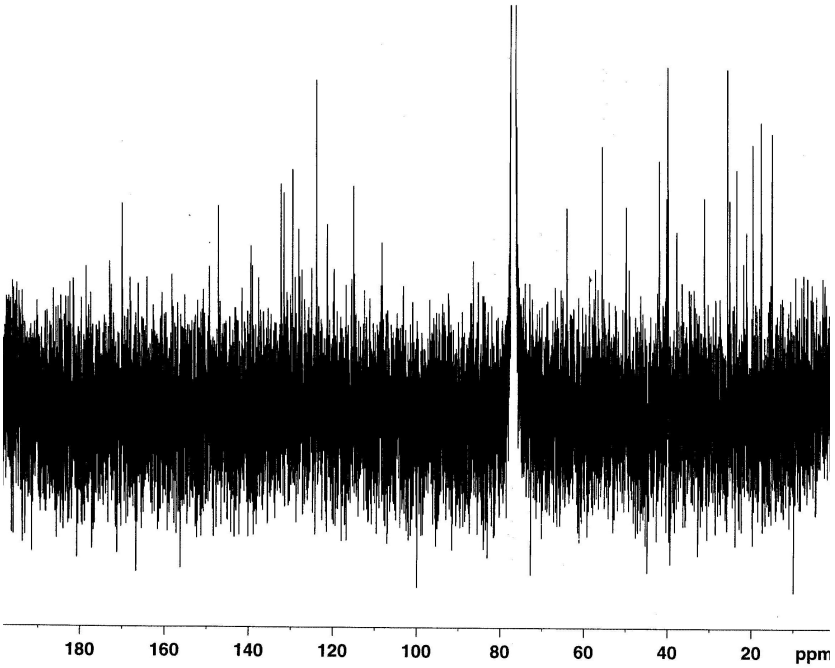

Figure A.14 ^{13}C NMR spectrum of callophycoic acid G (**7**) (125 MHz; $CDCl_3$)

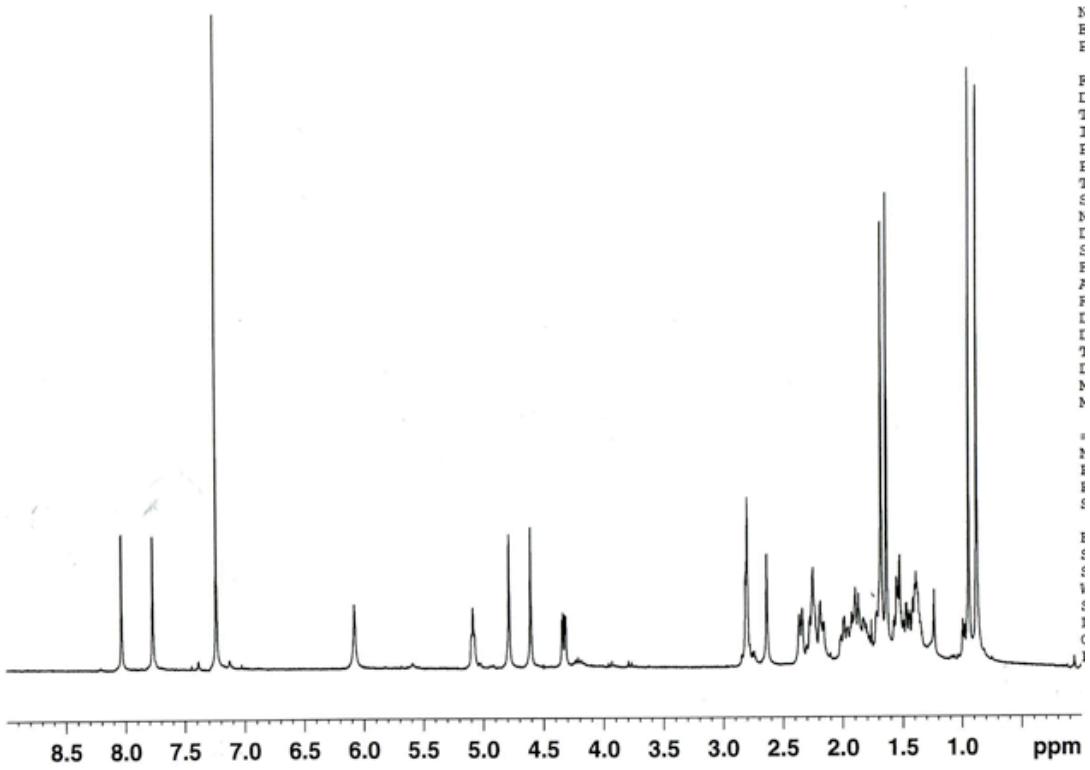

Figure A.15 ^{1}H NMR spectrum of callophycoic acid H (**8**) (500 MHz; $CDCl_3$)

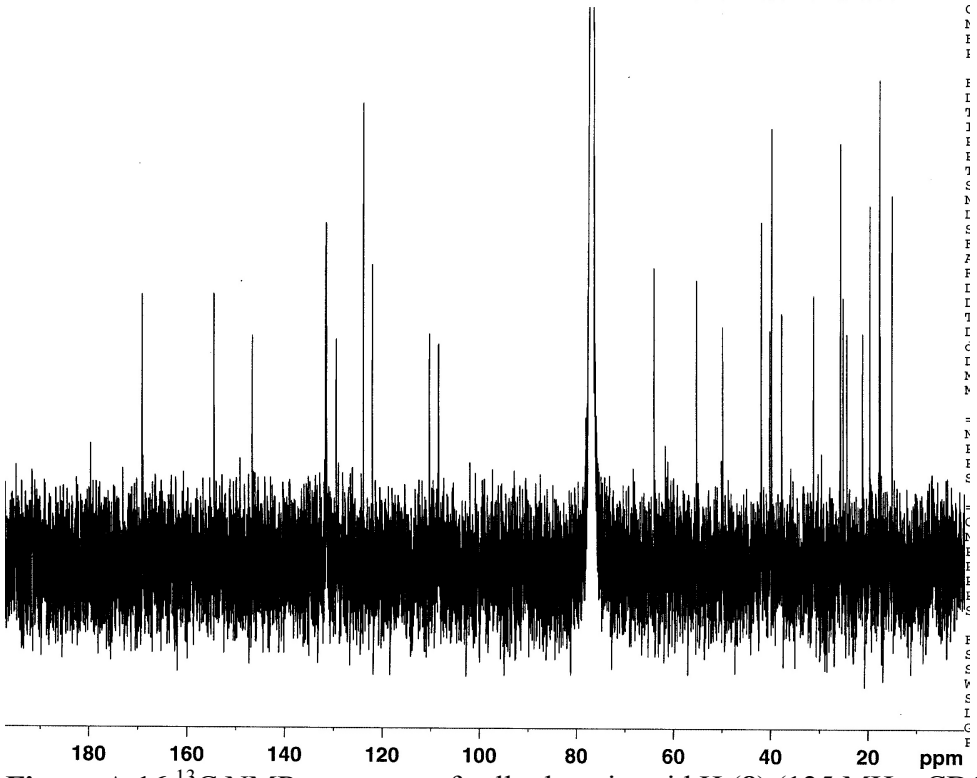

Figure A.16 ^{13}C NMR spectrum of callophycoic acid H (**8**) (125 MHz; $CDCl_3$)

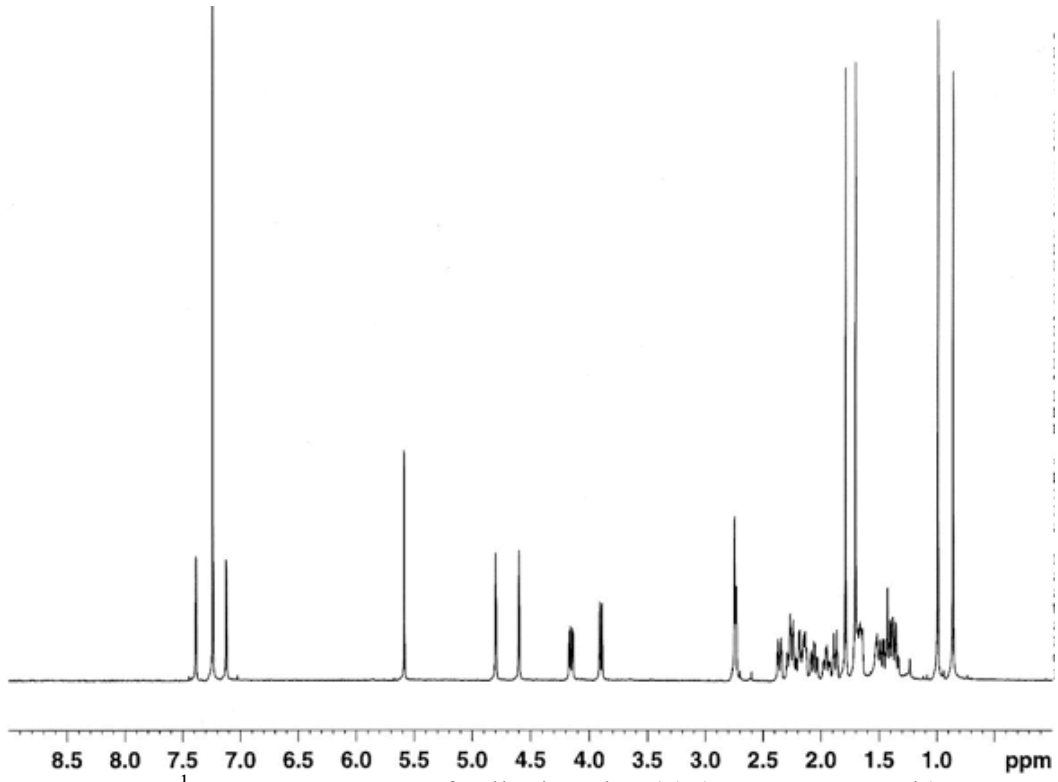

Figure A.17 ^{1}H NMR spectrum of callophycol A (**9**) (500 MHz; $CDCl_3$)

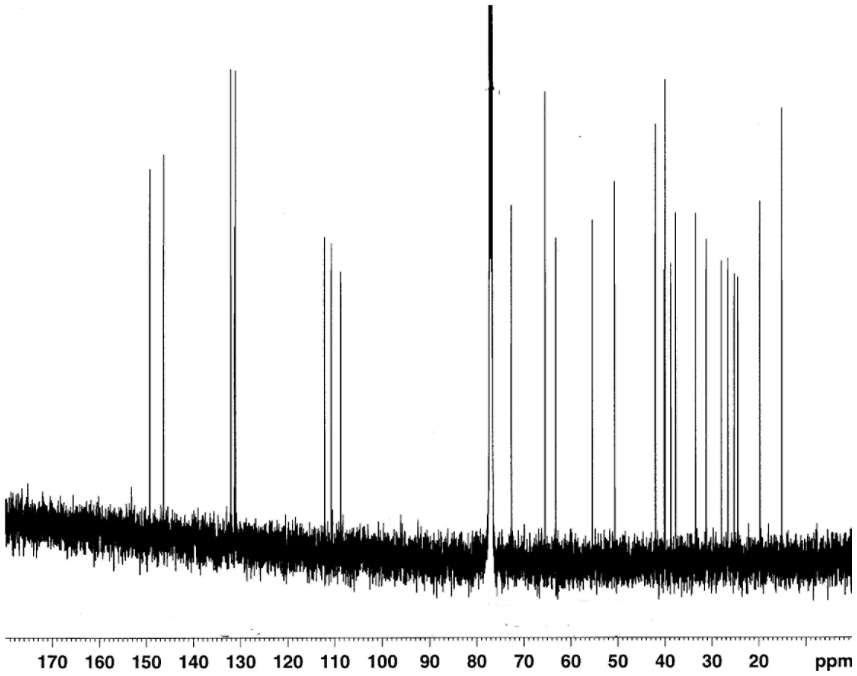

Figure A.18 ^{13}C NMR spectrum of callophycol A (**9**) (125 MHz; $CDCl_3$)

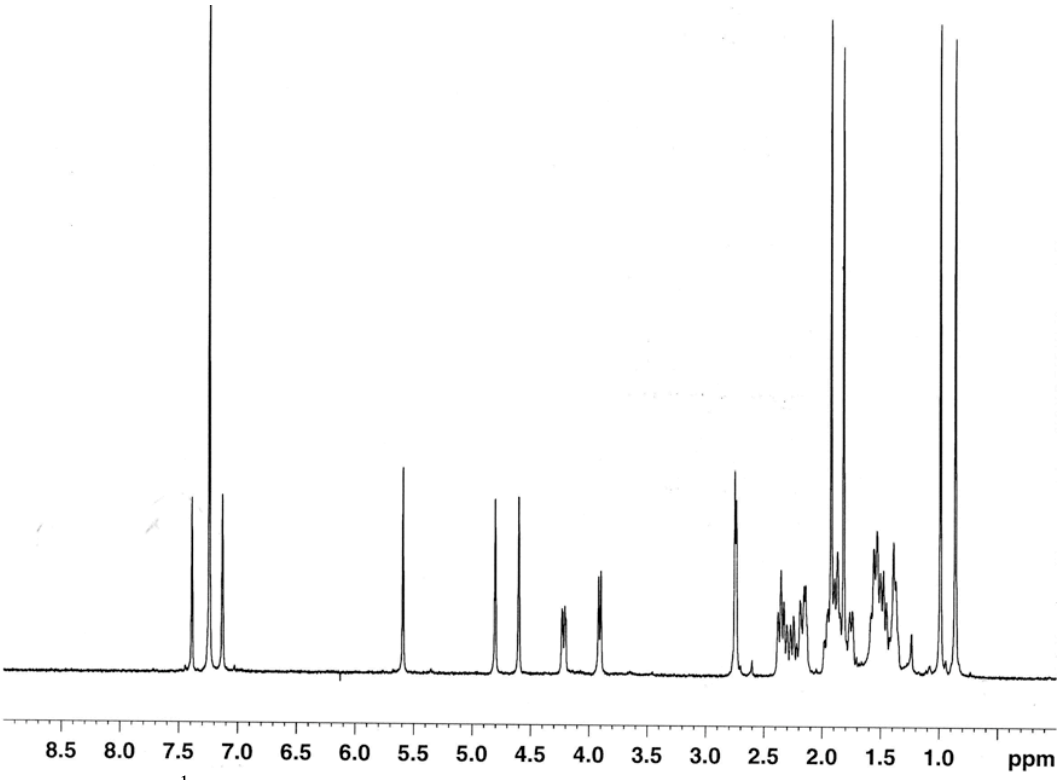

Figure A.19 ^{1}H NMR spectrum of callophycol B (**10**) (500 MHz; $CDCl_3$)

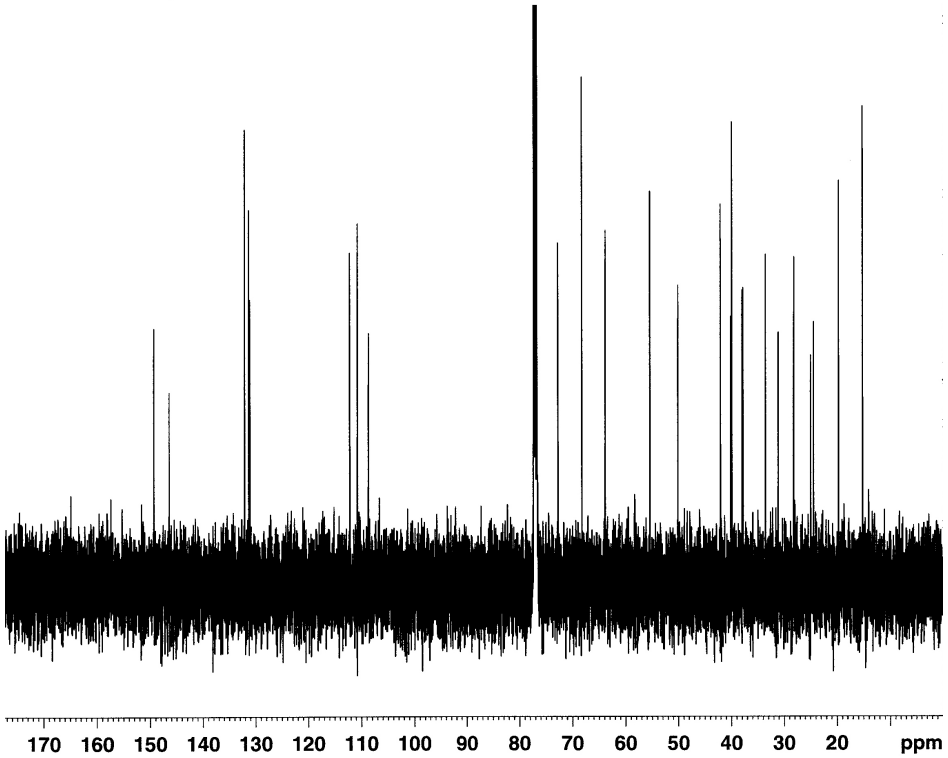

Figure A.20 ^{13}C NMR spectrum of callophycol B (**10**) (125 MHz; $CDCl_3$)

APPENDIX B

SUPPORTING INFORMATION FOR CHAPTER 3: ANTIMALARIAL NATURAL PRODUCTS FROM THE FIJIAN RED ALGA *CALLOPHYCUS SERRATUS*

Table B.1: COSY correlations for bromophycolides J-L (**1-3**). For diastereotopic protons with dissimilar chemical shifts, the proton whose chemical shift is listed first in Tables 1-2 of the main article is termed "a" and the other is "b". "NA" (not applicable) indicates that no proton signal exists for that position.

^{1}H at position #:	COSY correlations observed between protons listed on far left and those below:		
	1	**2**	**3**
3	-	-	-
5a	5b, 6	5b	5b
5b	5a	5a	5a
6	5a	NA	NA
7	NA	8a, 8b	NA
8a	8b, 9b	7, 8b	8b, 9b
8b	8a, 9a, 9b, 24	7, 8a, 9a, 9b	8a
9a	8b, 9b, 10	9b, 8b, 10	9b, 10
9b	8a, 8b, 9a, 10	9a, 8b	8a, 9a, 10
10	9a, 9b	9a	9a, 9b
12a	12b, 13a, 13b	12b, 13a, 13b	12b, 13b
12b	12a, 13a, 13b	12a, 13a, 13b	12a, 13b
13a	12a, 12b, 13b, 14	12a, 12b, 13b, 14	13b
13b	12a, 12b, 13a, 14	12a, 12b, 13a, 14	12a, 12b, 13a, 14
14	13a, 13b	13a, 13b	13b, 26a, 26b
16	17	17	17
17	16	16	16
20a	21a, 21b, 22	20b, 21a, 21b	20b, 21a
20b	NA	20a, 21a, 21b	20a, 21b, 23
21a	20, 21b, 22	20a, 20b, 21b	20a, 21b, 22
21b	20, 21a, 22	20a, 20b, 21a, 24b	20b, 21a, 22
22	20, 21a, 21b	NA	21a, 21b
23	-	-	20b
24a	8b	24b	-
24b	NA	24a, 21b	NA
25	-	-	-
26a	-	-	14, 26b, 27
26b	NA	-	14, 26a, 27
27	-	-	26a, 26b
28	-	NA	NA

Table B.2: HMBC correlations for bromophycolides J-L (**1-3**). For diastereotopic protons with dissimilar chemical shifts, the proton whose chemical shift is listed first in Tables 1-2 of the main article is termed "a" and the other is "b". "NA" (not applicable) indicates that no proton signal exists for that position.

^{1}H at position #:	HMBC correlations observed between protons listed on far left and carbons at positions listed below:		
	1	**2**	**3**
3	1, 5, 16, 18	1, 5, 16, 18	1, 5, 16, 18
5a	4, 7	7	3, 6, 7, 18, 19
5b	3, 4, 6, 7, 18, 19	4	3, 6, 7, 18, 19
6	-	NA	NA
7	NA	-	NA
8a	-	-	7, 22
8b	-	-	6
9a	-	-	-
9b	-	-	-
10a	11, 12	-	-
12a	-	-	-
12b	-	-	10, 11, 13
13a	-	-	11
13b	-	-	-
14	1, 12	1	15
16	1, 3, 18	-	1, 3, 18
17	2, 4	2	2, 4, 18
20a	-	-	-
20b	NA	-	22
21a	-	-	7, 19, 22
21b	-	-	7
22a	-	NA	20
23	6, 19, 20	6, 19, 20	6, 19, 20
24a	6, 7, 8, 22	7, 21	6, 7, 8, 22
24b	NA	7, 21	NA
25	10, 11, 12	10, 11, 12	10, 11, 12
26a	14, 15, 27	14, 15, 27	14, 27
26b	NA	NA	14, 15, 27
27	14, 15, 26	14, 15, 26	14, 15, 26
28	19	NA	NA
Aryl-OH	-	17, 18	4, 17, 18

Table B.3: Observed NOEs from NOESY and ROESY NMR experiments for bromophycolides J-L (**1-3**). For diastereotopic protons with dissimilar chemical shifts, the proton whose chemical shift is listed first in Tables 1-2 of the main article is termed "a" and the other is "b". Only NOEs important to determinations of stereochemistry are listed.

^{1}H at position #:	**NOE observed between protons listed on far left and protons at positions listed below:**		
	1	**2**	**3**
3	6	5a	
5a		3	24
5b	24		24
6	3, 8a, 20, 28		
7			
8a	6, 24		
8b	10, 24		
9a	10	10, 24a	
9b			22
10	8b, 9a, 25	9a, 25	25
12a	14	14	14
12b	14		14
13a	14	14	14
13b		14	14
14	12a, 12b, 13a	12a, 13a, 13b	12a, 12b, 13a, 13b
20a	6, 21b, 22, 28		
20b			
21a	23		
21b	20, 22		22
22	20, 21b		9b, 21b
23	21a, 24, 28		
24a	8a, 8b, 5b, 23	9a	5a, 5b
24b			
25	10	10	10
26			
27			
28	6, 23, 20		

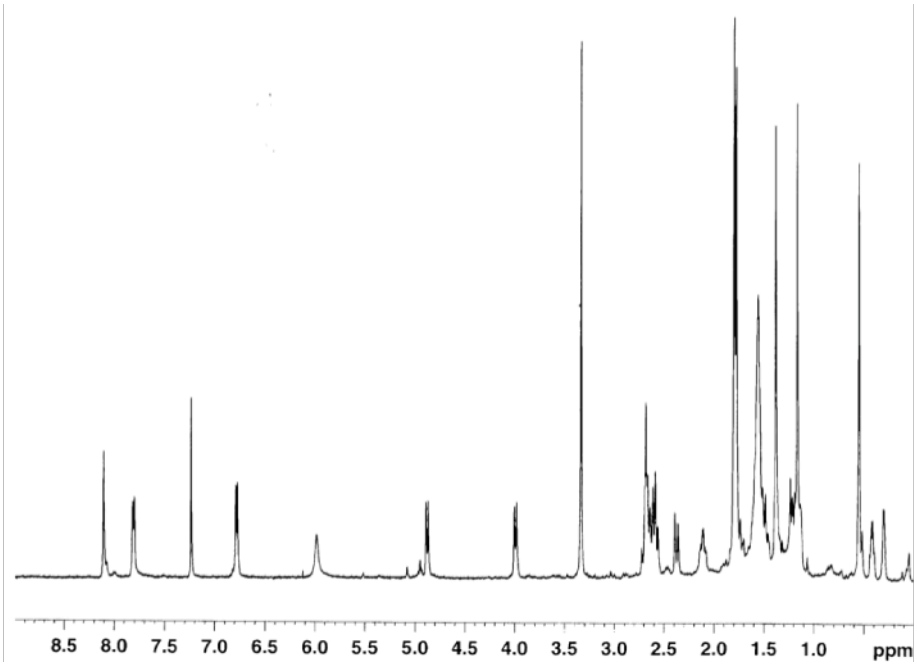

Figure B.1. ^{1}H NMR spectrum of bromophycolide J (**1**) (500 MHz; $CDCl_3$)

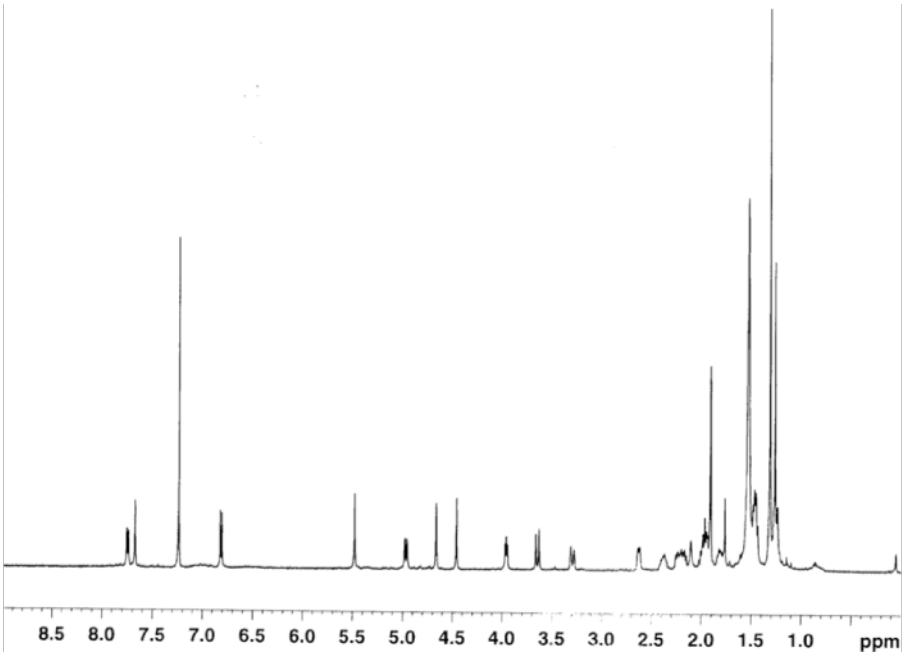

Figure B.2 ^{1}H NMR spectrum of bromophycolide K (**2**) (500 MHz; $CDCl_3$)

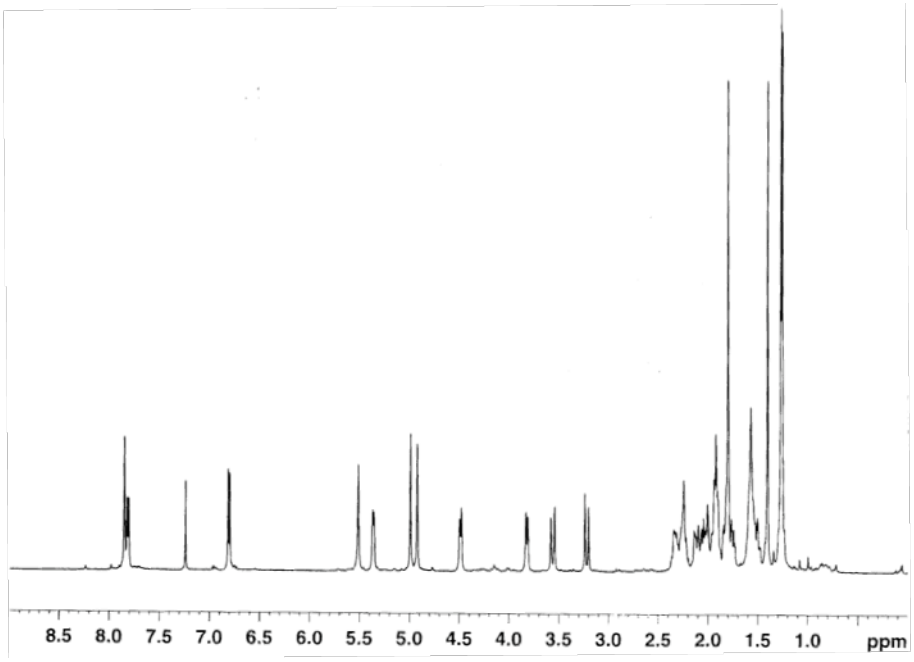

Figure B.3 ^{1}H NMR spectrum of bromophycolide L (**3**) (500 MHz; $CDCl_3$)

APPENDIX C

SUPPORTING INFORMATION FOR CHAPTER 5: SURFACE-MEDIATED ANTIFUNGAL CHEMICAL DEFENSES OF A TROPICAL SEAWEED

Additional experimental methods.

General. Semipreparative HPLC was performed using a Waters 1525 or 515 pump with a Waters 2996 diode-array UV detector or a Waters 2487 dual-wavelength absorbance detector. Compound purification was achieved with Agilent Zorbax SB-C18 and RX-SIL columns (5 μm, 9.4 × 250 mm). ^{1}H NMR spectra were collected in $CDCl_3$ on a Bruker DRX-500 instrument with a 5 mm broadband probe and referenced to residual $CHCl_3$ (7.24 ppm). LC-MS analyses were conducted with a Waters 2695 HPLC interfaced to a 2996 diode-array UV detector and Micromass ZQ 2000 electrospray ionization mass spectrometer using MassLynx 4.0 software and an Alltech Alltima C_{18} reversed-phase column (3 μm, 2.1 x 150 mm). HPLC grade solvents were used in semipreparative HPLC and DESI-MS, and optima grade solvents applied in LC-MS experiments (Fisher Scientific Co.). NMR solvents were obtained from Cambridge Isotope Laboratories. High resolution mass spectra were acquired using electrospray ionization with an Applied Biosystems QSTAR-XL hybrid quadrupole-time-of-flight tandem mass spectrometer and Analyst QS software. Epifluorescence and light microscopy experiments were conducted with an Olympus IX50 inverted microscope, and images collected with MagnaFire software (Optronics). Additional light micrographs were obtained with an Olympus dissecting scope (i.e. Fig. 3S). All statistical analyses were completed with either SYSTAT version 9 or GraphPad version 4.

The marine alga *C. serratus*. The red macroalga *Callophycus serratus* (Harvey ex Kutzing 1957) (family Solieriaceae, order Gigartinales, class Rhodophyceae, phylum Rhodophyta) was collected at depths from 1-30 m at several sites in Fiji. Ten collections were made in 2006 at Yanuca, Waitabu in Taveuni, Lavena in Taveuni, and Dravuni in Kadavu; GPS coordinates for each collection are provided in Table 1S. Immediately following collection, portions for quantitative whole tissue LC-MS experiments were extracted as described in main text. Remaining material was frozen at -20 °C until further processing. Samples for DESI-MS experiments and microscopic analyses were collected in 2008 at Yanuca (18° 22' 35" S, 177° 59' 72" E) and immediately preserved with 1% or 10% formalin in natural seawater until analysis. Samples for DESI-MS analyses were from separate plants collected on the reef at distances from 3 to 1000 m. Algal samples were identified based on comparison with previously described morphological traits (Littler and Littler, 2003), and vouchers deposited at the Georgia Institute of Technology and the University of the South Pacific in Suva, Fiji.

Table C.1 *Callophycus serratus* collection sites in Fiji and whole tissue natural concentrations of known secondary metabolites. Concentrations were determined by quantitative LC-MS of extracts from fresh plant material, and illustrate that bromophycolides and callophycoic acids/callophycols do not co-occur in individual specimens. ND denotes compounds that were not detected by selected ion recording ESI-MS. *deA denotes debromophycolide A.

		whole tissue concentration (μM)																			
		bromophycolide										callophycoic acid								callophycol	
ID	Collection site coordinates	A	B	C	D	E	F	G	H	I	de A*	A	B	C	D	E	F	G	H	A	B
G004	18°23'57"S 177°57'58"E	151	102	46.0	22.3	22.8	ND	40.8	31.2	50.0	ND	ND	ND	ND	ND	ND	ND	ND	ND	ND	ND
G021	18°22'47"S 177°59'37"E	165	107	24.0	10.0	35.0	ND	42.0	25.0	34.0	22.0	ND	ND	ND	ND	ND	ND	ND	ND	ND	ND
G039	18°22'43"S 177°59'41"E	ND	ND	ND	ND	ND	ND	ND	ND	ND	ND	1.9	10.2	257	181	ND	ND	187	48.1	61.9	23.8
G049	18°22'88"S 177°58'94"E	117	81.2	20.9	120	27.9	ND	30.4	29.6	19.5	8.3	ND	ND	ND	ND	ND	ND	ND	ND	ND	ND
G052	18°22'35"S 177°59'72"E	ND	ND	ND	ND	ND	ND	ND	ND	ND	ND	ND	2.1	252	131	ND	ND	241	78.4	92.5	33.3
G091	16°48'97"S 179°50'84"E	ND	ND	ND	ND	ND	ND	ND	ND	ND	ND	ND	ND	149	188	ND	ND	27.1	20.2	75.5	25.8
G100	16°52'31"S 179°52'68"E	103	146	37.9	17.7	26.1	ND	18.4	17.8	12.5	47.1	ND	ND	ND	ND	ND	ND	ND	ND	ND	ND
G113	18°42'49"S 178°32'35"E	ND	ND	ND	ND	ND	ND	ND	ND	ND	ND	ND	ND	174	160	ND	ND	8.3	ND	85.1	33.0
G118	18°41'62"S 178°30'72"E	ND	ND	ND	ND	ND	ND	ND	ND	ND	ND	ND	ND	261	178	ND	ND	113	93	72.4	25.9
G171	18°23'57"S 177°57'58"E	ND	ND	ND	ND	ND	ND	ND	ND	ND	ND	ND	ND	129	240	ND	ND	ND	ND	178	53.1

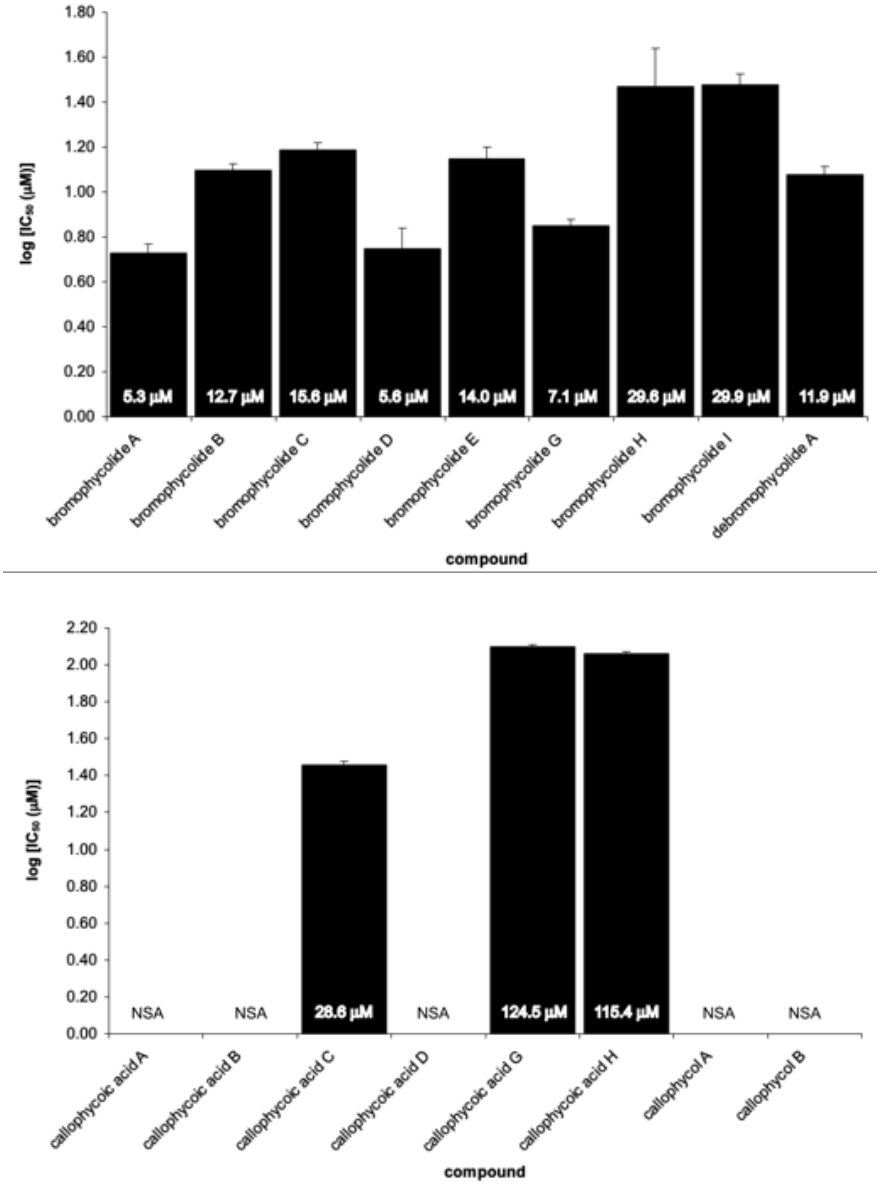

Fig. C.1 Experimental log IC_{50} values for growth inhibition of the fungus *L. thalassiae*, as determined by analysis of dose-response curves. Bars represent one standard error. IC_{50} values are indicated in white text within each data bar. NSA denotes compounds that were not significantly active at the maximum evaluated concentration of 300 μM ($p > 0.05$, $n = 3$, one-way ANOVA with Dunnett's post test).

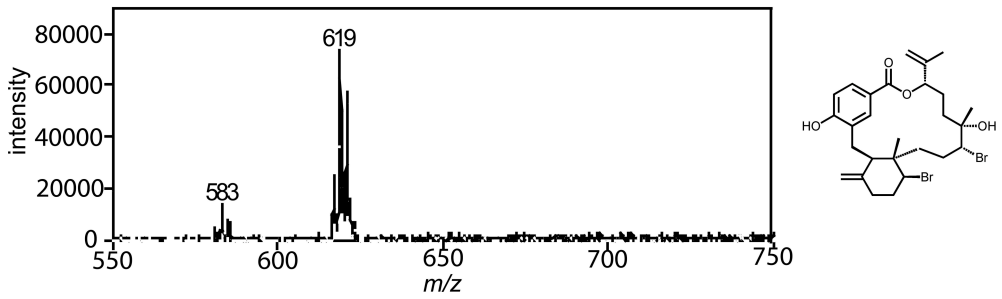

Fig. C.2 DESI mass spectrum of pure bromophycolide E (0.9 pmol/mm^2). The ion cluster centered at *m/z* 583 represents the molecular ion and *m/z* 619 represents the chloride adduct of bromophycolide E.

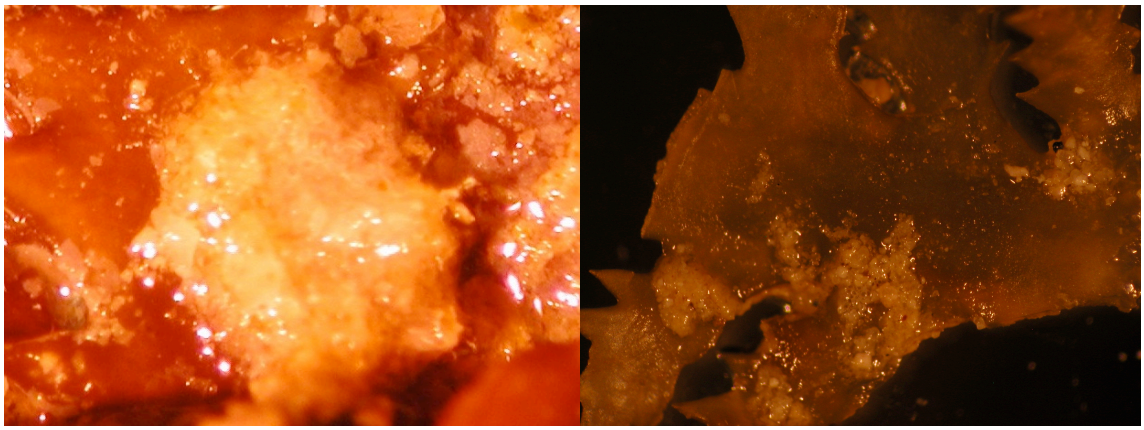

Fig. C.3 Light micrographs (~25× magnification) of bromophycolide-containing patches observed on intact *C. serratus* surfaces (preserved with 10% aqueous formalin).

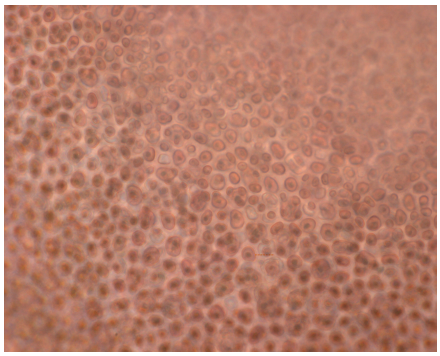

Pre DESI-MS analysis

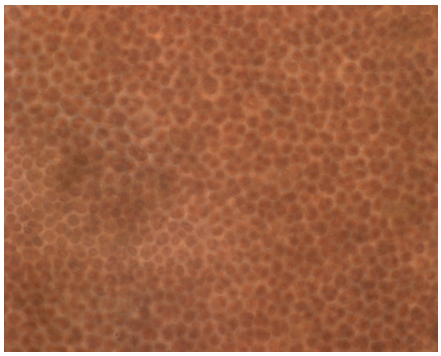

Post DESI-MS analysis

Fig. C.4 Light micrographs (100× magnification) of representative *C. serratus* fragment before (left) and after (right) DESI-MS analysis, indicating no obvious cell lysis caused by exposure to DESI source.

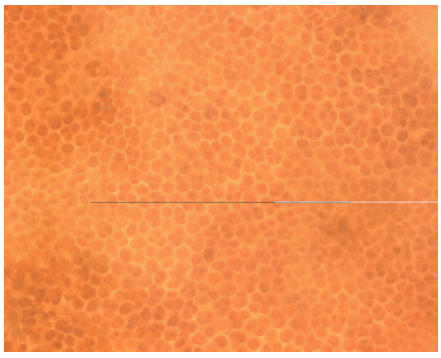

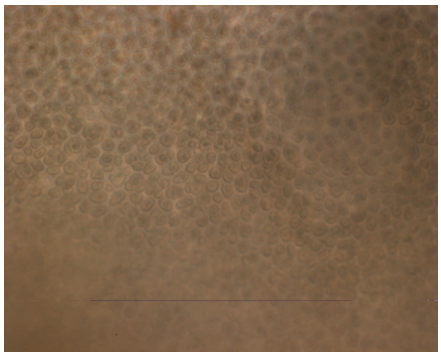

Fig. C.5 Representative light micrographs (100× magnification) of undamaged *C. serratus* tissue found beneath characteristic bromophycolide-containing surface patches.

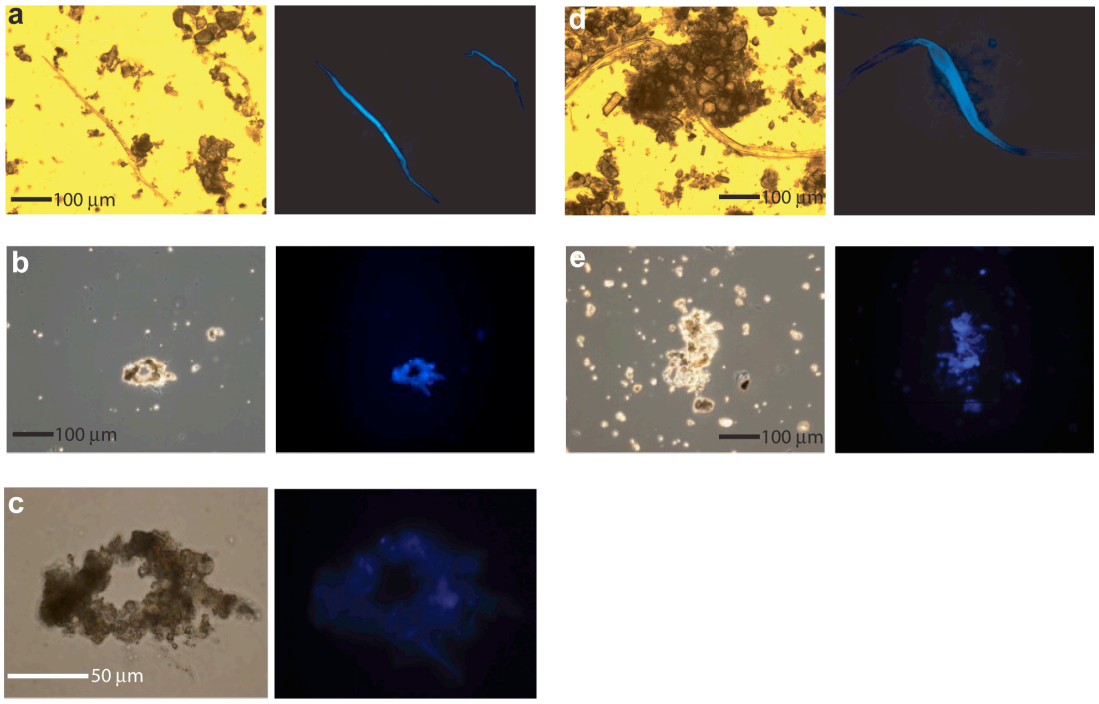

Fig. C.6 Light and epifluorescence micrographs of bromophycolide-containing patches from *C. serratus* surfaces. (a,b,d,e) 100× magnification light (left) and epifluorescence (right) micrographs of DAPI-stained patches removed from algal surfaces. (c) 400× magnification light (left) and epifluorescence (right) micrographs of DAPI-stained patches corresponding to 100× image from (b). Distinct stained nuclei, which would offer evidence for the presence of microbes, were not observed.

APPENDIX D

SUPPORTING INFORMATION: ECOLOGICAL LEADS FOR NATURAL PRODUCT DISCOVERY: NOVEL SESQUITERPENE HYDROQUINONES FROM A CRUSTOSE RED ALGA

Table D.1: COSY correlations for fijioic acids A-B (**1**-**2**). For diastereotopic protons with dissimilar chemical shifts, the proton whose chemical shift is listed first in Table 1 of the main article is termed "a" and the other is "b". "NA" (not applicable) indicates that no proton signal exists for that position.

^{1}H at position #:	COSY correlations observed between protons listed on far left and those below:	
	1	**2**
2	19	-
5	-	-
7a	5, 7b, 8	7b
7b	7a, 8	7a, 8
8	7a, 7b	7b
10a	10b, 11a, 11b	10b, 11b
10b	10a	10a, 11a, 11b
11a	10a, 11b, 12	10b, 11b
11b	10a, 11a, 12	10a, 10b, 11a, 12
12	11a, 11b	11b, 22
14	15a, 15b	15, 23a, 23b
15a	14, 16	14, 16
15b	14, 16	NA
16	15a, 15b, 18	15, 18
18	16	16
19	2	-
21	-	-
22	-	12
23a	-	23b
23b	-	23a

Table D.2: HMBC correlations for fijioic acids A-B (**1**-**2**). For diastereotopic protons with dissimilar chemical shifts, the proton whose chemical shift is listed first in Table 1 of the main article is termed "a" and the other is "b". "NA" (not applicable) indicates that no proton signal exists for that position.

^{1}H at position #:	**HMBC correlations observed between protons listed on far left and carbons at positions listed below:**	
	1	**2**
2	1, 3, 4, 19	1, 3, 4, 19
5	3, 4, 7, 20	3, 4, 7, 20
7a	5, 6, 8, 9, 17, 20	5, 6, 8, 9, 17, 20
7b	5, 6, 8, 9, 17, 20	5, 6, 8, 9, 17, 20
8	6, 7, 9, 10, 16, 17, 18	6, 7, 9, 16, 21
10a	21	-
10b	-	19, 21
11a	-	12
11b	10	-
12	22	10, 11, 13, 14, 22
14	8, 9, 10	8, 9, 12, 13, 15, 21, 23
15a	-	14, 16, 17
15b	-	NA
16	15	8, 14, 18
18	8, 16, 17	8, 16, 17
19	2, 4, 6, 20	2, 4, 6, 20
21	8, 9, 10, 14	8, 9, 10, 14
22	12, 13, 14, 23	11, 12, 13
23a	12, 13, 14, 22	12, 13, 14
23b	NA	12, 14

Table D.3: Observed NOEs from NOESY, ROESY, and 1D NOE NMR experiments, for fijioic acids A-B (**1**-**2**). For diastereotopic protons with dissimilar chemical shifts, the proton whose chemical shift is listed first in Table 1 of the main article is termed "a" and the other is "b". Only NOEs important to determinations of stereochemistry are listed.

^{1}H at position #:	**NOE observed between protons listed on far left and protons at positions listed below:**	
	1	**2**
2	-	-
5	-	7a
7a	-	5
7b	10b	10a
8	21	21
10a	-	7b
10b	7b	-
11a	22	-
11b	21, 22	21
12	14, 23	23b
14	12	22
15a	-	21, 23a
15b	-	NA
16	-	-
18	-	-
19	-	-
21	8, 22	8, 11b, 15
22	21, 11a, 11b	14, 23b
23a	12	15
23b	NA	12, 22